Entry Aerothermodynamics

- Review of basic fluid parameters
- Heating rate parameters
- Stagnation point heating
- Heating on vehicle surfaces
- Slides from 2012 NASA Thermal and Fluids Analysis Workshop: https://tfaws.nasa.gov/TFAWS12/Proceedings/Aerothermodynamics%20Course.pdf

© 2024 University of Maryland - All rights reserved
http://spacecraft.ssl.umd.edu

Entry Heating Background

- Orbital energy of 32 MJ/kg would melt any material if it were entirely internalized
- Spacecraft kinetic energy on entry is almost entirely dissipated by heating the atmosphere as it decelerates
  - Dependent on vehicle shape, size, and trajectory
  - Near peak heating, 1%-5% of thermal energy transferred to spacecraft
  - Example: Mars Pathfinder peak heat flux was 4000 W/cm^2, but only about 110 W/cm^2 was transferred to heat shield surface

Perspective on Heating Rate

- Energy density $\frac{E}{m} = \frac{V^2}{2} + g_o h$
- Note that water boils at 2.3 W/cm^2
  Carbon vaporizes at 60.5 W/cm^2
- In each case $g_o h$ is about 1% of total

Entry	V (km/s)	E/m (MJ/kg)
MER	5.6	16
Apollo	11.4	66
Mars Return	14.0	98
Galileo	47.4	1130

Earth-Based Testing of Entry Aerothermodynamics

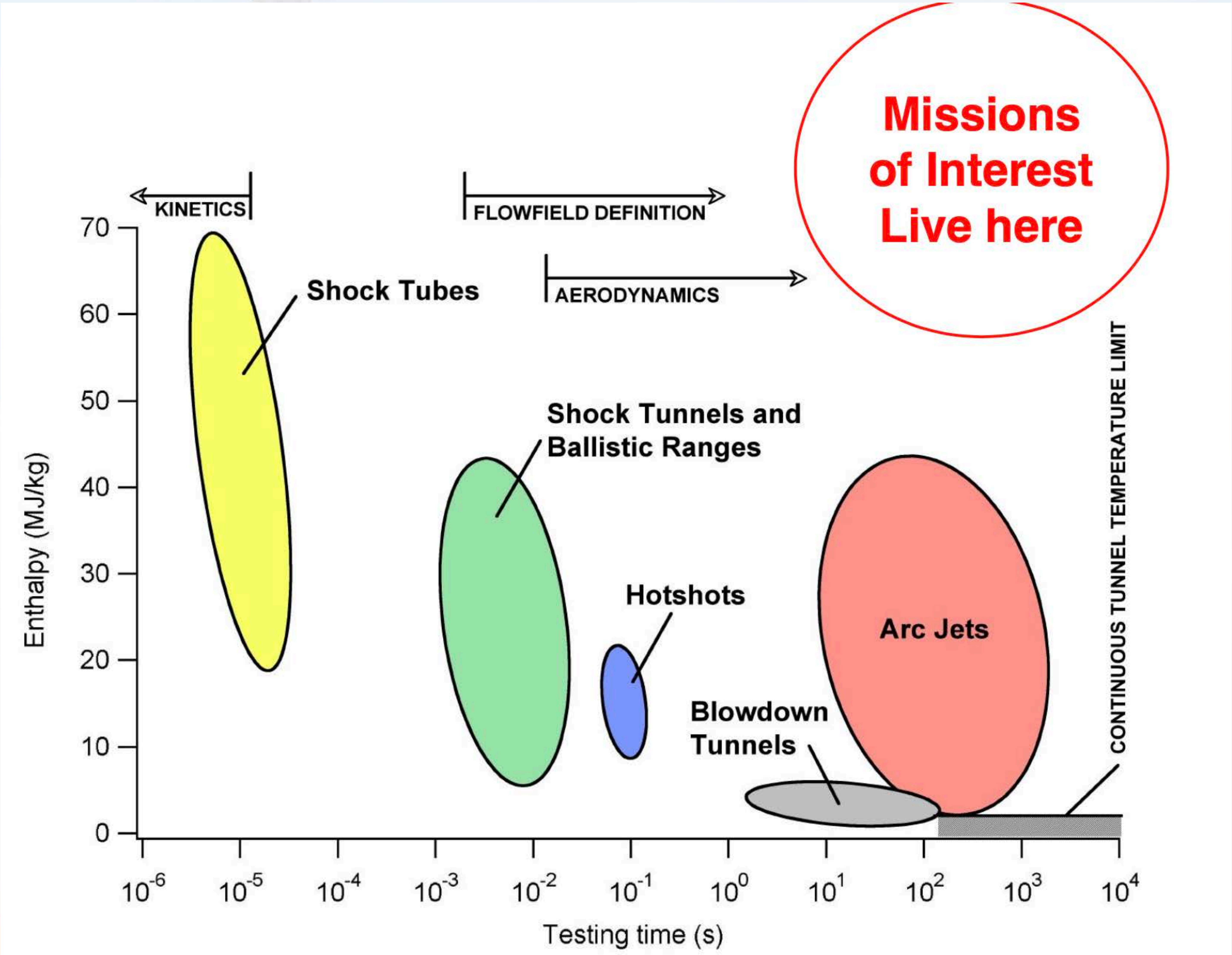

2012 NASA Thermal and
Fluids Analysis Workshop

Sharp vs. Blunt Entry Bodies

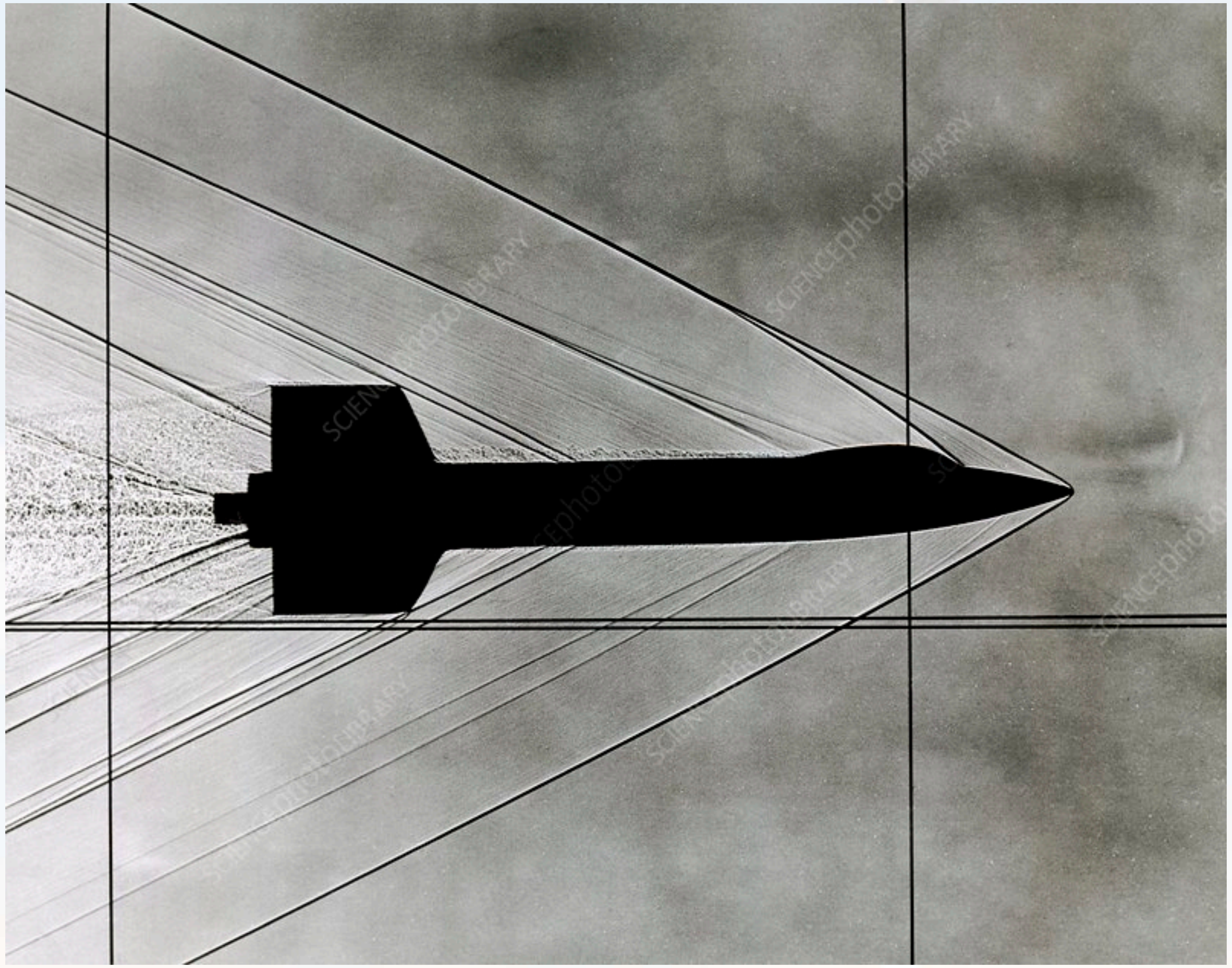

Low drag, highly maneuverable

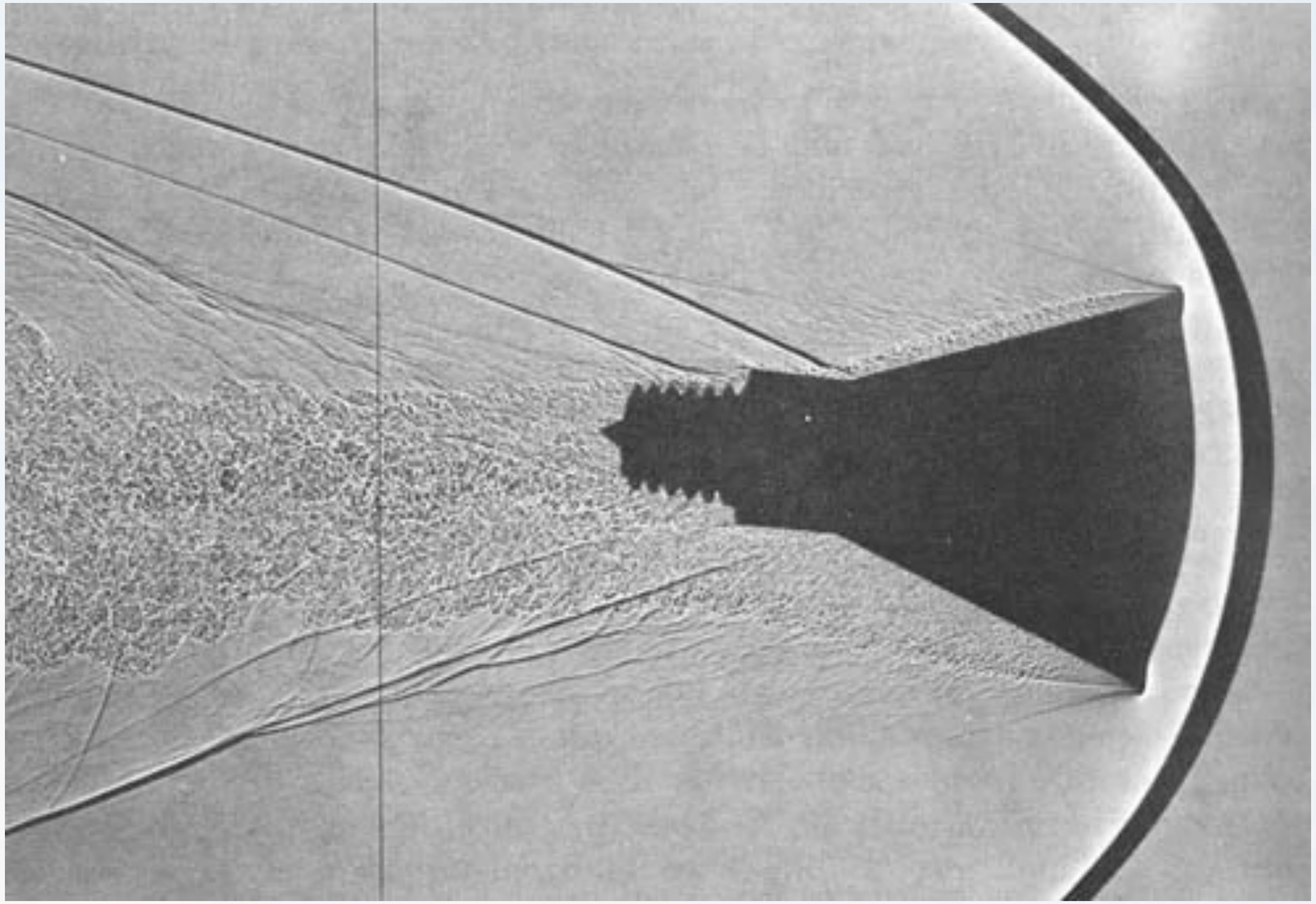

High drag, not very maneuverable

Advantages of Blunt Entry Bodies

- Strong shock waves
- Efficient energy dissipation
- Shck waves convert kinetic energy to internal energy
- Most of the energy convected to vehicle wake rather than vehicle surface
- Blunter is better!

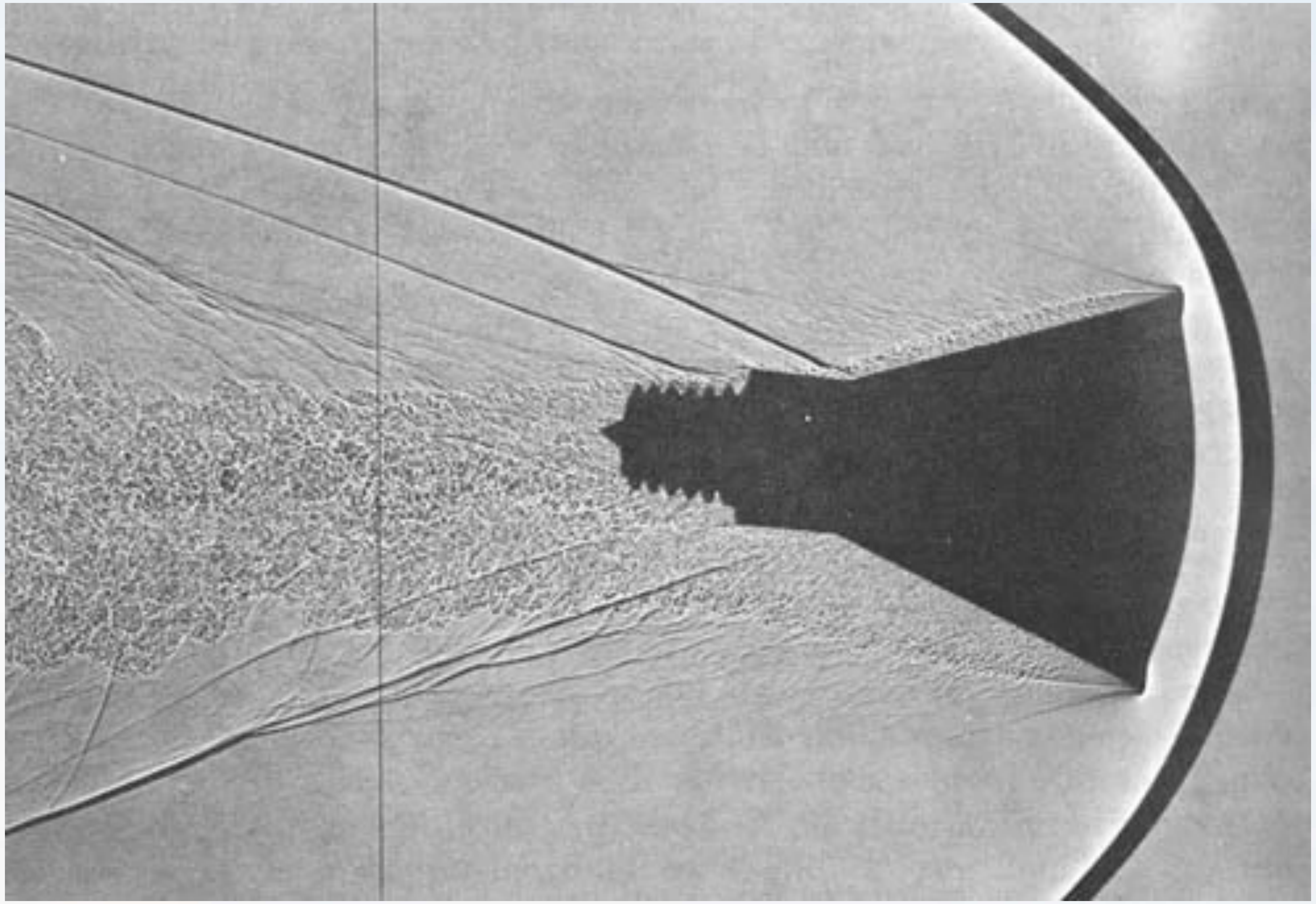

Hypersonic Flow Field around an Entry Vehicle

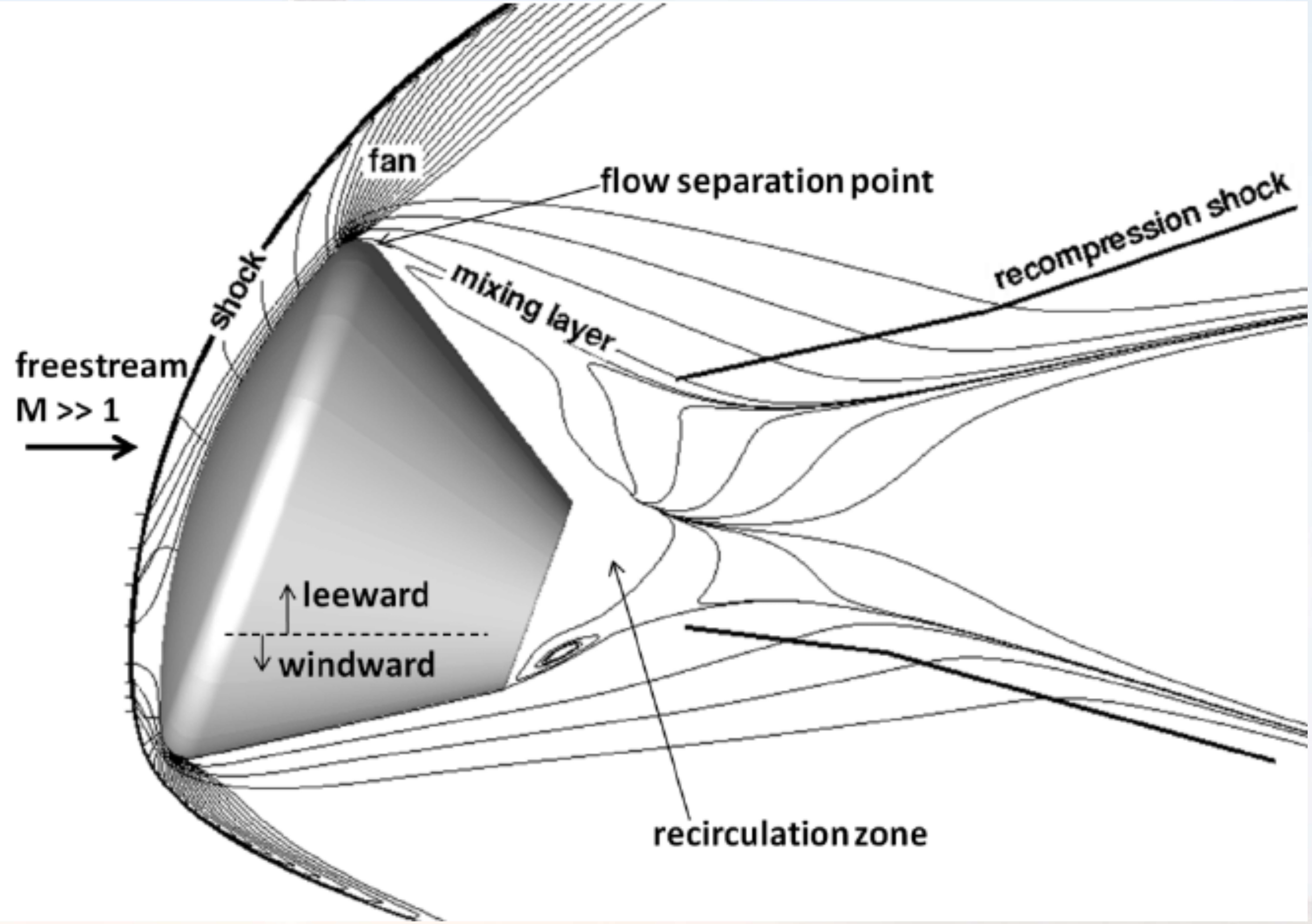

Ivey et.al., “Comparison of PLIF and CFD Results for the Orion CEV RCS Jets” AIAA 2011-713

Blunt Body Rationale

- Normal shock heats gas to thousands of degrees
- Much of the heat is conducted into the vehicle wake and propagated downstream – creates dissociation, ionization
- Velocity perturbation persists long downstream of the vehicle

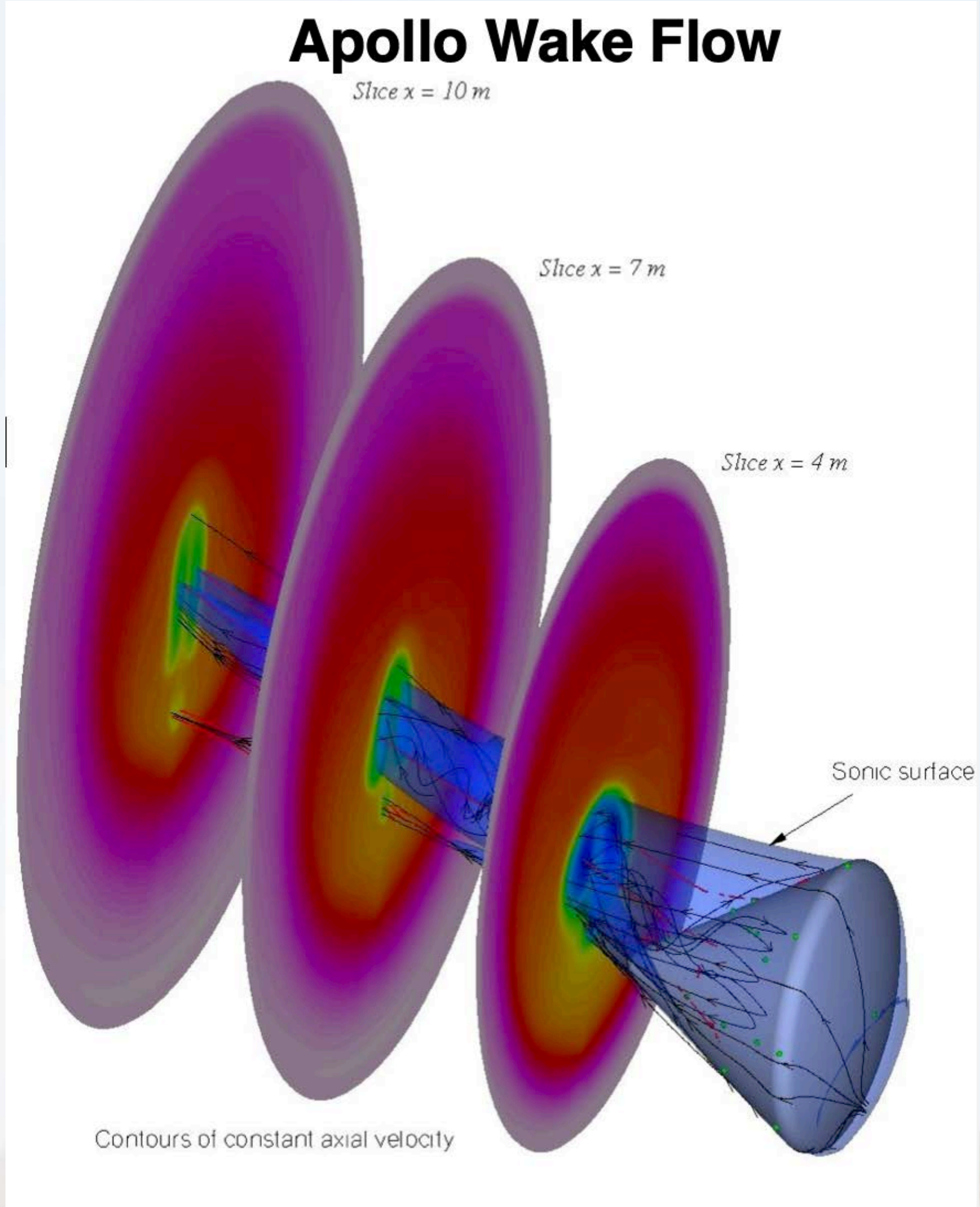

Definitions

- Heat rate q – instantaneous heat flux at a point on the vehicle <W / cm^2>
- Heat load Q – integration of heat rate with time over a trajectory <J / cm^2>
- Convective heating – heat flux into the vehicle from conduction ($\kappa \nabla T$)
- Catalytic Heating – heat flux to the vehicle via chemical reactions facilitated by surface; usually lumped in with convective heating
- Radiative hearing – heat flux to the vehicle from radiation produced by heated molecules in shock layer

What is Aerothermodynamics?

- **Accurate and conservative prediction of the heating environment encountered by an Earth or planetary entry vehicle**

- **Aerothermal modeling is coupled and entwined with Thermal Protection System (TPS) design**
  - The TPS is designed to withstand the predicted environment with risk-appropriate margin
  - For ablative systems, the flowfield and TPS interact with each other in non-reversible manner; the physics themselves are coupled

- **At its core, aerothermodynamics becomes the study of an energy balance at the surface of the material**

  - ➢ **Heat flux (with pressure & shear) used to select TPS material**
  - ➢ **Heat load determines TPS thickness**

Principles of Aerothermal Models

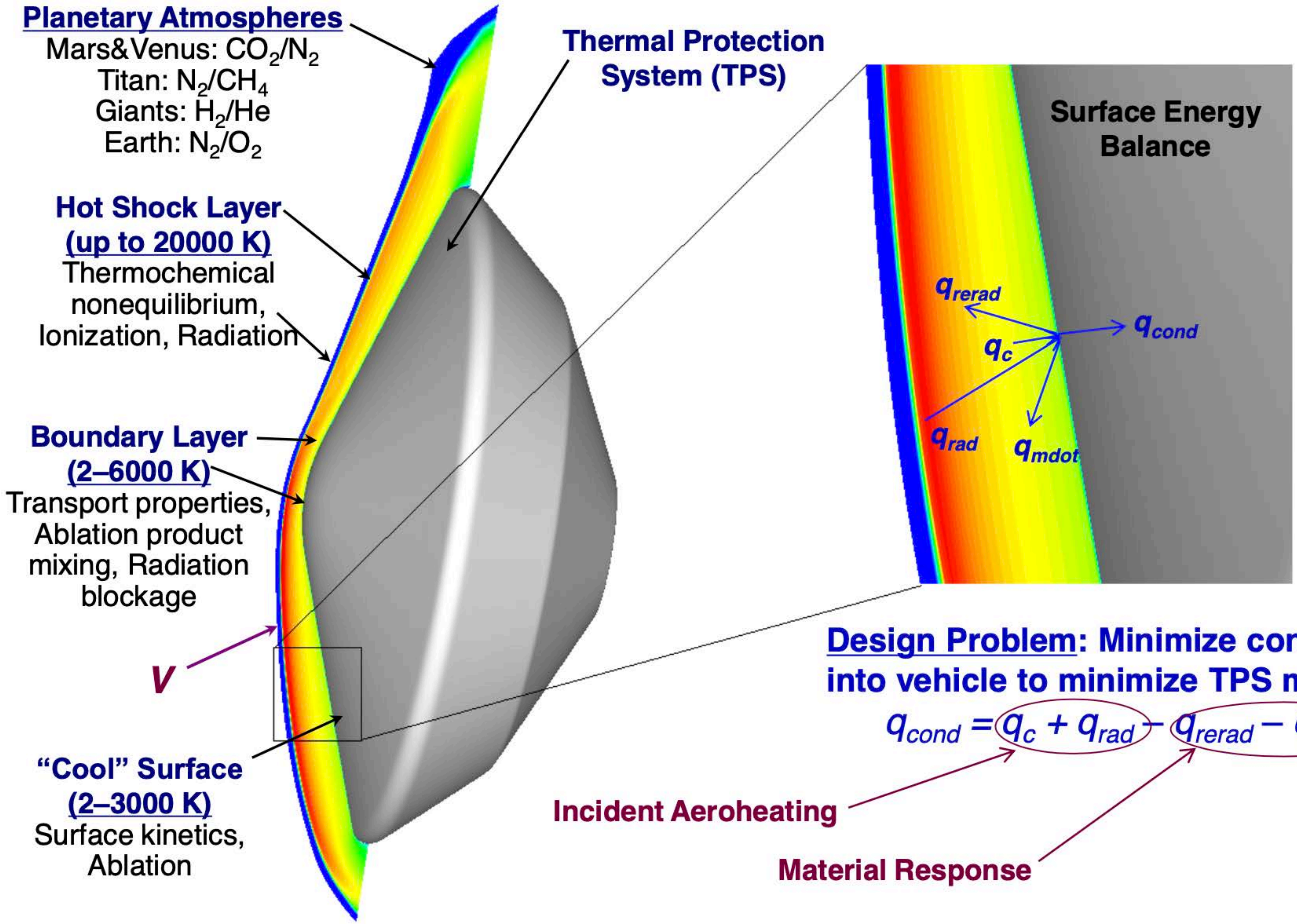

Design Problem: Minimize conduction into vehicle to minimize TPS mass/risk

$$q_{cond} = q_c + q_{rad} - q_{rerad} - q_{mdot}$$

Current State of the Art : CFD

- **The current SOA involves the steady solution of the reacting Navier-Stokes equations via CFD or DSMC methods**
- **Full 3D simulations possible in hours to days**
- **Longer time required for the simulation of OML details (steps, gaps, seals, windows, etc.**

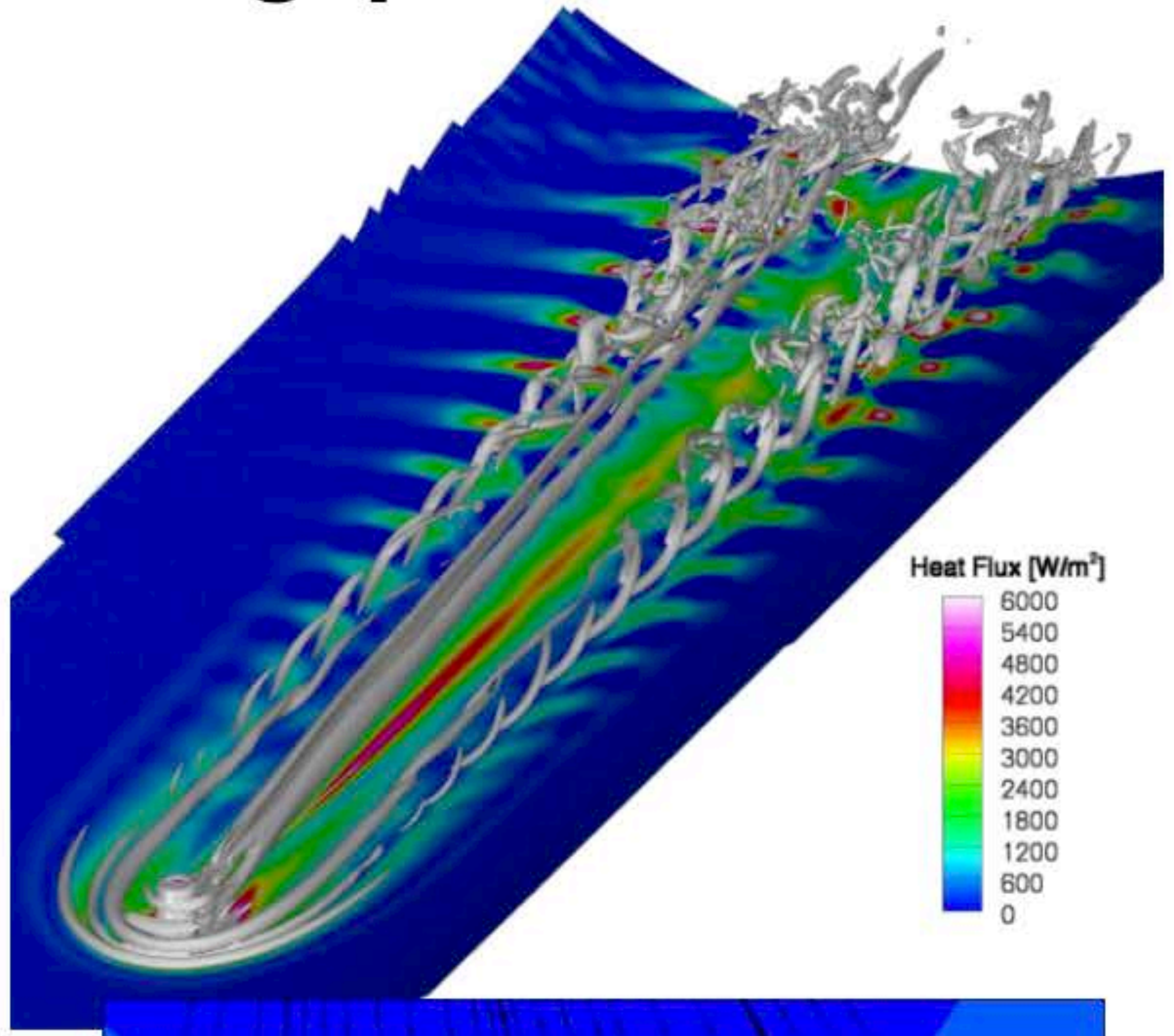

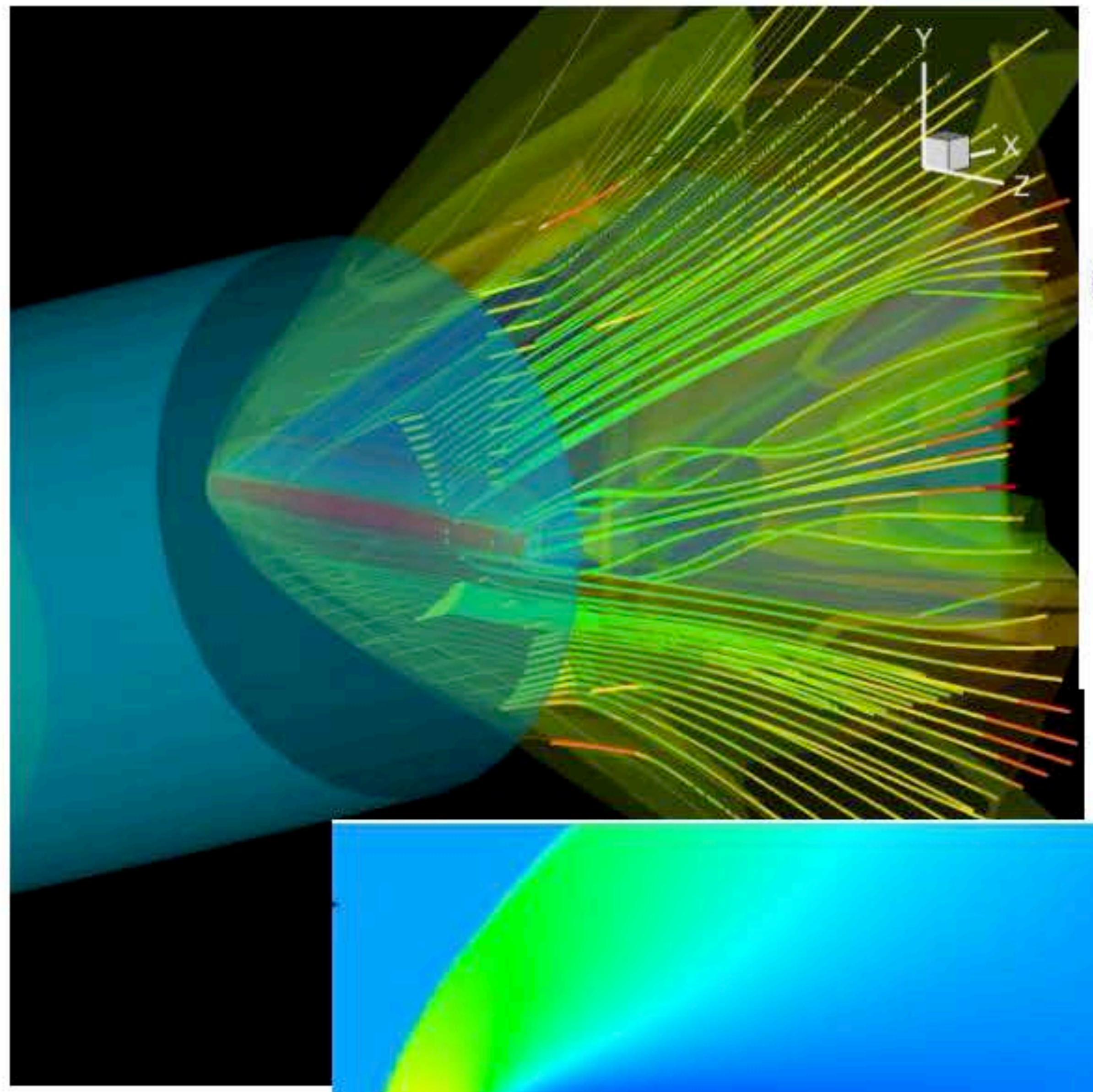

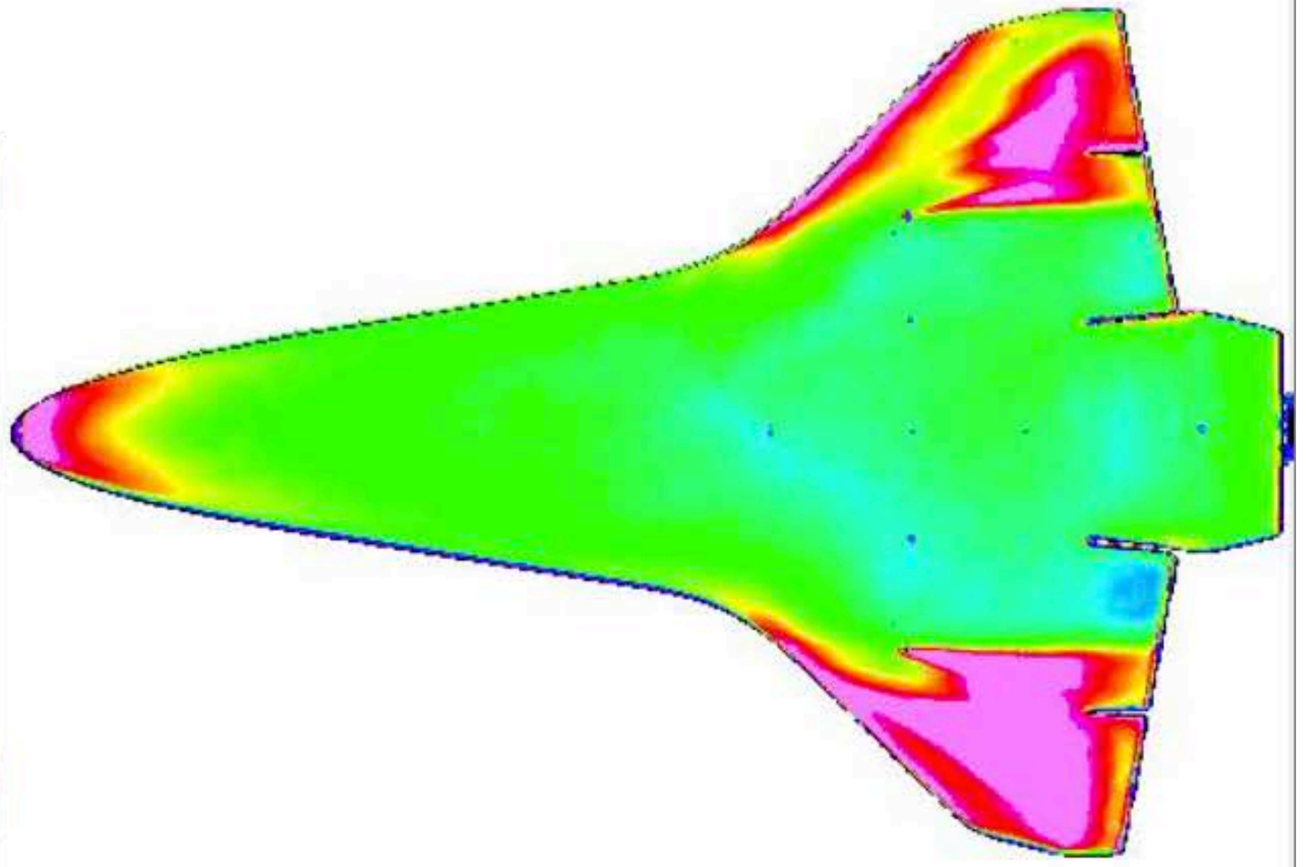

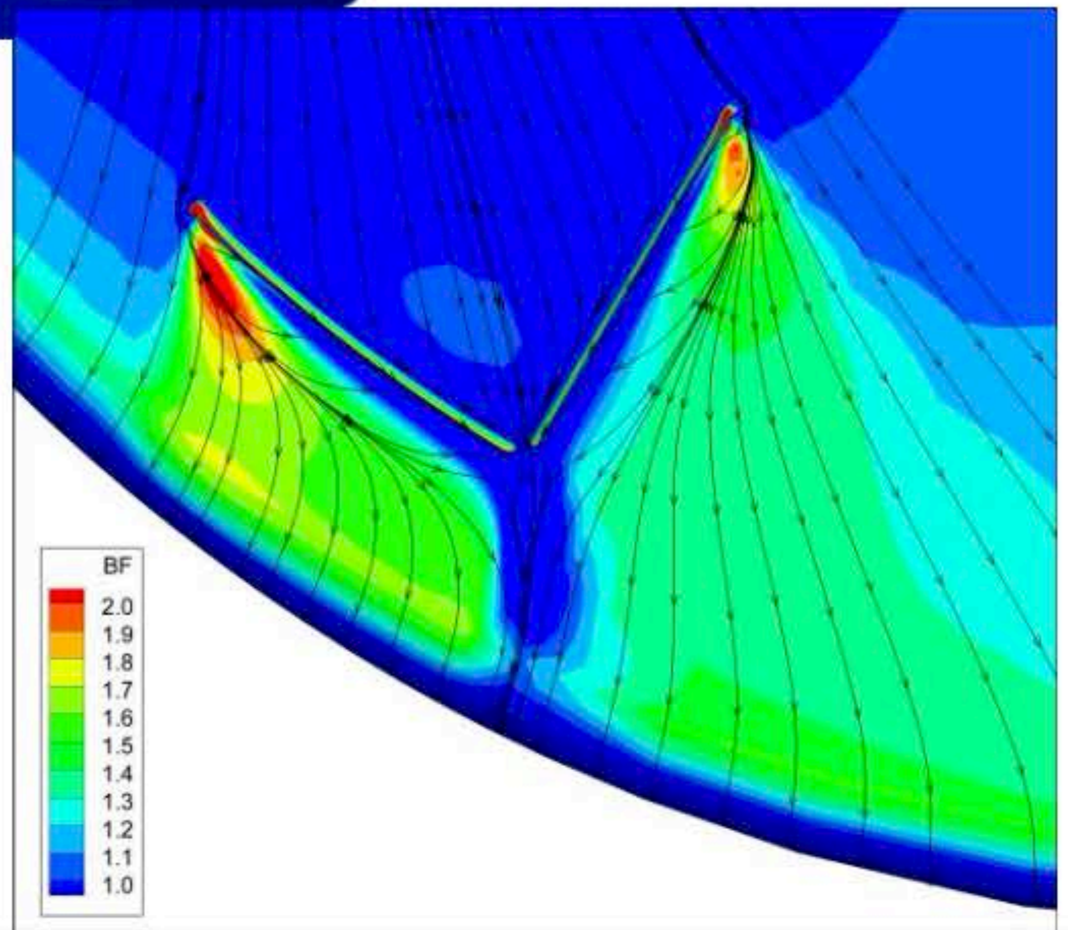

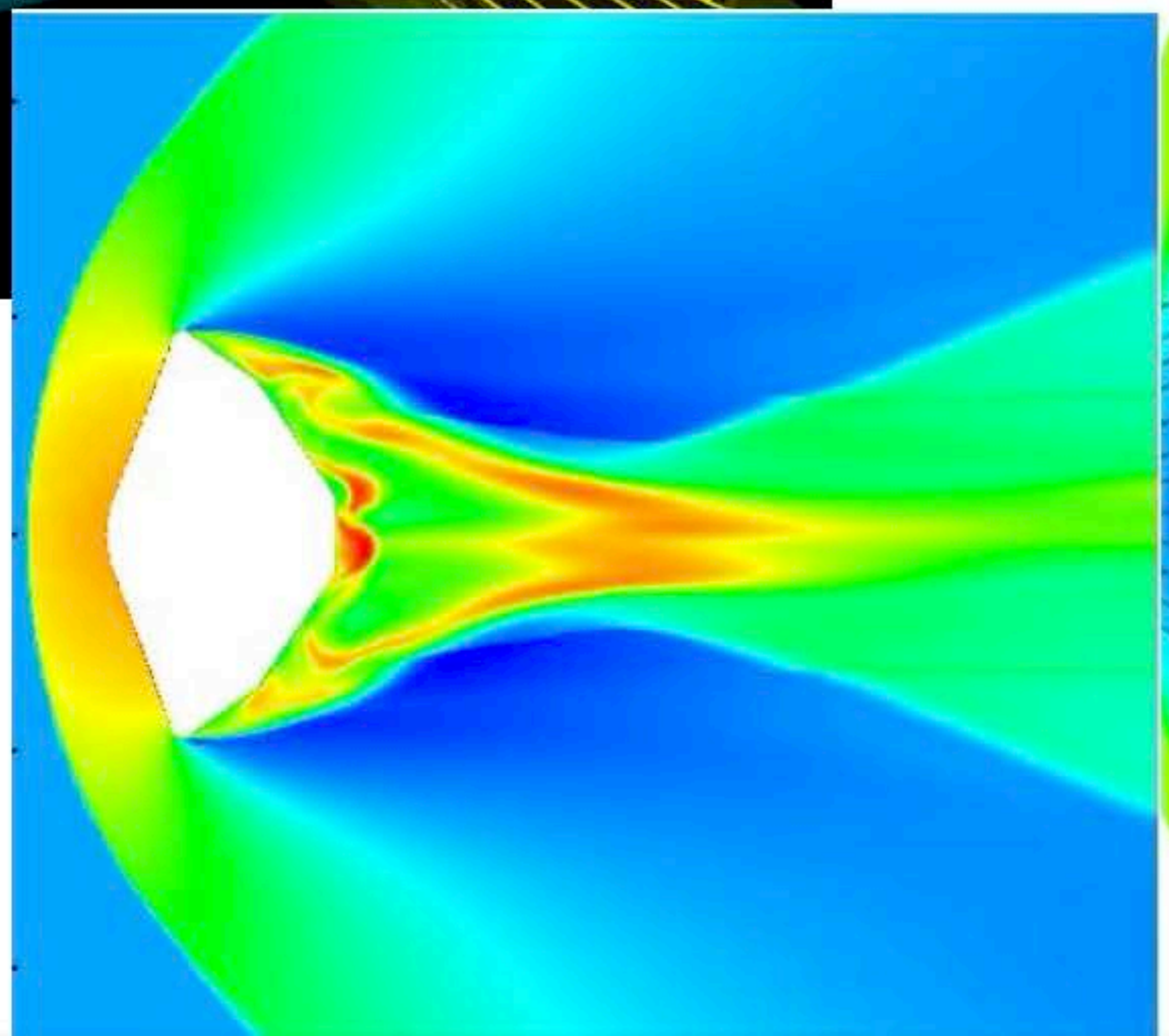

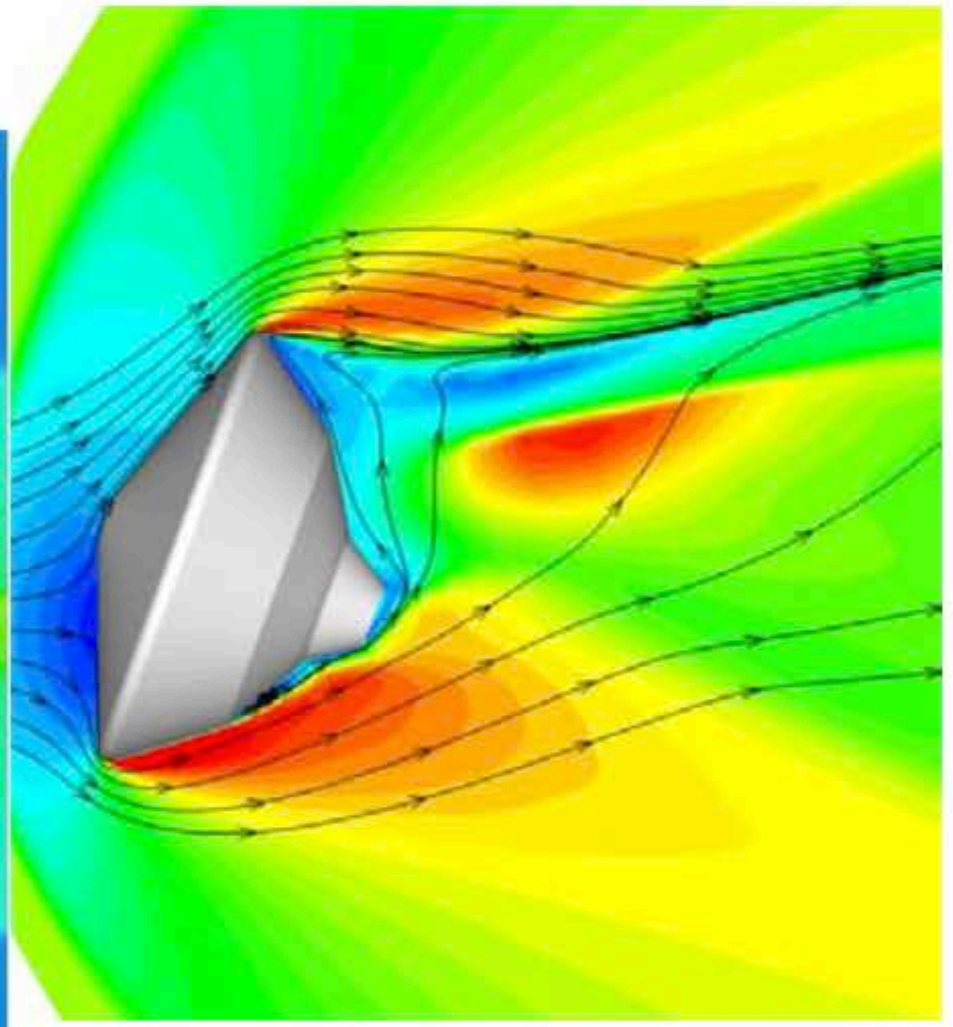

Why Engineering Methods?

With present computational abilities, why use engineering methods?

- CFD is a powerful tool, but high-fidelity simulations remain time (and resource) consuming

- Some applications of simple relationships for calculating non-ablating convective and radiative heating
  - Negligible computation time
  - Included in most atmospheric trajectory codes-stag. pt. heating
  - Initial estimates of heating rates and loads for use during conceptual design stage

- But most important:

➔In this day of commodity supercomputers it is all too easy to run simulations without truly understanding the physics involved or the trends that are expected. ***The fact that it "converged" doesn't make it right***. Engineering methods are based on sound approximations to theory and provide a valuable sanity check on CFD results

Stagnation Point Convective Heat Transfer Theory

- **Pioneering engineering theories were developed in the 1950's (missile technology)**

  Lees, L. "Laminar Heat Transfer Over Blunt-Nosed Bodies at Hypersonic Speeds," *Jet Propulsion*, pp. 256-269, Apr. 1956

  Fay, J.A. and Riddell, F.R., "Theory of Stagnation Point Heat Transfer in Dissociated Air," *Journal of Aeronautical Sciences*, Feb. 1958

- **Extensions to higher velocities were required to account for chemistry and ionization**

- **Many extensions and simplifications followed for specific applications, non-Earth atmospheres**

Stagnation Point Convective Heat Transfer Theory

- Early correlations for convective heating have the form

$$q_s \sim V^3 \left(\frac{\rho}{R_{nose}} \right)^{\frac{1}{2}}$$

- Why?
- At first thought, might expect heat flux to the surface to be proportional to freestream energy flux $\frac{1}{2}\rho V^3$
- From previous discussion, we would expect heat flux to decrease as bluntness (R_{nose}) increases, but what's the actual relationship?

Aerothermodynamic Heating

$q \equiv$ heating rate per unit area $\langle \mathrm{J/sec/m^2} \rangle$

$$q \equiv \frac{dQ}{dt} = k\left(T_r - T_w\right)$$

$k \equiv$ convective heat transfer coefficient $\left\langle \dfrac{J}{m^2 \sec K} \right\rangle$

$T_r \equiv$ recovery temperature $\langle K \rangle$

$T_w \equiv$ wall temperature $\langle K \rangle$

$$T_r = T_\infty \left(1 + \frac{\gamma - 1}{2} M^2\right)$$

Wall Temperature

$T_{w\ell} \equiv$ local wall temperature

$$\left(T_r - T_w\right)_\ell = \left(T_\infty - T_{w\ell}\right) + T_\infty \frac{\gamma - 1}{2} M^2$$

For high Mach numbers,

$$\left(T_r - T_w\right)_\ell = T_r - T_{w\ell} \cong T_\infty \frac{\gamma - 1}{2} M^2$$

Mach Number Manipulation

By definition,

$$M^2 = \frac{V^2}{a^2} = \frac{V^2}{\gamma RT}$$

$$M^2 T = \frac{V^2}{\gamma R} = \frac{V^2}{\left(c_p/c_v\right)\left(c_p - c_v\right)} = \frac{V^2}{c_p(\gamma - 1)}$$

$$T_r - T_{w\ell} = \frac{V^2}{2c_p}$$

Prandtl Number

$$Pr = \mu \frac{c_p}{K}$$

where $c_p \equiv$ specific heat at constant pressure

$K \equiv$ thermal conductivity

$\mu \equiv$ viscosity

$$\text{Pr} \propto \frac{\text{frictional dissipation}}{\text{thermal conduction}}$$

Pr $\approx$ 0.715 for air at standard conditions

Sutherland's Law (empirical)

Viscosity depends on temperature

$$\frac{\mu}{\mu_{\mathrm{ref}}} = \left(\frac{T}{T_{ref}}\right)^{3/2} \frac{T_{ref} + S}{T + S}$$

$$\text{for air: } \mu_{ref} = 1.789 \times 10^{-5} \frac{\mathrm{kg}}{\mathrm{m} \cdot \mathrm{sec}}$$

$$T_{ref} = 288 \text{ K}$$

$$S = 110 \text{ K}$$

$\Longrightarrow$ good to several thousand degrees

Stanton Number

Applies to boundary layer problems

$$S_T = \frac{q_w}{\rho_e v_e \left(H_{aw} - H_w\right)}$$

$$H \equiv \text{ enthalpy} = c_p T \text{ for perfect gas}$$

$$H_w = \text{ enthalpy at the wall}$$

$$H_a w = \text{ enthalpy at an adiabatic wall}$$

$$\text{for } H_{aw}, \quad \left(\frac{\partial T}{\partial z}\right)_w = 0$$

Approximating H_{aw}

$$H_o = H_e + \frac{u_e^2}{2} \Longleftarrow \text{ total enthalpy at edge of boundary layer}$$

$$H_{aw} = H_e + r\frac{u_e^2}{2} \qquad r \equiv \text{ recovery factor}$$

$$H_{aw} = H_e + r\left(H_o - H_e\right)$$

for incompressible flow, $r \approx \sqrt{P_r} = 0.845$ for air @ STP

r only decreases 2.4 % from M = 0 to M = 16

$\Longrightarrow$ fairly constant!

Reynold's Analogy

Relates the convective heat transfer coefficient k to the local skin friction coefficient

$$c_{f\ell} = \tau_w \frac{\rho_\infty}{2} V^2$$

$\tau_w \equiv$ local wall stress $\langle Pa \rangle$

$$k = \frac{1}{2} c_{f\ell} c_{p\ell} \rho_\ell V_\ell$$

$Q \equiv$ total heat transfer rate

$$Q = \int_{S_{wet}} q ds = \int_{S_{wet}} k \left(T_r - T_w \right) ds$$

Reynold's Analogy (2)

$$\frac{S_T}{c_f} = \frac{1}{2} P_r^{-2/3}$$

$c_f \equiv$ skin friction coefficient

$$\text{since } P_r \approx 1, \quad S_T \approx \frac{c_f}{2} \Longleftarrow \text{Reynold's Analogy}$$

Fay-Riddell Method

- **<u>Convective</u>: derived from boundary layer and stagnation point theories**

w = wall
e = edge

Fay & Riddell (1958):

Boundary layer eqns, similarity transformation

$$\dot{q}_w = \frac{0.763}{(\mathrm{Pr}_w)^{0.6}} (\rho_e \mu_e)^{0.4} (\rho_w \mu_w)^{0.1} \left[(h_o)_e - h_w \right] \left[1 + (Le^{0.52} - 1) \frac{h_d}{(h_o)_e} \right] \left[\left(\frac{du_e}{dx} \right)_t \right]^{0.5}$$

Velocity gradient from mod. Newtonian theory ~(1/R_n)

$$\frac{du_e}{dx} = \frac{1}{R} \sqrt{\frac{2(p_e - p_\infty)}{\rho_e}}$$

Significant advance, but still requires many quantities that are not readily available to designer

Allows for chemistry effects, non-unity Pr, Le (Prandtl, Lewis numbers)

Simplified Methods

Chapman Equation (Earth):

$$q_s = 1.63 \times 10^{-4} \left(\frac{\rho}{R_n} \right)^{\frac{1}{2}} V^3 \left(1 - \frac{h_w}{h_\infty} \right)$$

$$h_\infty = \int_0^T C_p T dt + \tfrac{1}{2} V_\infty^2$$

"hot wall correction" can frequently be neglected in hypersonic flow ($h_w << h_\infty$)

Sutton Graves:

$$q_s = k \left(\frac{\rho}{R_n} \right)^{\frac{1}{2}} V^3$$

k = 1.7415e-4 (Earth)
k = 1.9027e-4 (Mars)

(SI units)

- **Calculated for specific atmosphere (Earth or Mars), accounting for thermodynamics.**
- **Above assume a fully catalytic surface; equivalent expressions for non catalytic wall are available.**

Hot Wall Correction Term

- Negligible above about 100 W/cm² assuming radiative equilibrium
- Actual effect is smaller than this for ablative TPS

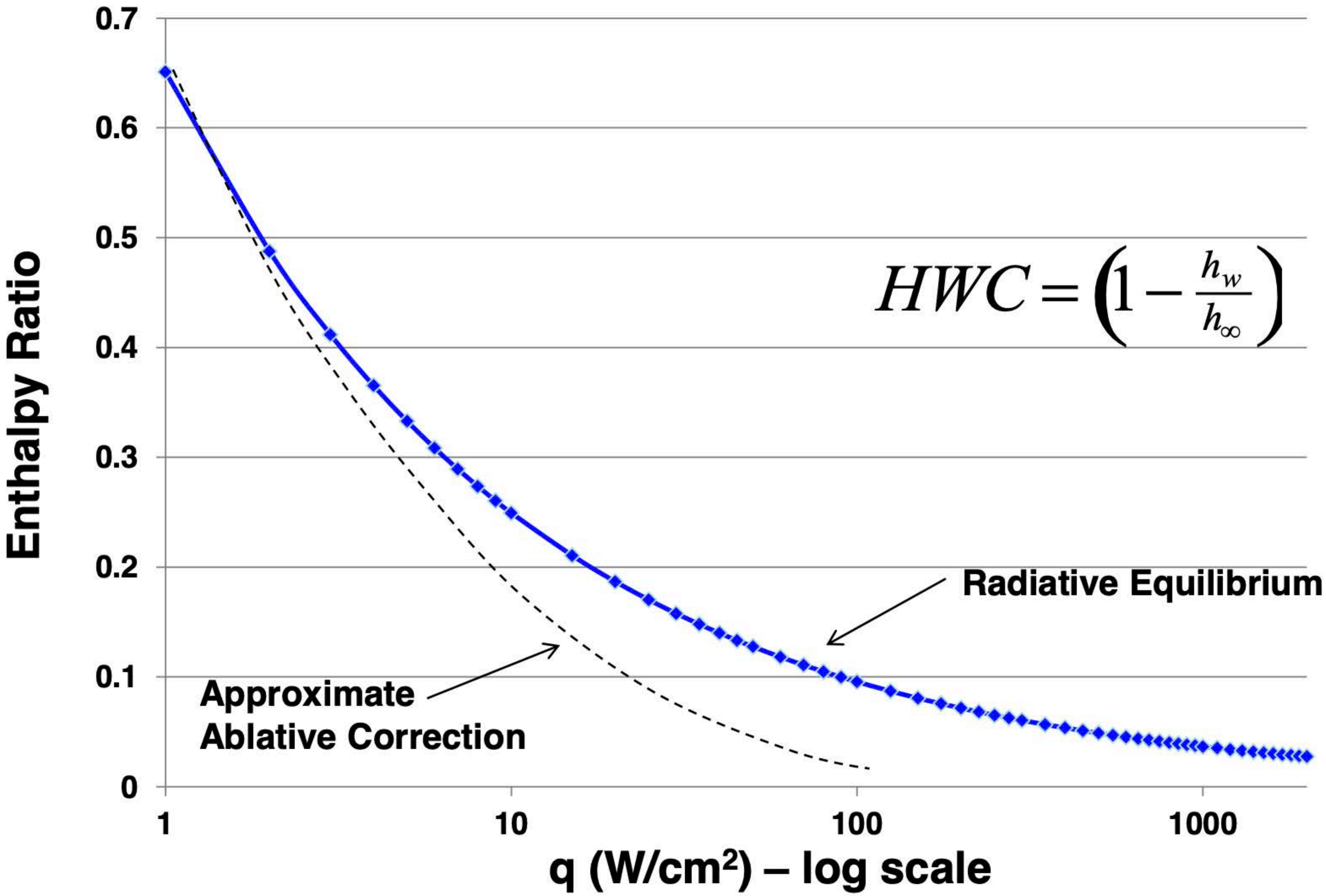

$$HWC = \left(1 - \frac{h_w}{h_\infty}\right)$$

Generalized Chapman Method

$$q_{c,0} = \frac{C}{\sqrt{R_n}} (\rho_\infty)^m (V_\infty)^n \left[1 - \frac{h_w}{h_\infty} \right];$$

Earth : **m = 0.5,** **n = 3**
Mars: **m = 0.5,** **n = 3.04**

C is derived for problem of interest

Powerful design tool - can be used to approximate heating from a small number of CFD “anchor points” even away from the stagnation point by letting *C*, *m*, and *n* be curve fit coefficients

Nuance – Effective Nose Radius

- **Prior correlations are straightforward and require only readily available quantities**
- **However, there is a nuance. All are dependent on the effective nose radius of the vehicle under investigation**
- **For a hemisphere, $R_{eff} = R_n$, but corrections are required for other vehicle shapes.**
- **For example, Apollo was a truncated sphere, with an effective radius almost twice the base radius of the capsule. MER/MSL use sphere-cones, where the conical flank increases the effective radius of the nose**
- **For bodies with a rounded corner, Zoby and Sullivan have computed tables of effective radius as a function of R_b/R_n and R_c/R_b:**

Zoby, E. and Sullivan E, “Effects of Corner Radius on Stagnation Point Velocity Gradients on Blunt Axisymmetric Bodies,” Journal of Spacecraft and Rockets, Vol. 3, No. 10, 1966.

Nuance – Effective Nose Radius (2)

When does it matter?

Can the flow "tell" that the nose is finite?

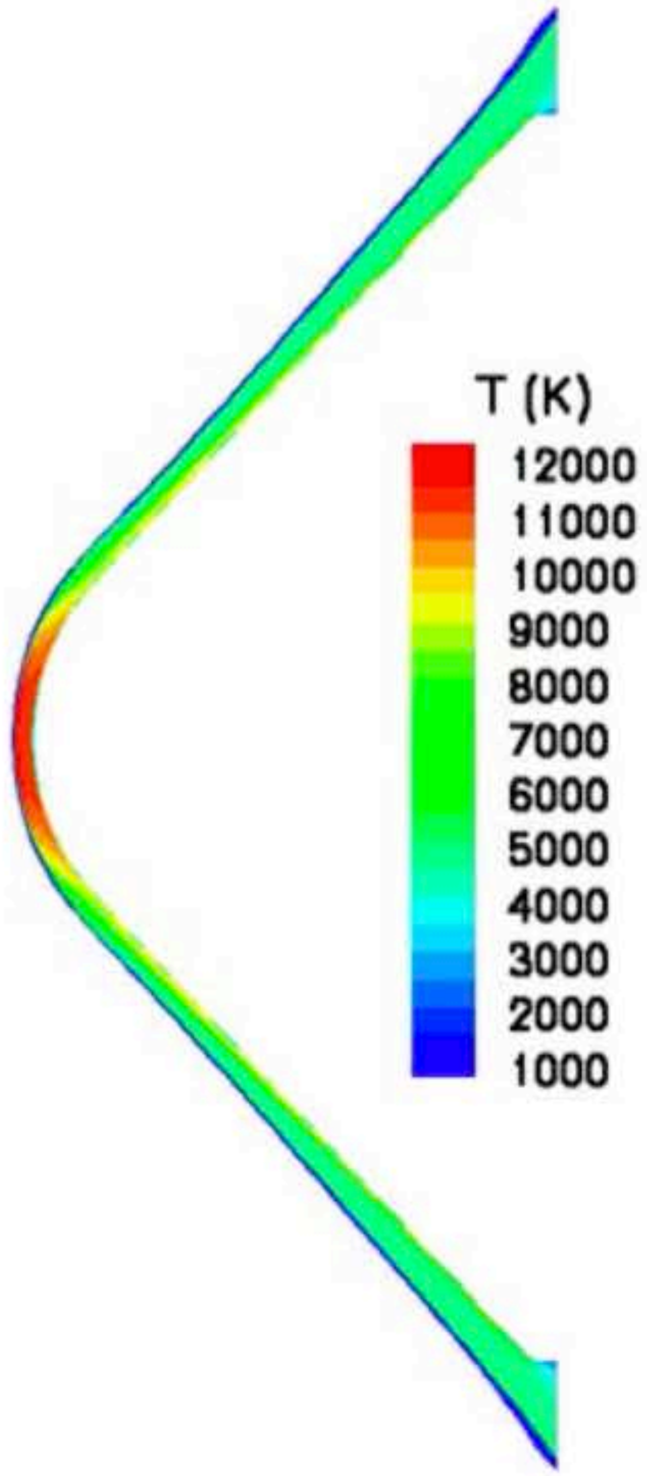

45° Sphere-Cone
Supersonic Oblique Shock
$R_{eff} = R_n$

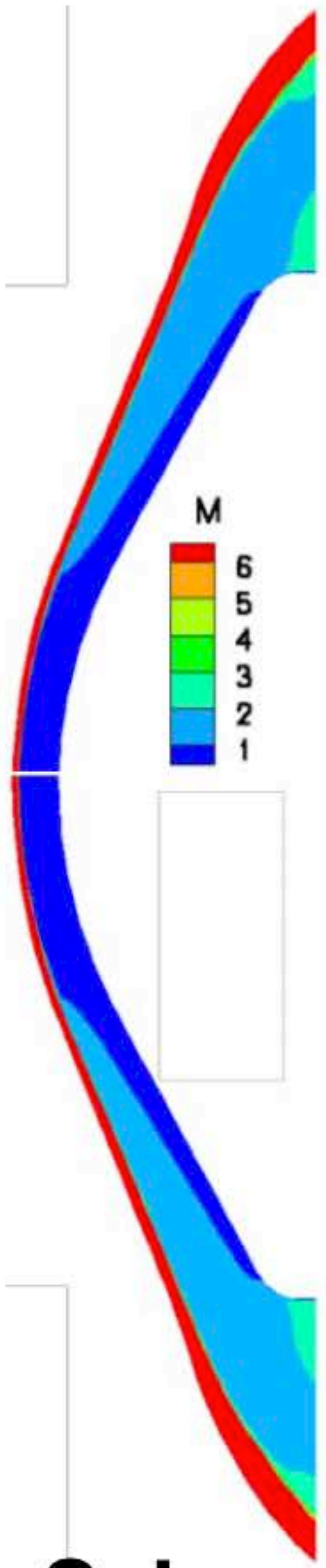

60° Sphere-Cone
Subsonic Shock
$R_{eff} > R_n$

Theory of Stag. Pt. Radiative Heat Transfer

- Theory is less intuitive, more involved
- Atoms or molecules are excited by collisions. Excited species can emit a photon that carries energy with it
- Photons are emitted isotropically, and travel effectively instantaneously
- Radiative heating is the integration of those photons that hit the surface times the energy they carry; intuitively should be proportional to the size of the radiating volume
- Partition functions for excited states imply a near exponential dependence on temperature
- Radiation is coupled to the fluid mechanics for two reasons:
  - Emitted photons carry energy out of control volume (adiabatic cooling)
  - Photons can be absorbed in the boundary layer and heat the gas

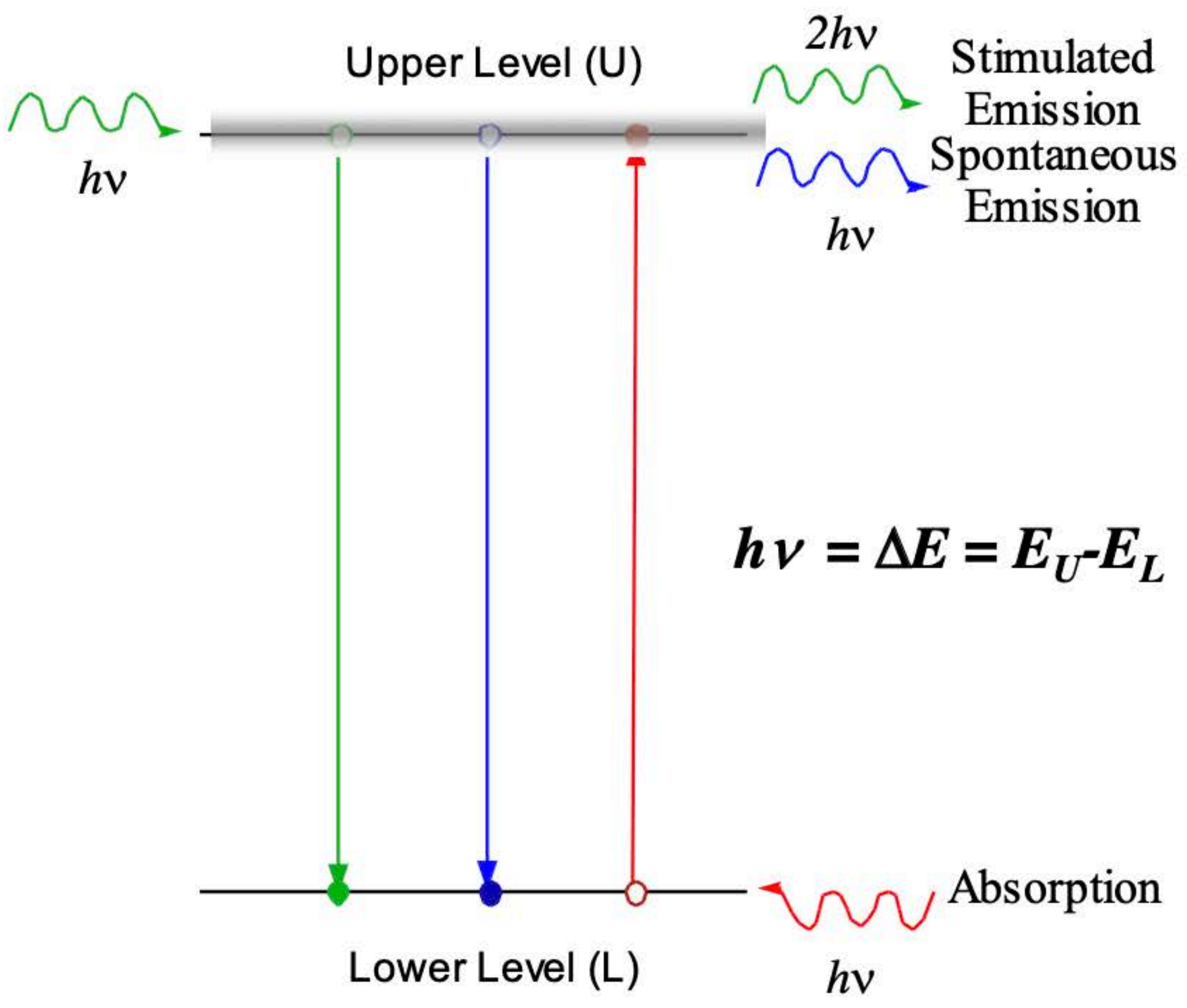

$$h\nu = \Delta E = E_U - E_L$$

$$\frac{N_i}{N} = \frac{g_i e^{-\frac{E_i}{kT}}}{\sum_j g_j e^{-\frac{E_j}{kT}}} = \frac{g_i e^{-\frac{E_i}{kT}}}{Q}$$

LTE-Plasma

Relative Importance of Radiation vs Convection

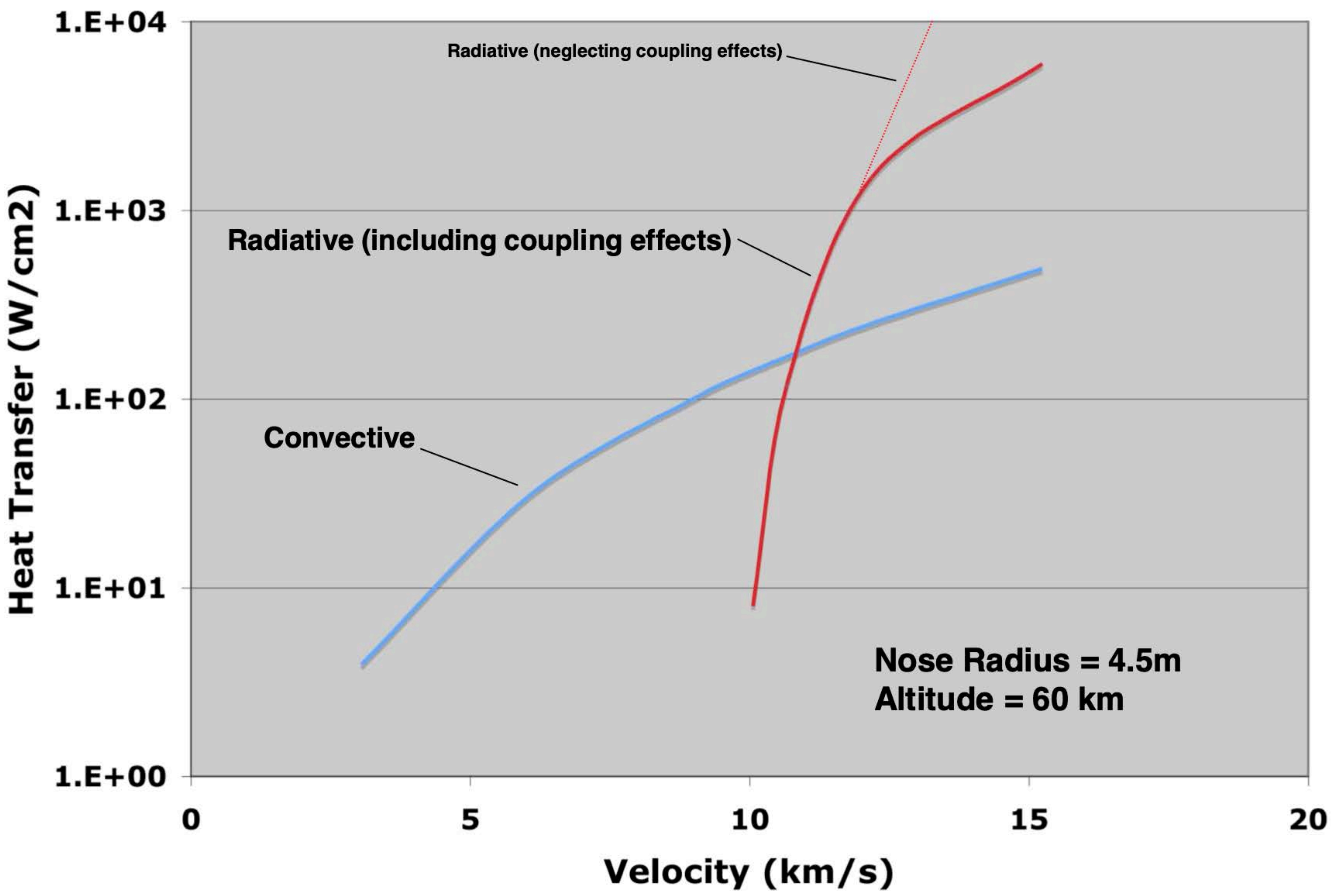

Adapted from Anderson, Hypersonic and High Temperature Gas Dynamics, Fig. 18.10

Theory of Stag. Pt. Radiative Heat Transfer

Martin:

$$q_r \sim r_n^{1.0} \rho_\infty^{1.6} V_\infty^{8.5}$$

- Earth

Direct dependence on R_n agrees with intuitive argument about radiating volume

Tauber-Sutton:

$$\boxed{q_r = C_i r_n^a \rho_\infty^m f_i \left(V_\infty \right)}$$

Earth : a ~ 1, m ~ 1.2
Mars: a = 0.526, m ~ 1.2

f_i are tabulated, near exponential at moderate velocity

- based on tabulated data, equilibrium shock theory

Theory is less intuitive, more involved. Typically relies on table lookups and has limited range of validity

Fortunately, radiation is not a major issue for many problems of interest: Mars (moderate velocity), LEO return, Titan

Importance of Radiative Cooling

- The shock layer is cooled by the emission of photons. Clearly this effect will become more important as a larger fraction of the total shock layer energy is converted to photons
- Tabular or engineering expressions for stagnation point radiation typically ***include*** the radiative cooling effect
- However it is very important to recognize this phenomenon when computing radiation from CFD data (inherently uncoupled operation)
- Goulard proposed a non-dimensional parameter that is essentially the ratio of total energy flux to that lost to radiation:

$$\Gamma = \frac{2q_{R,unc}}{\frac{1}{2}\rho V^3}$$

- The net radiative heating can then be computed from (Tauber-Wakefield):

$$q_{R,coup} = \frac{q_{R,unc}}{\left(1 + \kappa\Gamma^{0.7}\right)}$$

- Where κ is an atmosphere-specific constant
  - κ = 2 for Titan
  - κ = 3.45 for Earth
  - κ ~ 3 for Mars/Venus

Example - Galileo Probe

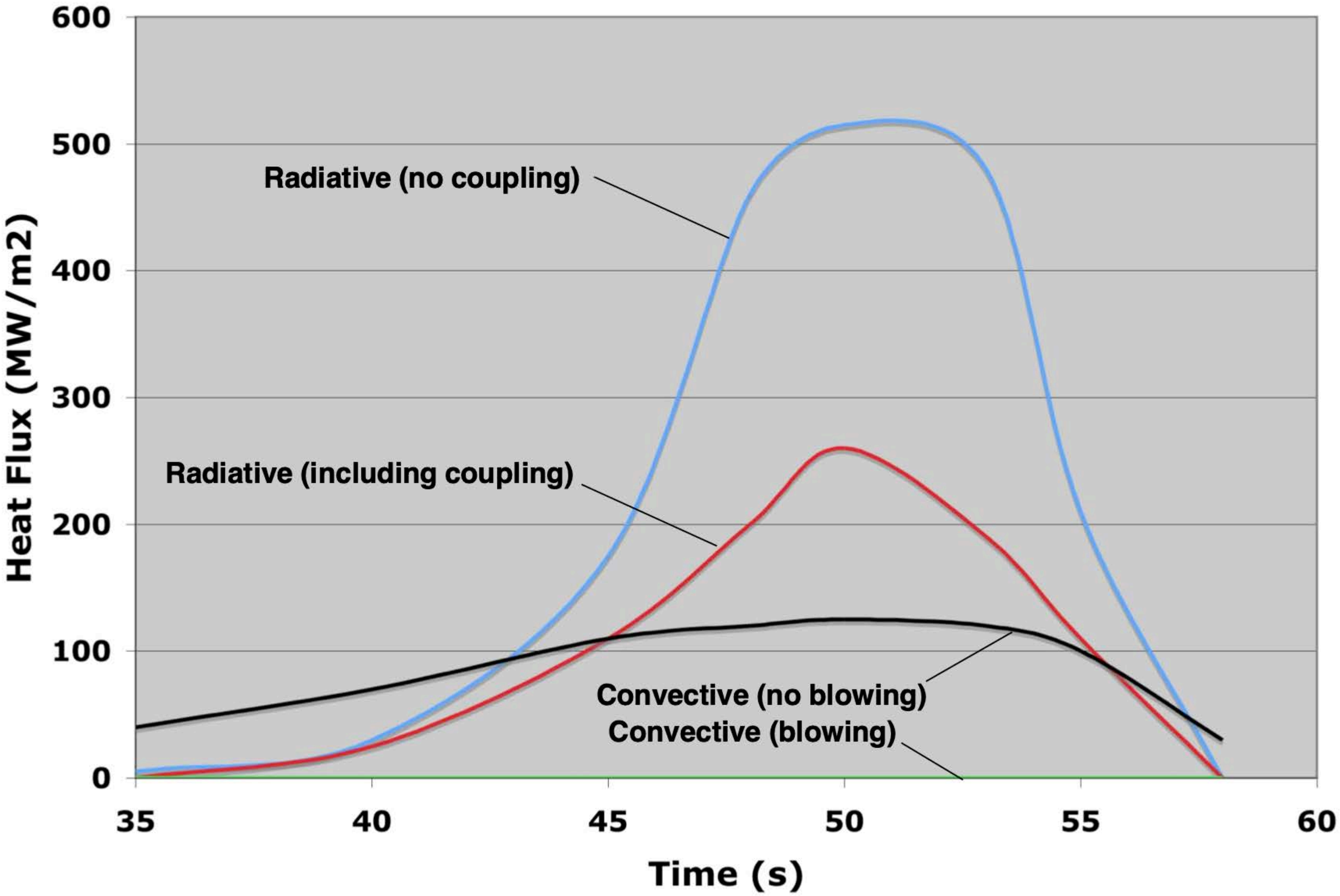

Adapted from Anderson, Hypersonic and High Temperature Gas Dynamics, Fig. 18.16

Wall Temperature Estimation

- **How hot does the TPS surface get?**
- **A body radiates heat at a rate proportional to the 4th power of its temperature**
- **Stefan-Boltzmann Law:** $q_{rerad} = \varepsilon \sigma T^4$
  - where ε is the emissivity of the TPS (ε = 1 for a blackbody), σ is the Stefan-Boltzmann constant (σ = 5.67e-8 W/m^2/K^4), and T is the wall temperature (assumes the ambient temperature is much lower)
- **The wall heat flux balance is in general given by the sum of heat into the material minus reradiation, conduction, and material response. A primary function of TPS is to minimize conduction (good insulator), and thus, neglecting material response we can assume that:**

$$q_{rerad} \sim q_{conv} + q_R$$

which can readily be solved for Tw.

- **Examples:**
  - Orbiter peak heating (Tw = 1600 K)
  - MER peak heating (Tw = 1725 K)
  - Orion peak heating (Tw = 3360 K)
    - – by this point we are overpredicting by ~20% due to material response effects

Engineering Methods

- Tauber, M., “A Review of High-Speed, Convective Heat Transfer Computation Methods,” NASA TP-2914, Jul. 1989.
- Tauber, M., Bowles, J., and Yang, L., “Use of Atmospheric Braking During Mars Missions,” *Journal of Spacecraft and Rockets*, Sept.-Oct. 1990, pp. 514-521.
- Tauber, M., Yang, L. and Paterson, J., “Flat Surface Heat-Transfer Correlations for Martian Entry,” *Journal of Spacecraft and Rockets*, March-April 1993, pp.164-169.
- Compton, D. L. and Cooper, D. M., “Free-Flight Measurements of Stagnation Point Convective Heat Transfer at Velocities to 41,000 ft/sec,” NASA TN D-2871, Jun. 1965.
- Marvin, J. G. and Deiwert, G. S., ”Convective Heat Transfer in Planetary Atmospheres,” NASA TR R-224, Jul. 1965.
- Kaattari, G. E., “Effects of Mass Addition on Blunt Body Boundary Layer Transition and Heat Transfer”, NASA TP-1139, 1978.
- Tauber, M. E. and Sutton, K., “Stagnation Point Radiative Heating Relations for Earth and Mars Entries”, Journal of Spacecraft and Rockets, Jan.-Feb. 1991, pp. 40-42.
- Page, W. A. and Woodward, H. T., “Radiative and Convective Heating during Venus Entry”, AIAA Journal, Oct. 1972, pp.1379-1381.
- Tauber, M. E., “Some Simple Scaling Relations for Heating of Ballistic Entry Bodies”, Journal of Spacecraft and Rockets, July 1970, pp. 885-886.
- Chapman, G.T., “Theoretical Laminar Convective Heat Transfer & Boundary Layer Characteristics on Cones at Speeds to 24 km/s,” NASA TN D-2463, 1964
- Sutton, K. and Graves, R.A., “A General Stagnation Point Convective Heating Equation for Arbitrary Gas Mixtures,” NASA TR- R-376, 1971
- Fay, J.A, and Riddell, F.R, “Theory of Stagnation Point Heat Transfer in Dissociated Air,” *J. Aeronautical Sciences*, **25**, 1958, pp. 73-85,121.

Distributed Heating on a Sphere

- It can be shown that the heat transfer rate along the body varies according to

$$\frac{q}{q_{stag}} \approx \cos\theta$$

for angles as large as 45° (in theory) and 70° (in practice)

- This expression permits us to integrate the total heat flux into a spherical nose as

$$\int q dA = q_{stag} \int \cos\theta dA$$

$$dA = 2\pi y R_n d\theta = 2\pi R_n^2 \sin\theta d\theta$$

$$\int q dA = 2\pi R_n^2 q_{stag} \int_0^{\pi/2} \sin\theta \cos\theta d\theta = \pi R_n^2 q_{stag}$$

- For a laminar boundary layer, the heat input to a hemisphere is ~ equal to the product of stag. point heating times the projected area

Distributed Heating on a Sphere (2)

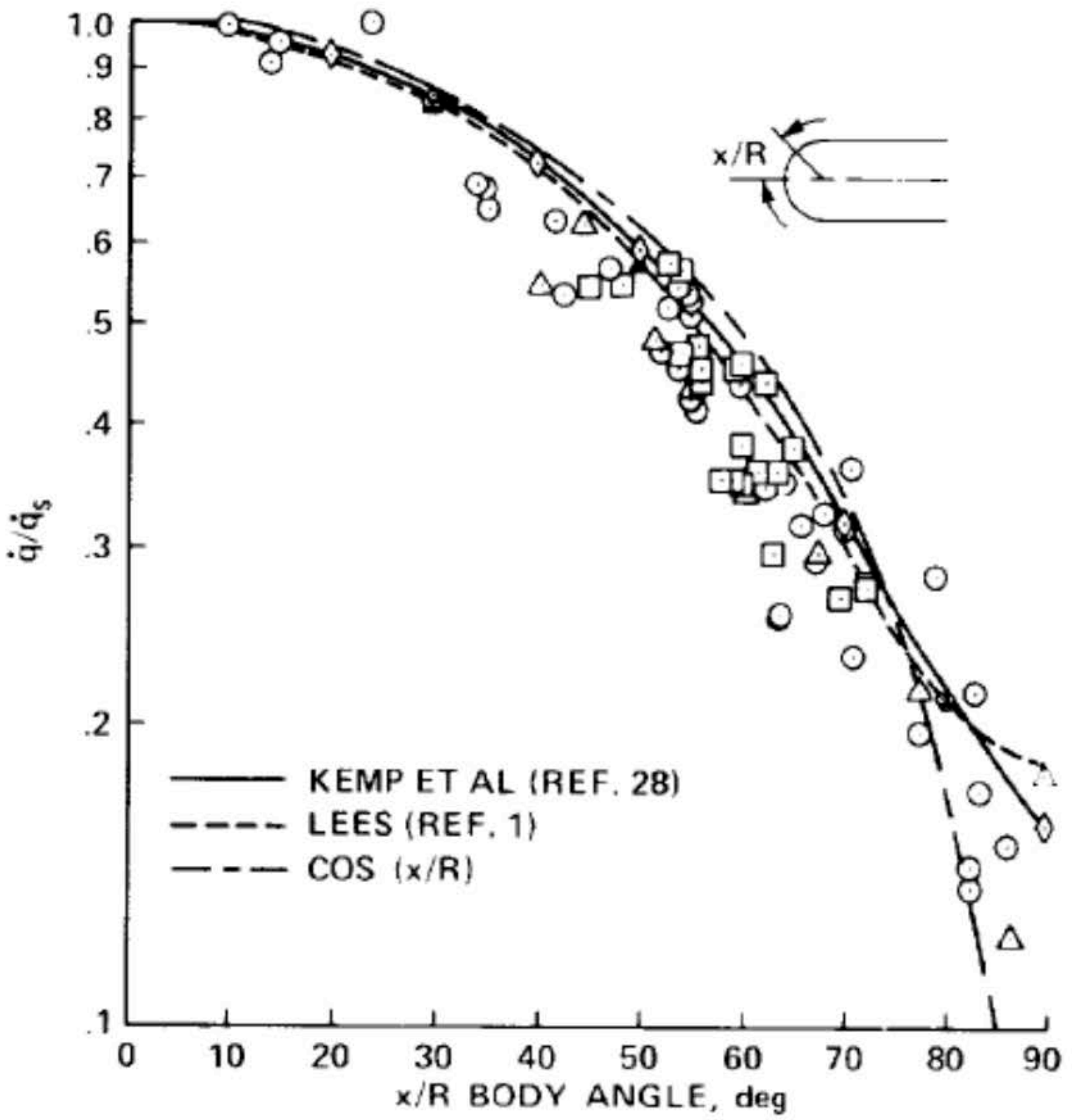

Figure 5.– Heat-transfer distribution on hemisphere cylinder. (From ref. 28; reprinted with permission of The American Institute of Aeronautics and Astronautics.)

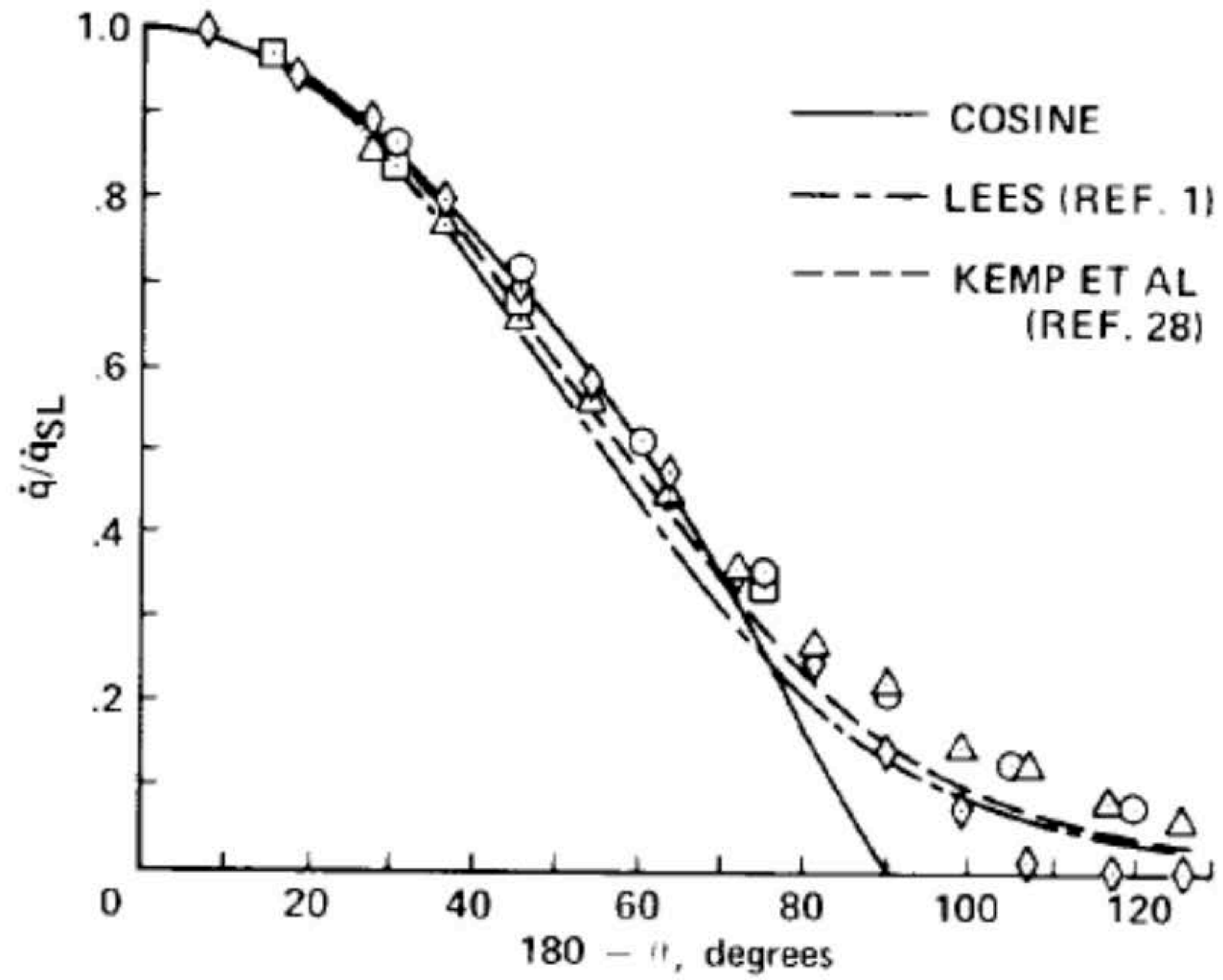

Figure 6.– Comparison of predicted and measured heat flux distributions on a circular cylinder normal to a stream.

Local Similarity – Flat-Faced Cylinder

- **Local similarity methods (see e.g. Anderson) can be extended to other geometries**
- **Take for example a flat-faced cylinder with a rounded corner**
- **For this case, local similarity theory (and more sophisticated methods) show that the stagnation point is not the highest heating location; rather heating is higher on the corner**
  - Physically, the large favorable pressure gradient causes the boundary layer to thin. This increases the magnitude of ∇h, which increases heat transfer per previous arguments. The magnitude of increase is inversely related to the radius of curvature.

Distributed Heating - Flat-Faced Cylinder

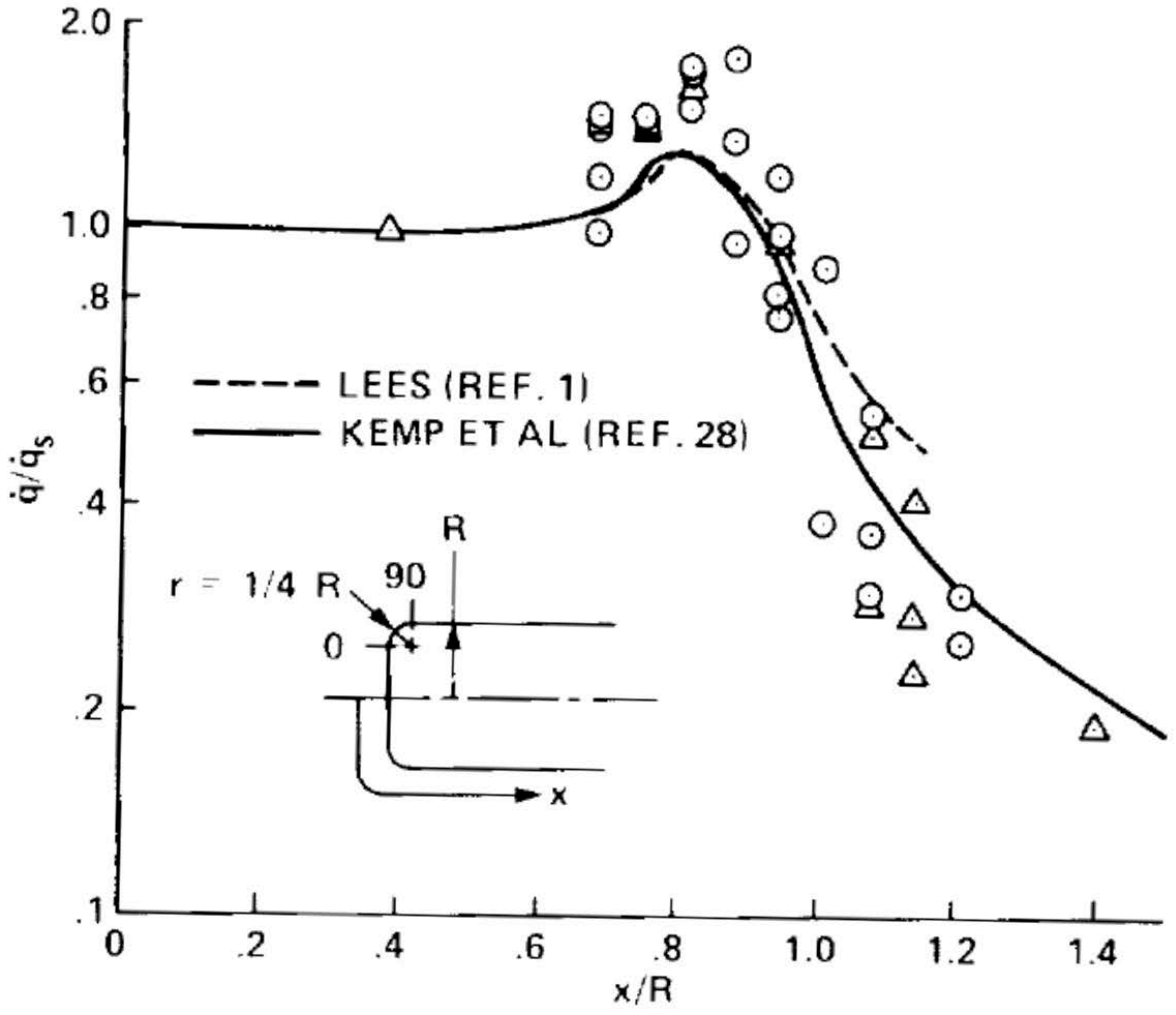

Figure 7.– Heat-transfer distribution on flat-nosed body. (From ref. 28; reprinted with permission of The American Institute of Aeronautics and Astronautics.)

Distributed Heating – Approximate Methods

- **Many other approximate methods have been developed for the calculation of heating on other geometries, e.g. wings, attachment lines.**
- **Detailed assessment is beyond the scope of these lectures, but the interested student can read further in:**

Tauber, M.E., "A Review of High Speed Convective Heat Transfer Computation Methods," NASA TP 2914, 1989

Trajectory Effects

- The discussion up to now has focused on the calculation of an instantaneous heat flux (primarily at the stagnation point).
- However, the heating on the vehicle is obviously coupled to the trajectory flown, and thus it is important to develop expressions that quantify the relationship between heating and trajectory.
- You have already learned two basic trajectory equations (Allen-Eggers and Equilibrium Glide); lets start with Allen-Eggers
- For simplicity, lets use the simplest of convective heating relationships:

$$q_s \sim (\rho)^{\frac{1}{2}} V^3$$

Intuition Check 1

Two identical ballistic vehicles enter the atmosphere. One is on a steep entry trajectory and one is on a shallow entry trajectory. Which has the higher peak heat flux? Load?

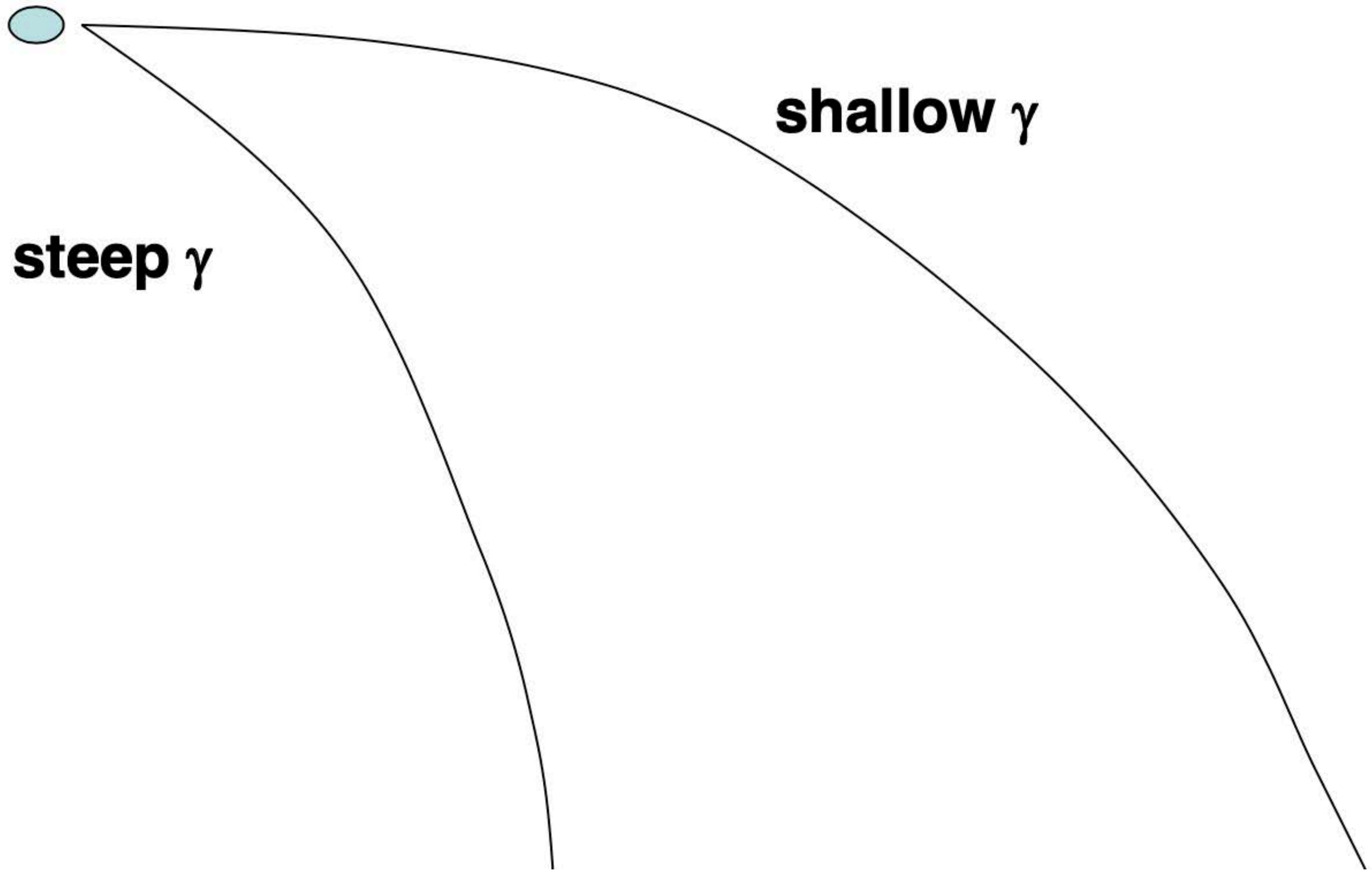

Intuition Check 2

Two ballistic vehicles enter the atmosphere on an identical flight path angle. One has a higher ballistic coefficient. Which has the higher peak heat flux? Load?

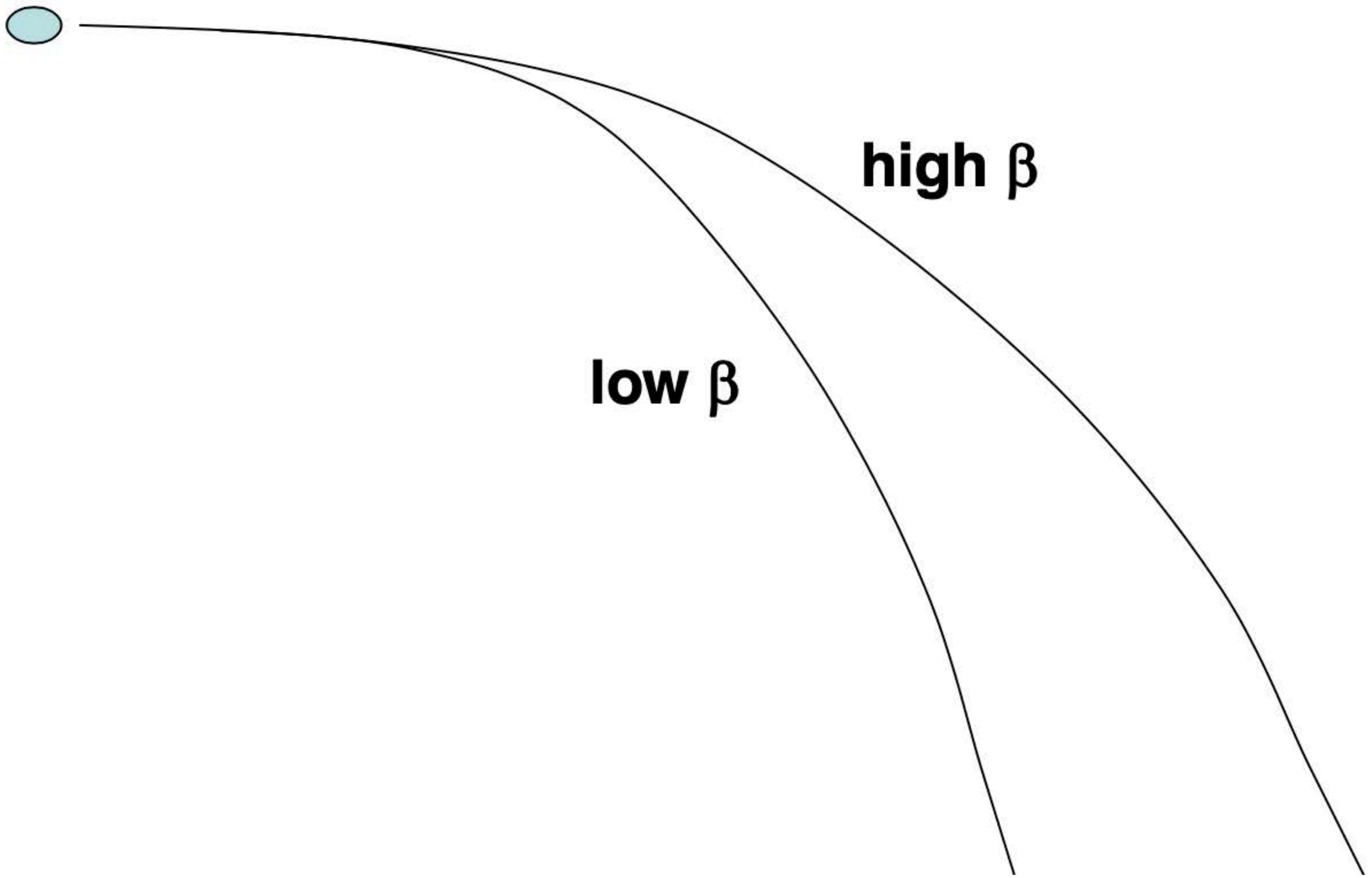

Allen-Eggers Trajectory Equation

$$V = V_{atm}\exp\left[Ce^{-h/H}\right] = V_{atm}\exp\left[C\frac{\rho}{\rho_o}\right]$$

$$C = \frac{H\rho_0}{2\beta\sin\gamma}$$

V_{atm} = Velocity at atmospheric interface
$\beta = m/C_D A$
Exponential atmosphere assumed
Ballistic entry

- Substitute above for V into approximate heating equation:

$$q_s \sim (\rho)^{\frac{1}{2}}\left(V_{atm}^3\exp\left[3C\frac{\rho}{\rho_o}\right]\right)$$

- Differentiate w.r.t density:

$$\tfrac{1}{2}(\rho)^{-\frac{1}{2}}\left(V_{atm}^3\exp\left[3C\frac{\rho}{\rho_o}\right]\right) + (\rho)^{\frac{1}{2}}\left(\frac{3C}{\rho_o}\right)\left(V_{atm}^3\exp\left[3C\frac{\rho}{\rho_o}\right]\right) = \frac{dq_s}{d\rho}$$

Allen-Eggers Trajectory Equation (2)

- Looking for a maximum of q_s, which should occur when $dq_s/q\rho = 0$:

$$1 + 6C\frac{\rho}{\rho_o} = 0$$

- So the density of maximum convective heating is:

$$\boxed{\rho^*_{q\,\max} = -\frac{\rho_o}{6C} = \frac{\beta \sin\gamma}{3H}}$$

- For a given atmospheric scale height, the density (altitude) of peak heating increases with ballistic coefficient and flight path angle

Allen-Eggers Trajectory Equation (3)

- So, in the exponential atmospheric model

$$\frac{\beta \sin\gamma}{3H} = \rho_o e^{-h^*/H}$$

$$-\frac{h^*}{H} = \ln\left(\frac{\beta \sin\gamma}{3H\rho_o}\right)$$

- The altitude and velocity of peak heating are given by:

$$\boxed{h^*_{q\max} = -H \ln\left(\frac{\beta \sin\gamma}{3H\rho_o}\right)}$$

$$\boxed{V^*_{q\max} = V_{atm} \exp\left[\frac{C}{\rho_o}\left(\frac{-\rho_o}{6C}\right)\right] = V_{atm} e^{-1/6} = 0.846 V_{atm}}$$

Allen-Eggers Trajectory Equation (4)

- As in the case of the previously derived expression for the velocity at peak deceleration, the velocity at peak heating is a function only of the entry velocity.
- Recall that $V_{gmax} = 0.606V_{atm}$. Therefore, peak heating occurs earlier in the entry than peak deceleration. In fact, it can be shown that

$$h^*_{q\max} \approx 1.1 h^*_{g\max}$$

- We are now in the position of being able to calculate the peak stagnation point convective heat rate for a ballistic entry vehicle
- Substitute the evaluated expressions for V_{qmax} and ρ_{qmax} into the Sutton-Graves Equation:

$$q_{s,\max} = k\left(\frac{1}{R_n}\right)^{\frac{1}{2}}\left(\frac{\beta\sin\gamma}{3H}\right)^{\frac{1}{2}}\left(.6055V_{atm}^3\right)$$

- In addition to the nose radius dependence shown earlier, we now see that peak heating rate increases with increasing ballistic coefficient and flight path angle

Heat Load

- Stagnation point heat load is just the time integration of the heat flux

$$Q_s = \frac{k}{\sqrt{R_n}} \int \rho^{\frac{1}{2}} V^3 dt$$

- How do we convert this to an integral that we now how to evaluate (redefine *dt* through change of variables)? Lets borrow some logic from the Equations of Motion:

$$\sin\gamma = -\frac{dh}{ds} \; ; \qquad V = \frac{ds}{dt}$$

$$dt = \frac{ds}{V} = -\frac{dh}{V\sin\gamma}$$

- Using the exponential atmosphere model we can write this in terms of dρ

Heat Load (2)

- Exponential atmosphere model

$$\rho = \rho_o e^{-h/H}$$

- Differentiate: $$\frac{d\rho}{dh} = -\frac{\rho_o}{H} e^{-h/H} = -\frac{\rho}{H}$$

- Substitute into dt: $$dt = \frac{H d\rho}{\rho V \sin\gamma}$$

- Now we can substitute into the heat load integral:

$$Q_s = \int q_s dt = \frac{k}{\sqrt{R_n}} \frac{V_{atm}^2 H}{\sin\gamma} \int_0^{\rho_o} \rho^{-\frac{1}{2}} \exp\left[\frac{2C\rho}{\rho_0}\right] d\rho$$

$$Q_s \sim k V_{atm}^2 \left[\frac{\beta}{R_n \sin\gamma}\right]^{\frac{1}{2}}$$

After some manipulation…

Heat Rate vs. Heat Load

- Quantitative expression can be derived from approximate evaluation of the integral:

$$\boxed{Q_s \approx k V_{atm}^2 \left[\frac{\beta}{\rho_o} \left(\frac{\pi H}{R_n \sin\gamma} \right) \right]^{\frac{1}{2}}}$$

k is the Sutton-Graves constant

- Compare the derived expressions for heat rate and heat load:

$$q_{s,\max} = k \left(\frac{1}{R_n} \right)^{\frac{1}{2}} \left(\frac{\beta \sin\gamma}{3H} \right)^{\frac{1}{2}} \left(.6055 V_{atm}^3 \right) \qquad Q_s = k V_{atm}^2 \left[\frac{\beta}{\rho_o} \left(\frac{\pi H}{R_n \sin\gamma} \right) \right]^{\frac{1}{2}}$$

- Heat rate increases with both β and γ, while heat load increases with β, but decreases with γ
- This leads to a second mission design trade (the first was R_n and its impact on drag, convective heating, and radiative heating):
- The selection of γ becomes a trade between peak heat rate (TPS material selection), and total heat load (TPS thickness and mass)

Intuition Check 1

Two identical ballistic vehicles enter the atmosphere. One is on a steep entry trajectory and one is on a shallow entry trajectory. Which has the higher peak heat flux? Load?

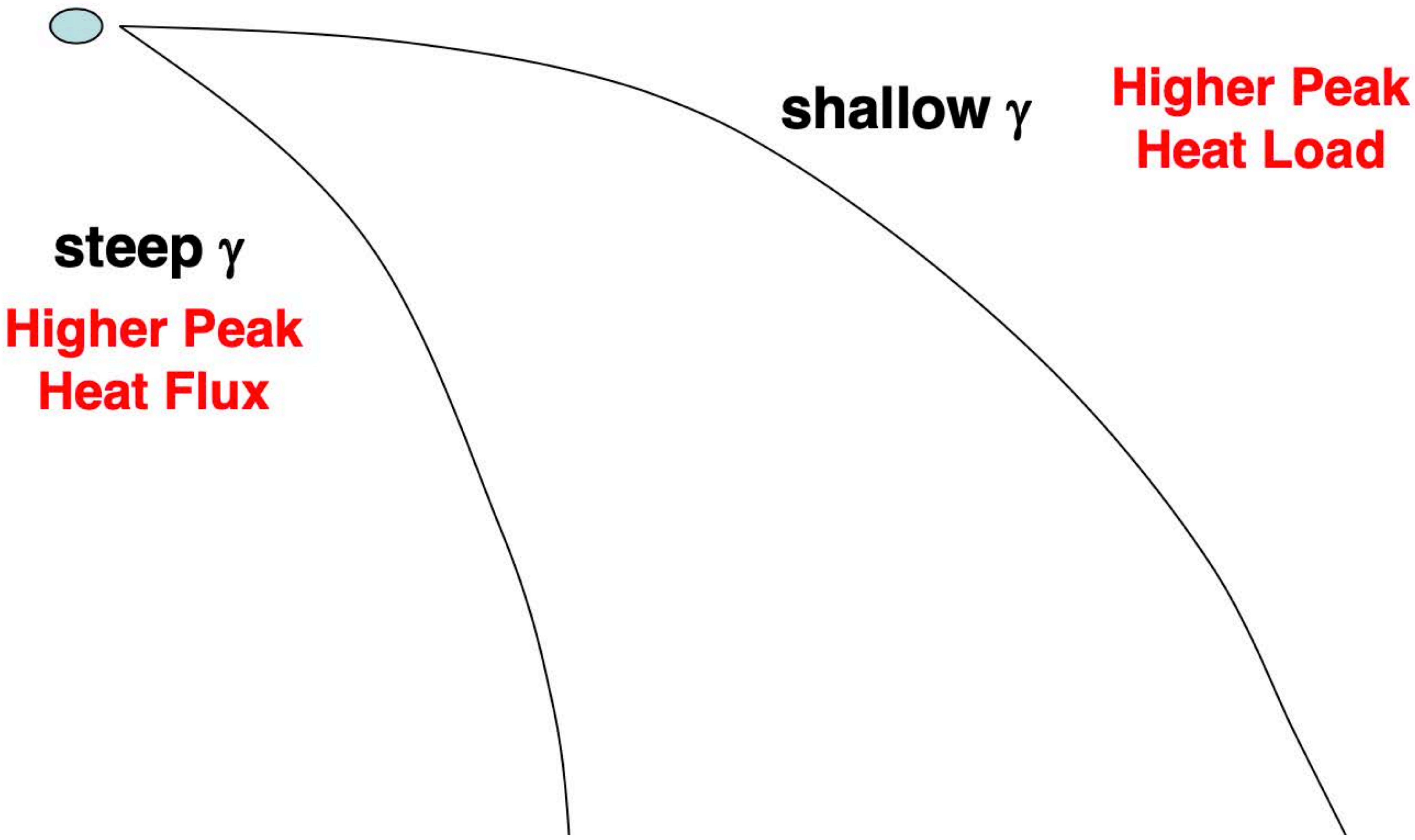

Intuition Check 2

Two ballistic vehicles enter the atmosphere on an identical flight path angle. One has a higher ballistic coefficient. Which has the higher peak heat flux? Load?

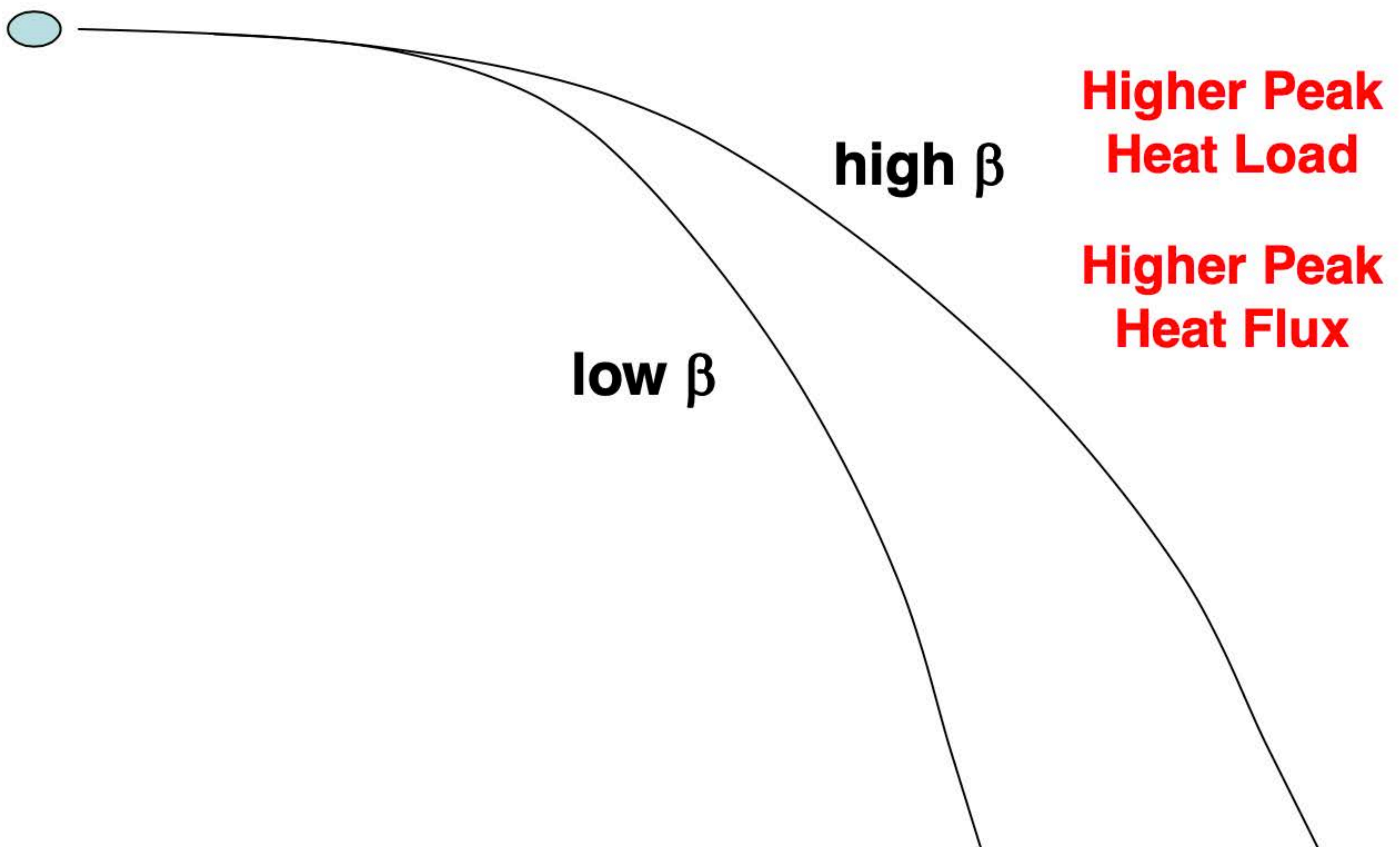

Mars Entry Heating Example

Entry Flight Path Variation

$\beta = 90\ kg/m^2$; $V_i = 5.5\ km/s$

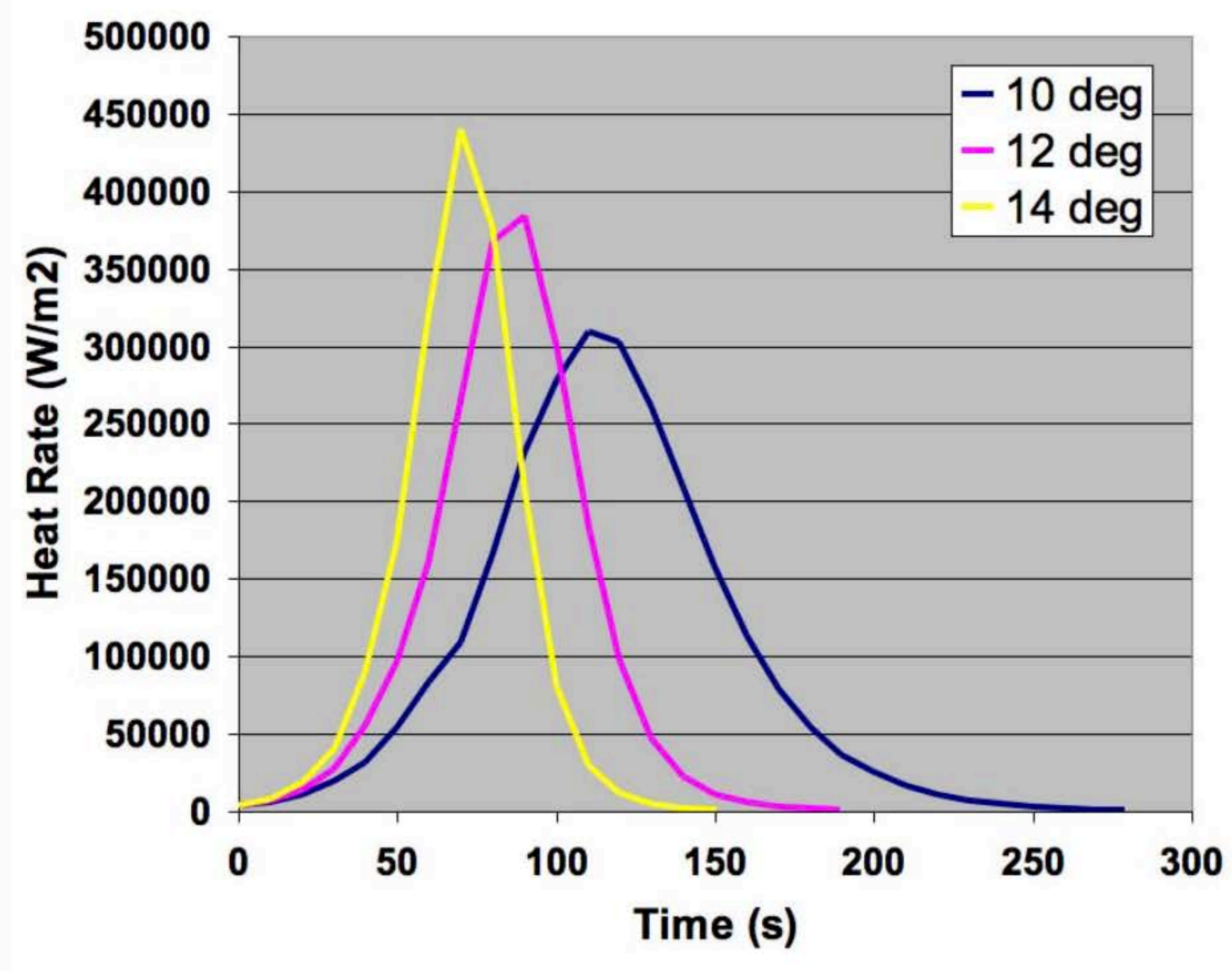

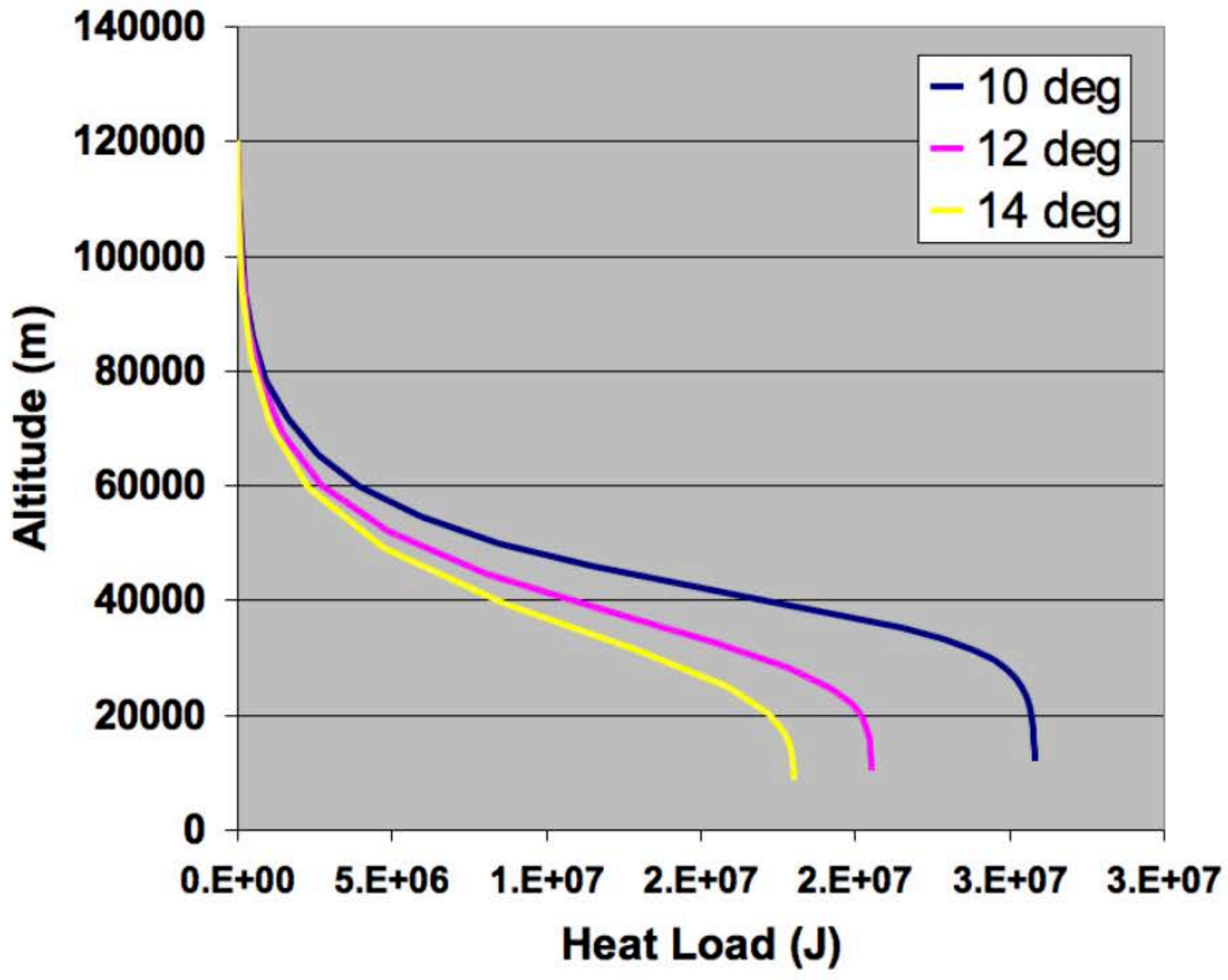

Heat rate falls and heat load grows as FPA decreases

Mars Entry Heating Example

Ballistic Coefficient Variation

γ = -12 deg; V_i = 5.5 km/s

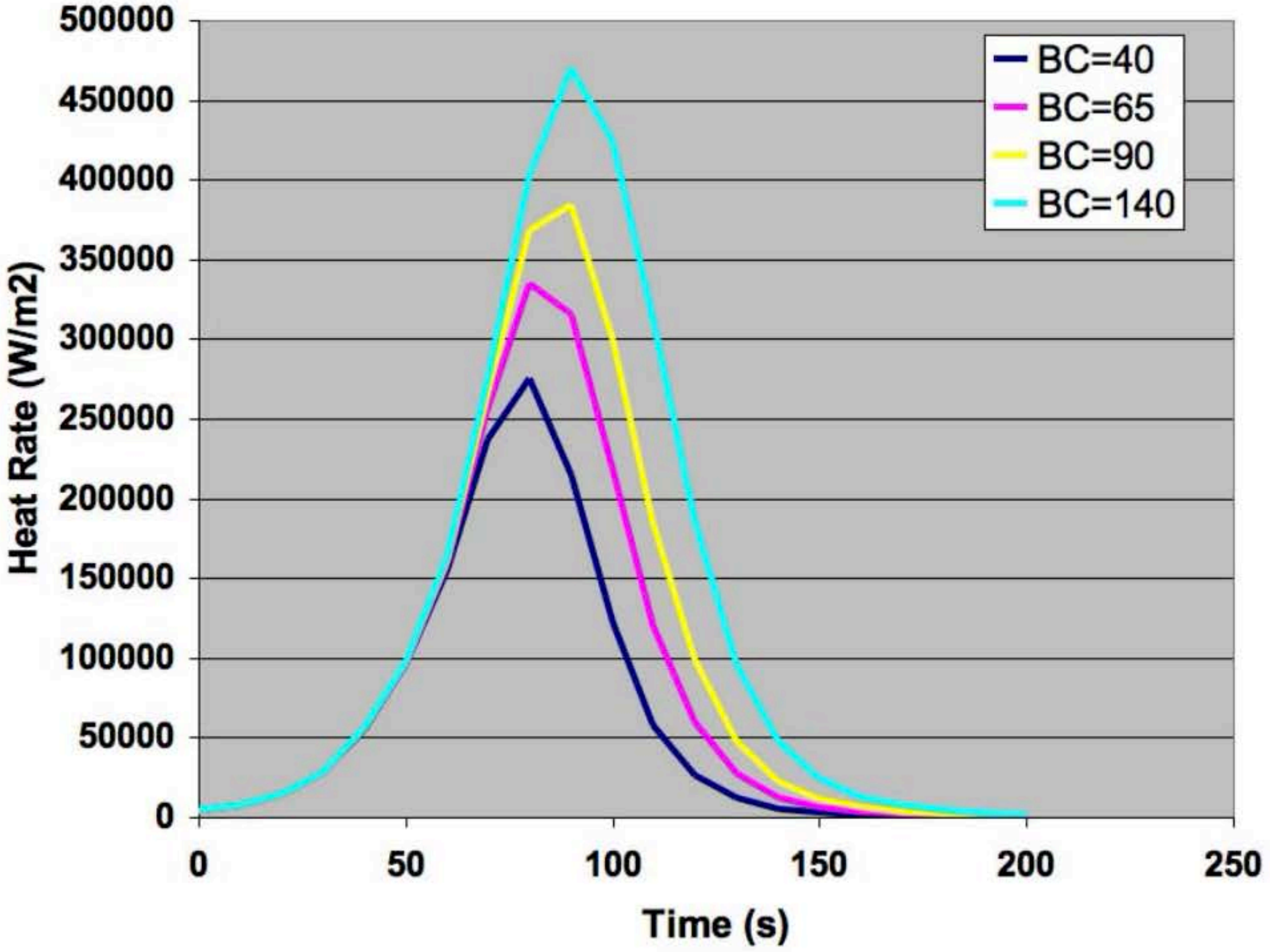

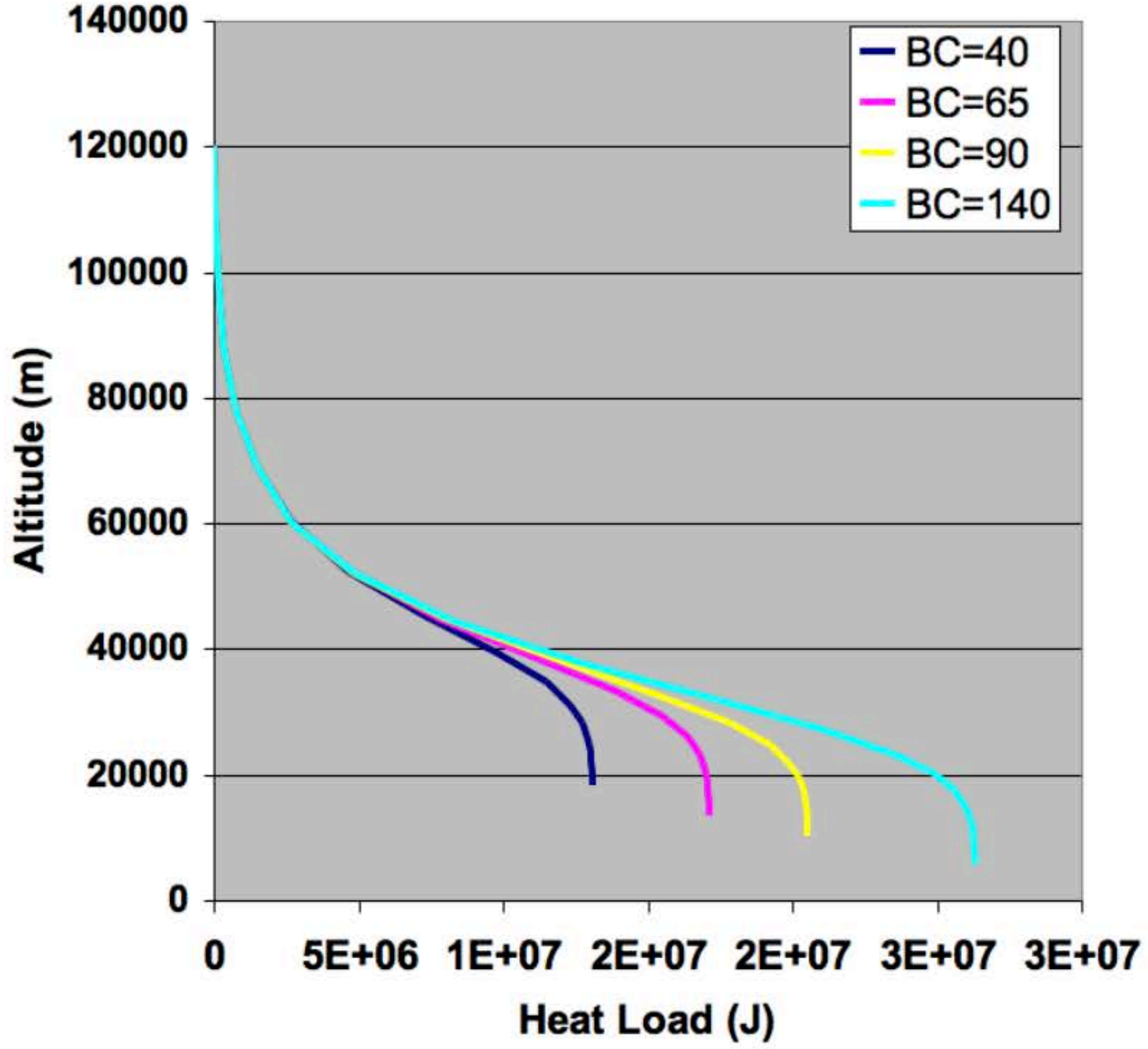

Rising ballistic coefficient raises heat rate and load

Equilibrium Glide Entry

- Can perform the same analysis of an equilibrium glide (lifting) entry
- Details are left as an exercise for the student

$$V^*_{q\,\max} = \sqrt{\tfrac{2}{3}}V_c \qquad \text{(for } V_{atm} \geq \sqrt{\tfrac{2}{3}}V_c\text{)}$$

$$q_{s\,\max} = 1.94 \times 10^4 \left[\frac{1}{R_n}\left(\frac{\beta}{L/D}\right)\right]^{\frac{1}{2}}$$

$$Q_s \approx 2.05 \times 10^7 \left[\frac{\beta}{R_n}\left(\frac{L}{D}\right)\right]^{\frac{1}{2}} \left[\sin^{-1}\left(\frac{V_{atm}}{V_c}\right) - \frac{V_{atm}}{V_c}\left(1 - \left(\frac{V_{atm}}{V_c}\right)^2\right)^{\frac{1}{2}}\right]$$

- Compare to Allen-Eggers; similar dependence on β, but a lifting body (L/D > 1) will have heat flux inversely dependent on L/D and heat load directly dependent on L/D

Numerical Example: MER

- **What is the peak stagnation point heating for the MER example previously examined ($R_n = 0.5R_b$)?**
- **At peak heating:**

  V_{qmax} = 0.846*5.45 = 4.61 km/s

  R_n = 2.65/4 = 0.6625 m

  h = 40.87 km

  ρ = 3.11e-04 kg/m^3

- **From the Allen-Eggers expressions derived herein:**

$$q_s = k\left(\frac{\rho}{R_n}\right)^{\frac{1}{2}} V^3 = 1.9027\times10^{-4}\left(\frac{3.11\times10^{-4}}{0.6625}\right)^{\frac{1}{2}}(4610)^3 = 40.4 \ \mathrm{W/cm^2}$$

$$T_w = \left(\frac{q_w}{\varepsilon\sigma}\right)^{\frac{1}{4}} = \left(\frac{40.4\times10^4}{0.8\cdot5.67\times10^{-8}}\right) = 1727K$$

(literature quoted values range from 40-44 W/cm^2 based on CFD)

Other Trajectory Effects

- **Prior discussion focused on impact of trajectory on stagnation point heating**

- **However, trajectory selection has other aerothermal impacts as well**

- **Transition to turbulence**
  - Can dramatically increase heating levels away from stagnation point (4-6 times laminar levels)
  - Governed by Reynolds number ($\rho uL/\mu$), therefore exacerbated by large entry bodies, steeper flight path angle, higher entry velocity, higher ballistic coefficient

- **Heat soak**
  - Longer trajectory time increases the amount soak of energy into the TPS, which increases the amount of TPS required to protect the structure (a given TPS tends to be less efficient as peak heat flux drops but heat load stays constant)

Orbiter Thermal Imagery

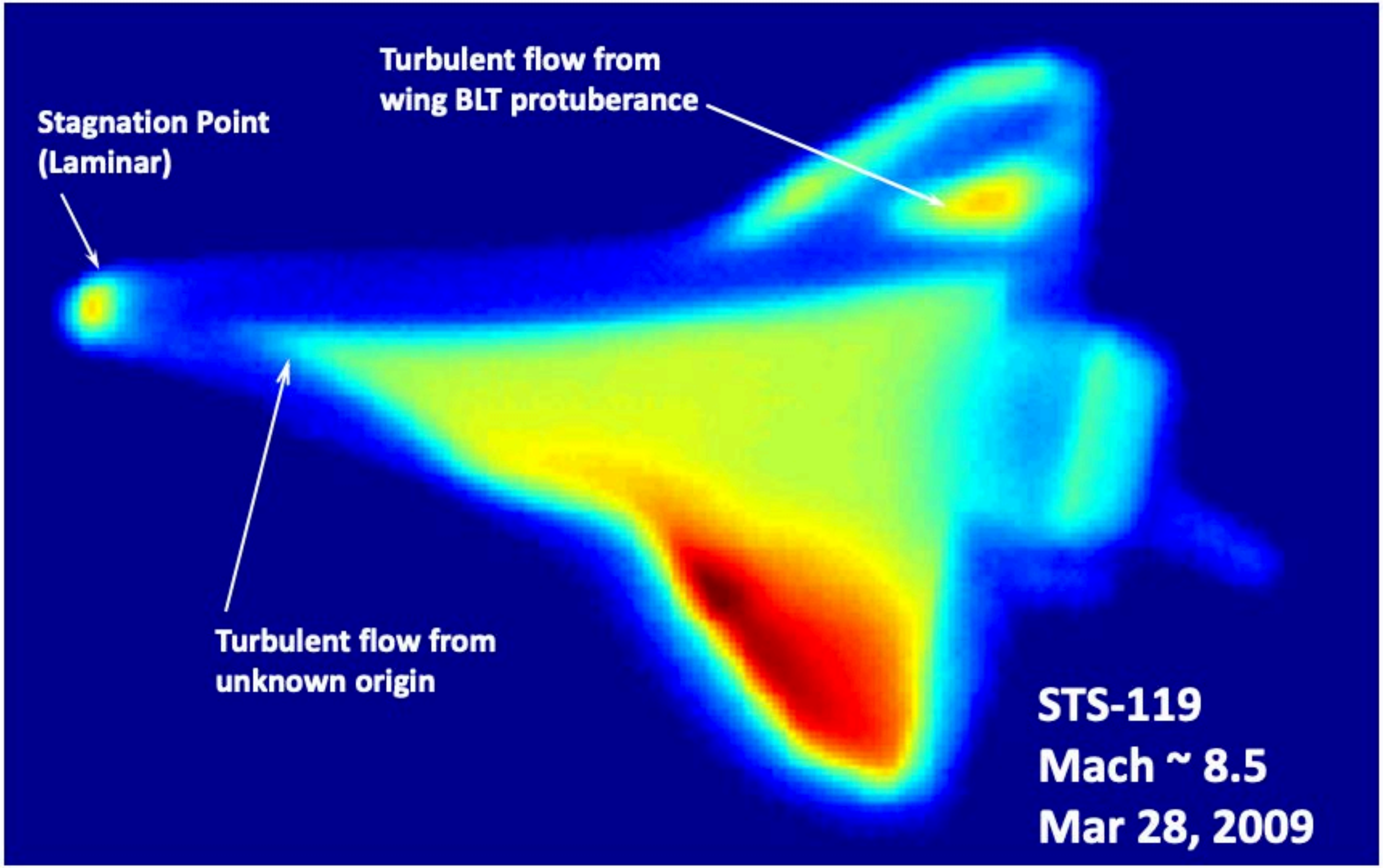

CFD Process for Entry Vehicle Design

- High fidelity CFD tools based on 20-year old methodologies
- Recent advances in parallel computing, efficient implicit algorithms have enabled rapid turnaround capability for complex geometries
- Full body three-dimensional CFD is an integral part of the design of all planetary and Earth entry TPS

Shuttle RCC Repair Concept Evaluation

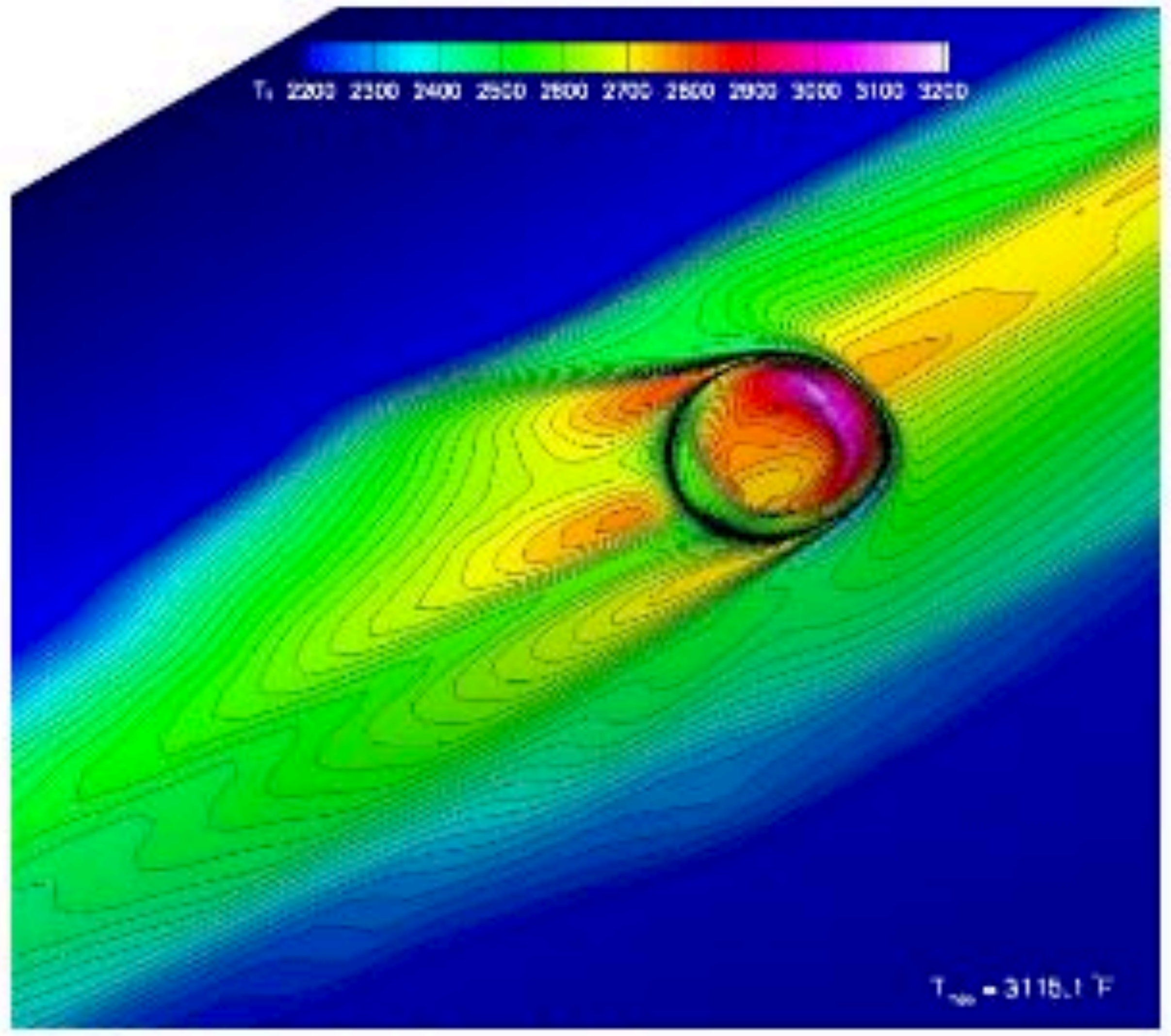

Genesis Penetration Analysis

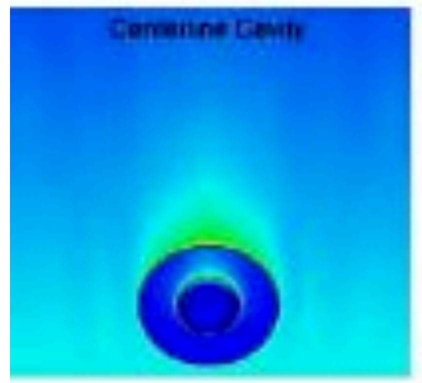

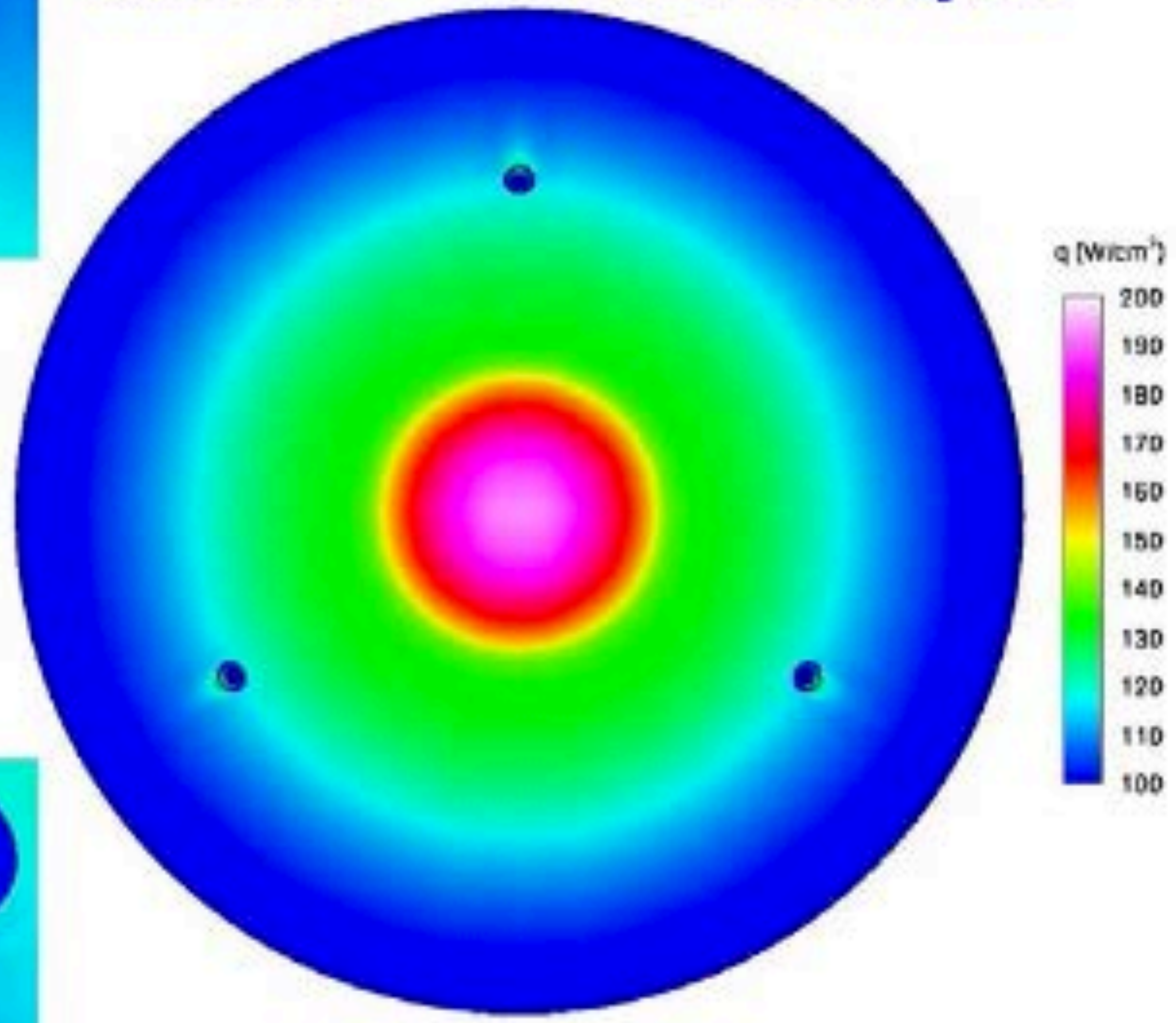

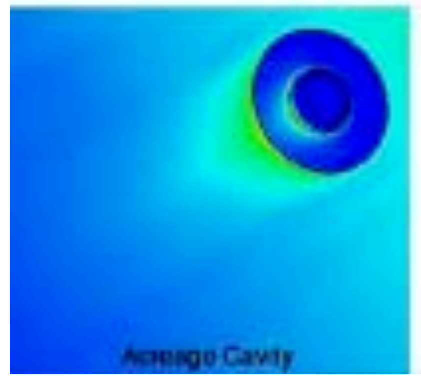

Arc Jet Model Simulation

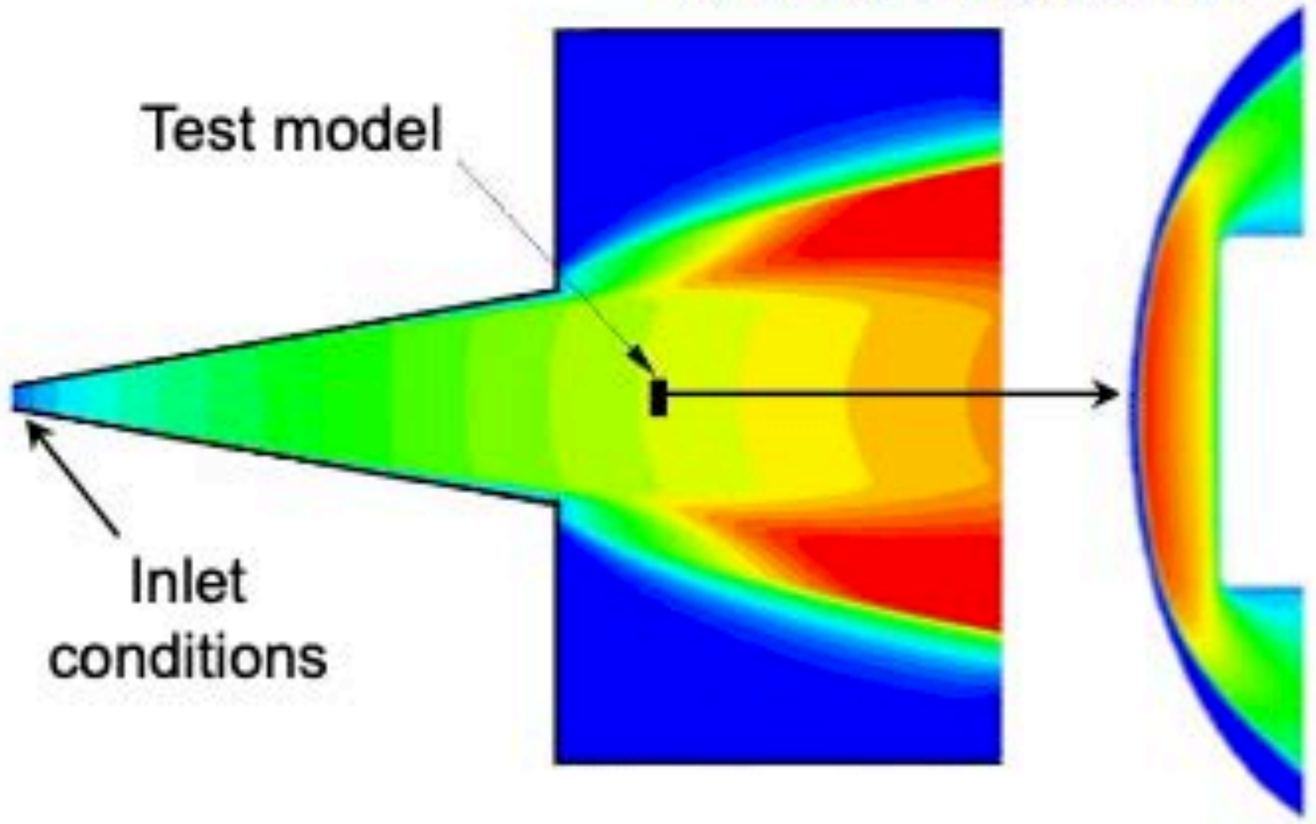

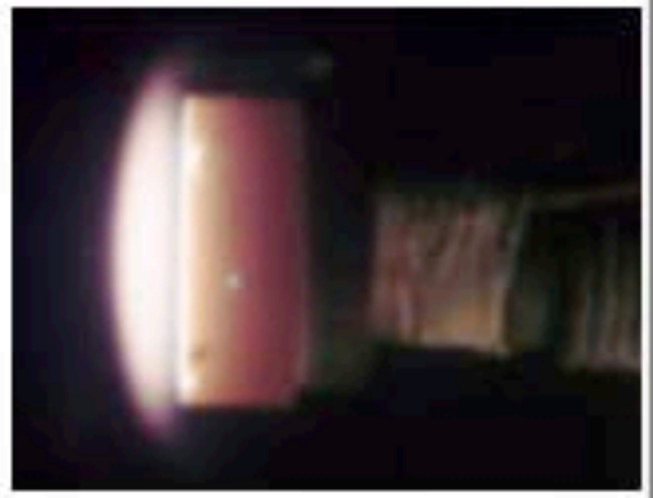

Nozzle flow CFD simulation | Model CFD simulation | Arc jet test

Aerothermal Modeling Needs for Entry

- **Needs are both physics and process driven**
  - process improvements are important for modeling complex geometries - not covered in this presentation
  - physical model improvements are important across the spectrum of NASA missions
- **Gaps are destination <u>and</u> mission specific**
  - shock layer radiation in particular will dominate aeroheating for some missions and be unimportant for others
  - sensitivity analysis must be performed for each candidate mission
- **Gaps can be divided into general categories**
  - reacting gas physical models
  - surface kinetics
  - transition and turbulence
  - afterbody heating
  - shock layer radiation modeling
  - coupling between radiation/material response/fluid dynamics/aerodynamics
  - unsteady separated flows (wakes, control surface shock-BL interaction)
  - geometry effects

Transition and Turbulence

- **Transition is less of a concern for blunt capsules**
  - shorter trajectories, smaller surface area leads to less heat load augmentation
  - single use ablative TPS can withstand heating if mass penalty not large – design to fully turbulent
- **Conclusion: Transition cannot be accurately predicted for most problems of interest. Designs must rely on testing and conservatism.**
- **Acreage turbulent heating predictions generally within 25% for orbital Earth entries (RANS), but additional developments are required for chemistry, blowing, roughness**
- **DNS, LES, DES type models under development to replace current RANS**

70º Sphere-Cone:

Hypersonic Flight in Ballistic Range

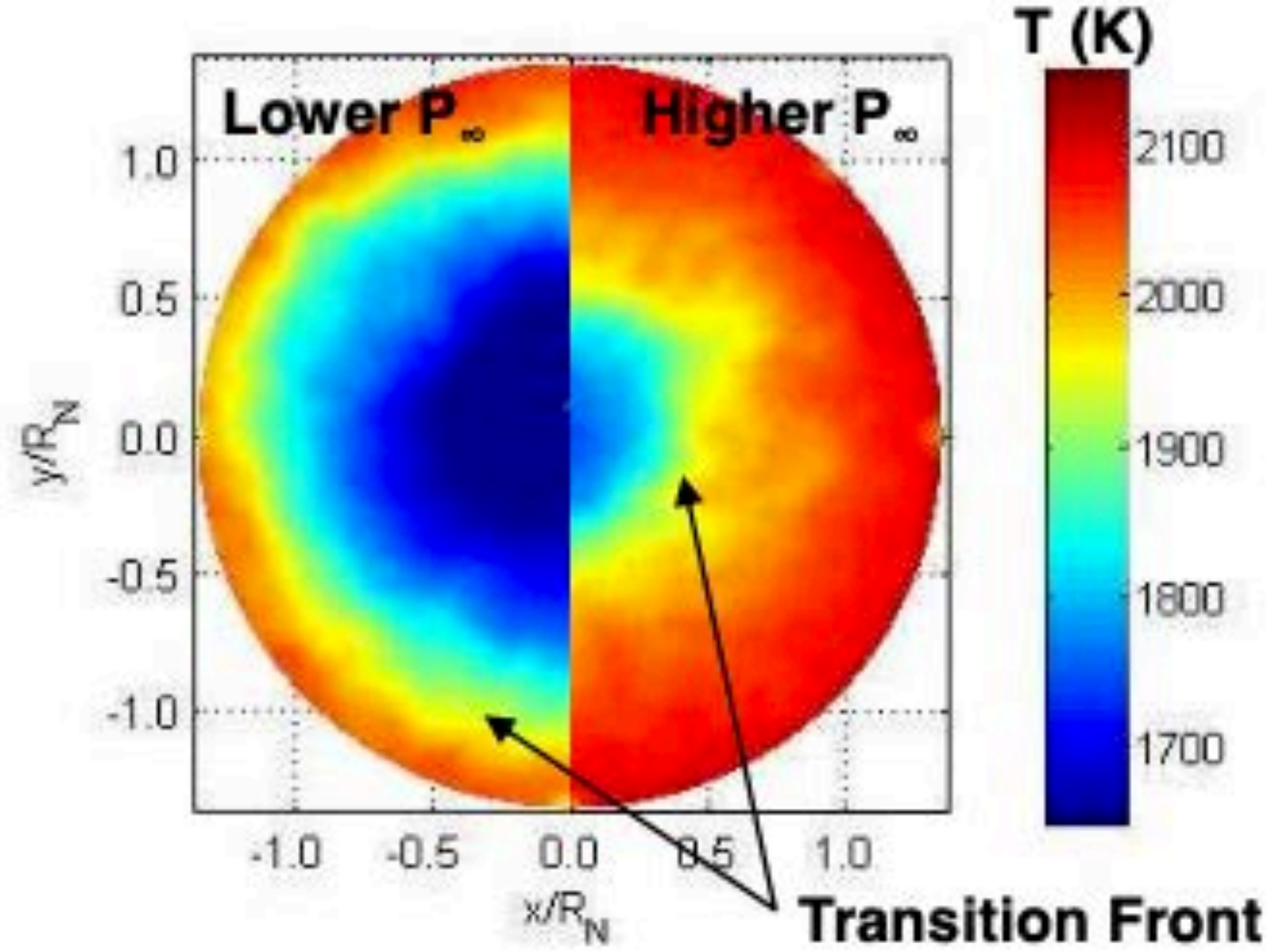

Mars Science Laboratory

Peak Heating Condition

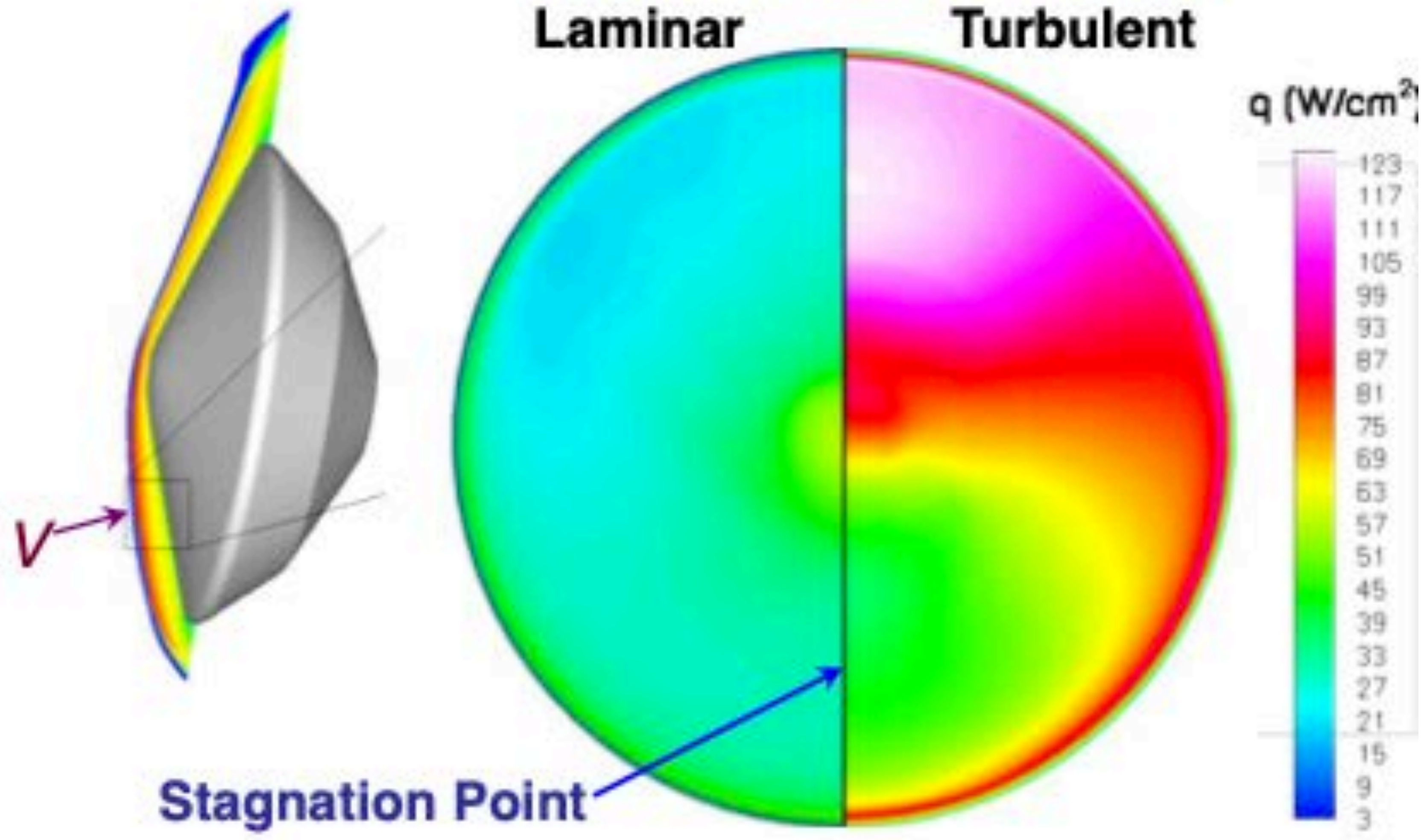

Turbulence and Surface Roughness

- ➢ **Previous discussion centered on smooth wall turbulence**
- ➢ **However, all ablators develop a roughness pattern that can augment heating**
- ➢ **Analysis for MSL based on correlations from WT experiments and DoD RV data**
  - 1mm roughness → potential for up to 50% augmentation to baseline smooth wall predictions
  - if true, roughness has eaten up entire turbulent heating uncertainty!
- ➢ **Roughness can also lead to a positive feedback loop → vortical structures are generated that augment roughness**

Effects of Roughness on Heating

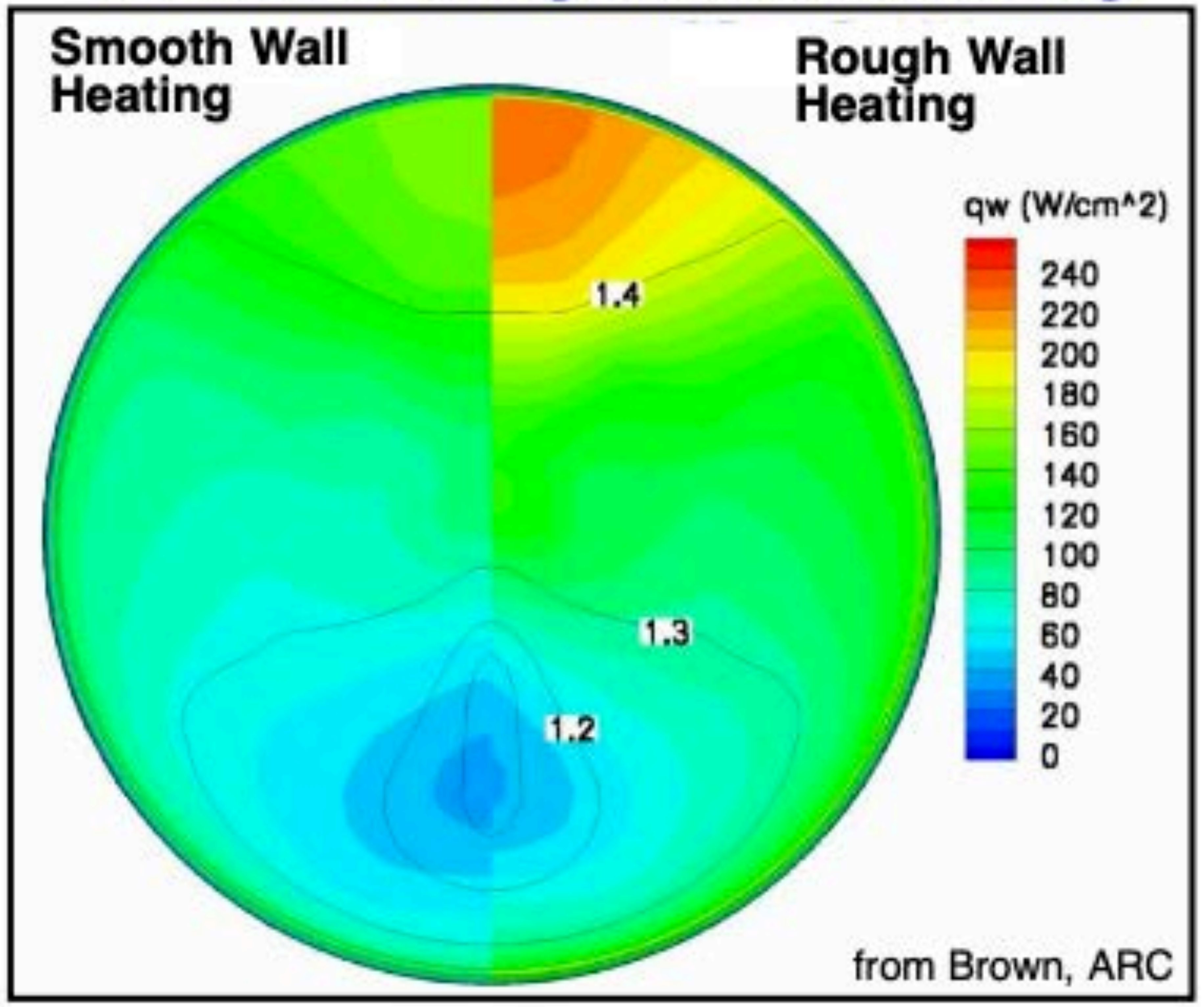

from Brown, ARC

Surface Catalysis

- **No validated model exists for Mars:**

  $CO + O$; $O + O$; $CO + O_2$
- **As a consequence, Mars entry vehicles are designed assuming a worst case scenario**
  - so called “supercatalytic” wall
- **For MSL there is a factor of four difference in heating between the various models**

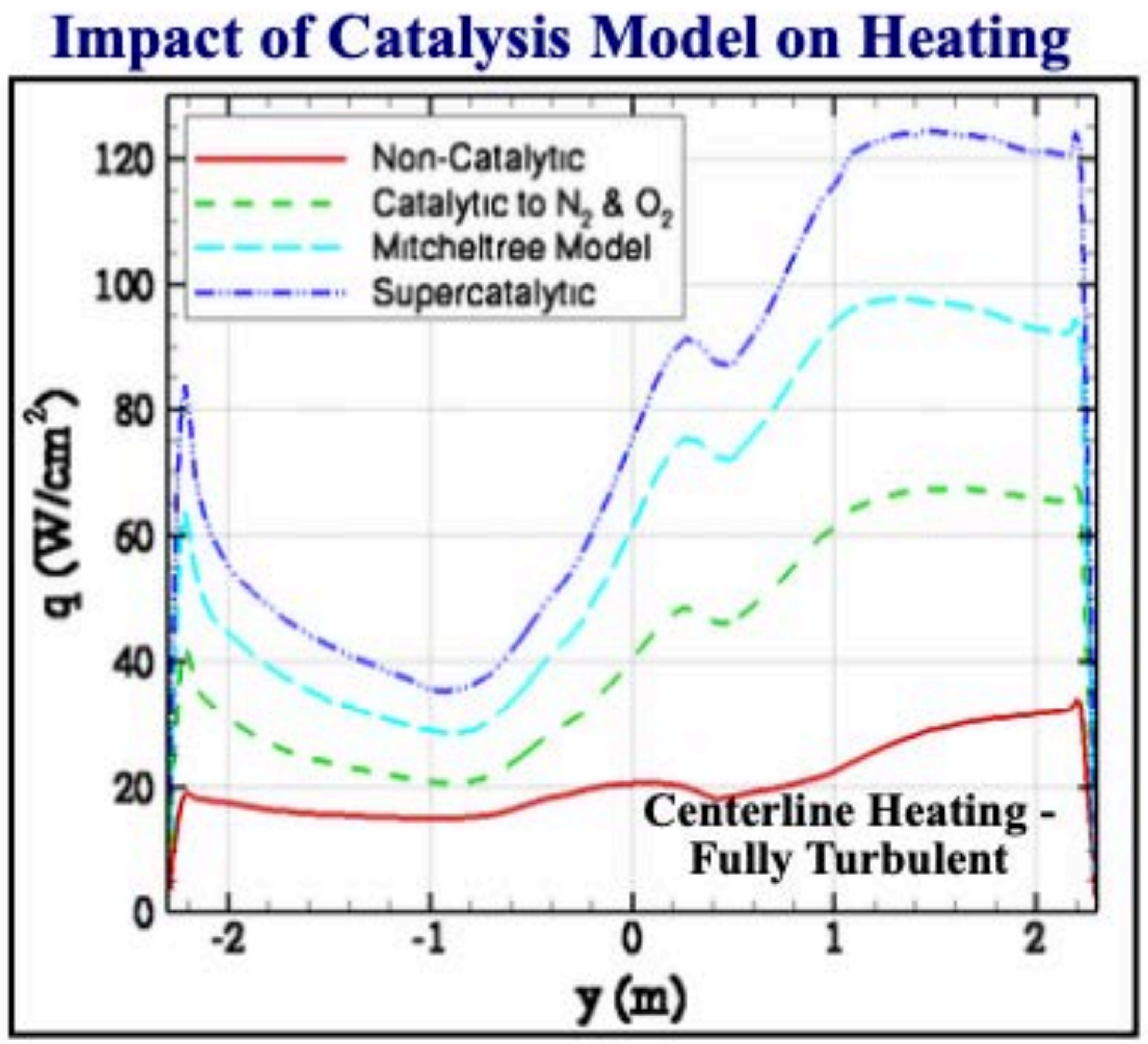

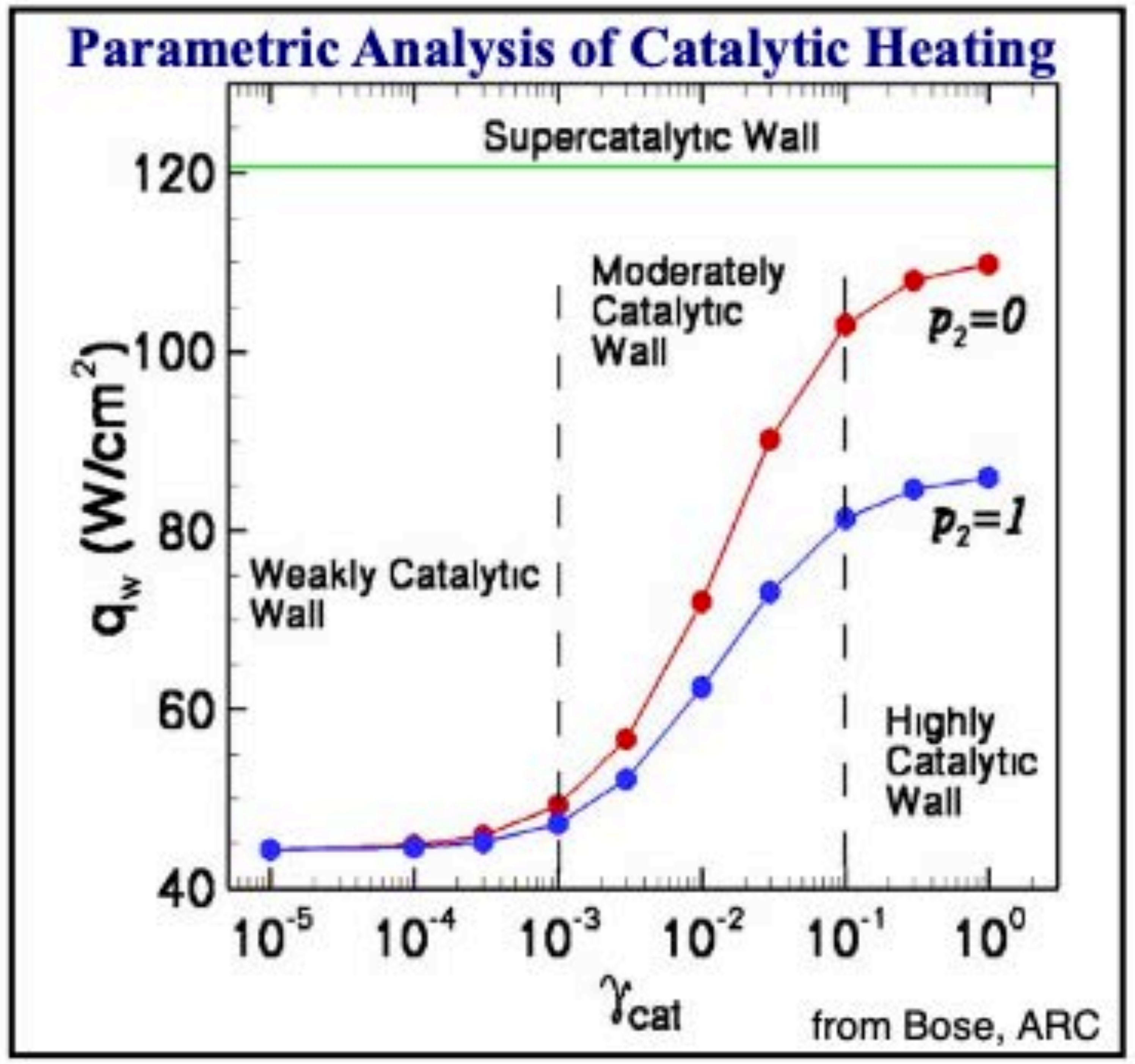

- **What are the key gaps?**
  - quantum chemistry to determine reaction rates (gas phase and gas-surface)
  - MD simulations of key GSI processes
  - experimental data on TPS materials at relevant conditions

Afterbody Heating

- **Wake flows are much harder to simulate than forebody**
  - separated, low density, unsteady, nonequilibrium flowfield
  - significant code-to-code differences still exist
- **Current uncertainty levels ~50-300%**
  - primary reason: lack of validation; we have not quantified how good (or bad) we are

MSL Afterbody Heating

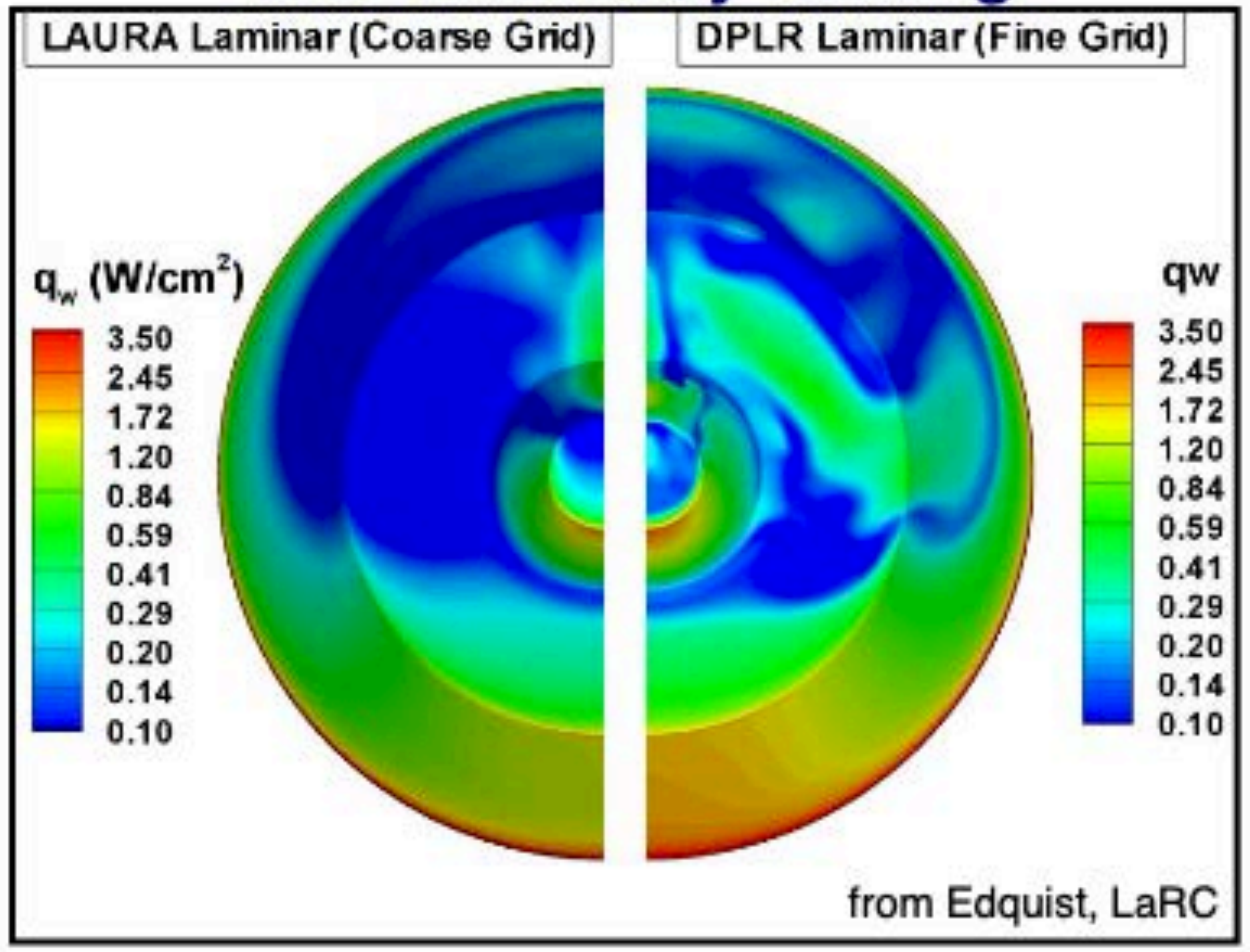

CFD Validation with AS-202 Flight Data

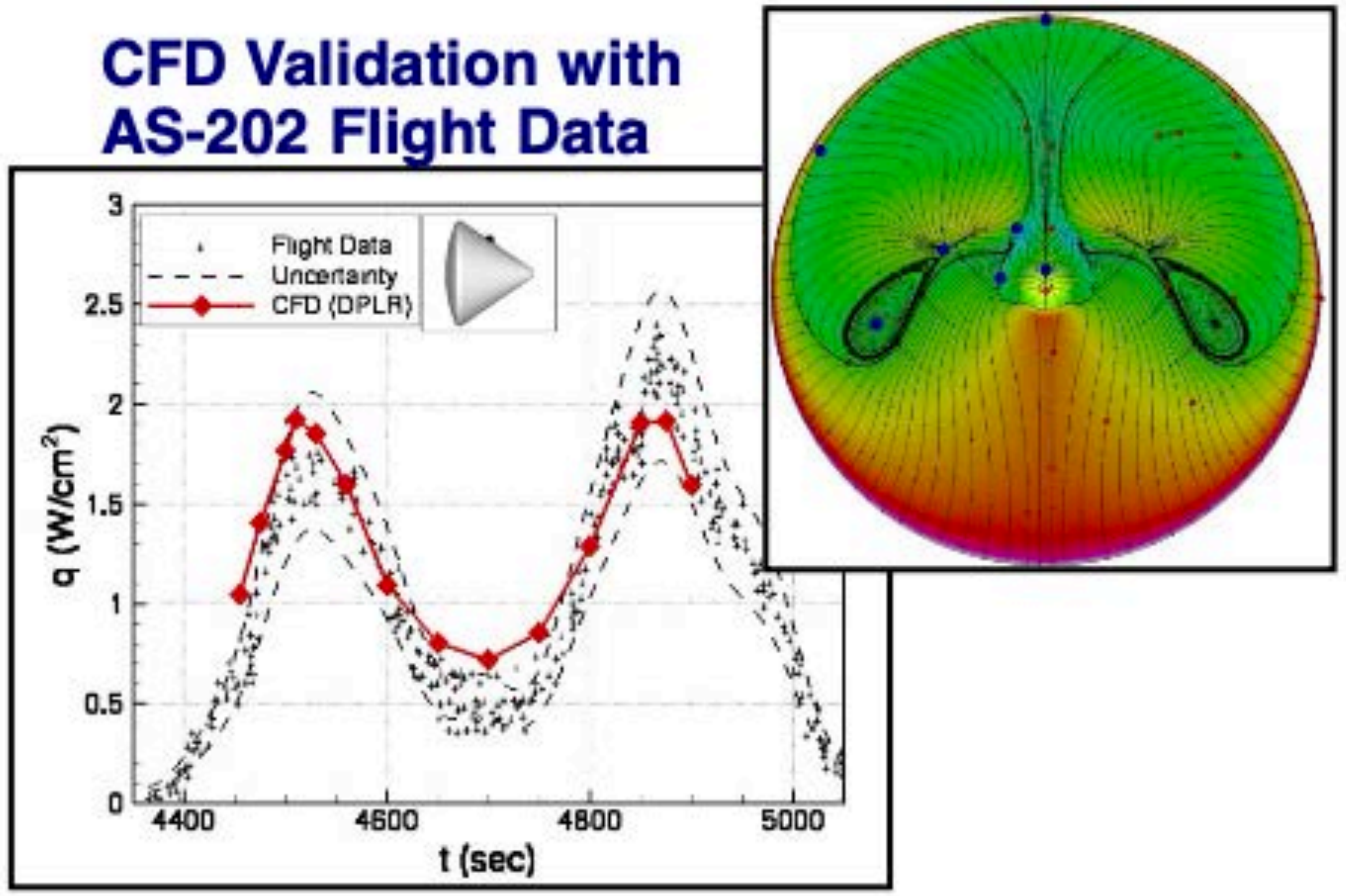

- **What are the key gaps?**
  - additional ground test data (including free flight or stingless models)
  - explore advanced methods (DES, LES) for hypersonic separated flows
  - advocate for additional flight data

Singularity Heating

- **Now throw OML singularities (such as RCS thrusters) into the wake flow**
  - does not make things easier!
- **MSL is actively guided; thrusters must fire during hypersonic entry**
  - predicted locally high heating rates necessitated a late change in backshell TPS for MSL (with significant cost and mass penalty)

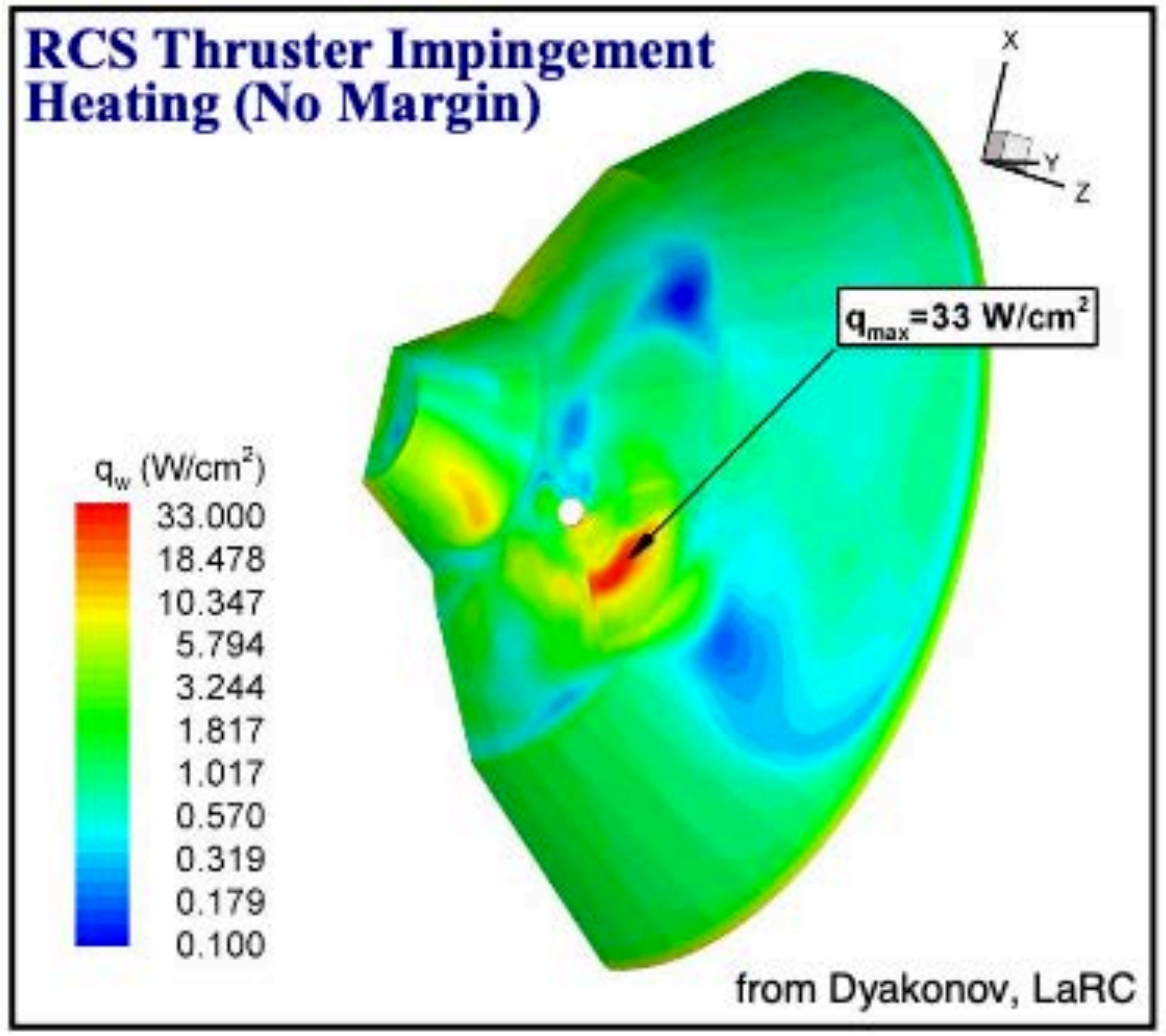

from Dyakonov, LaRC

MSL RCS Thruster Design (Preliminary)

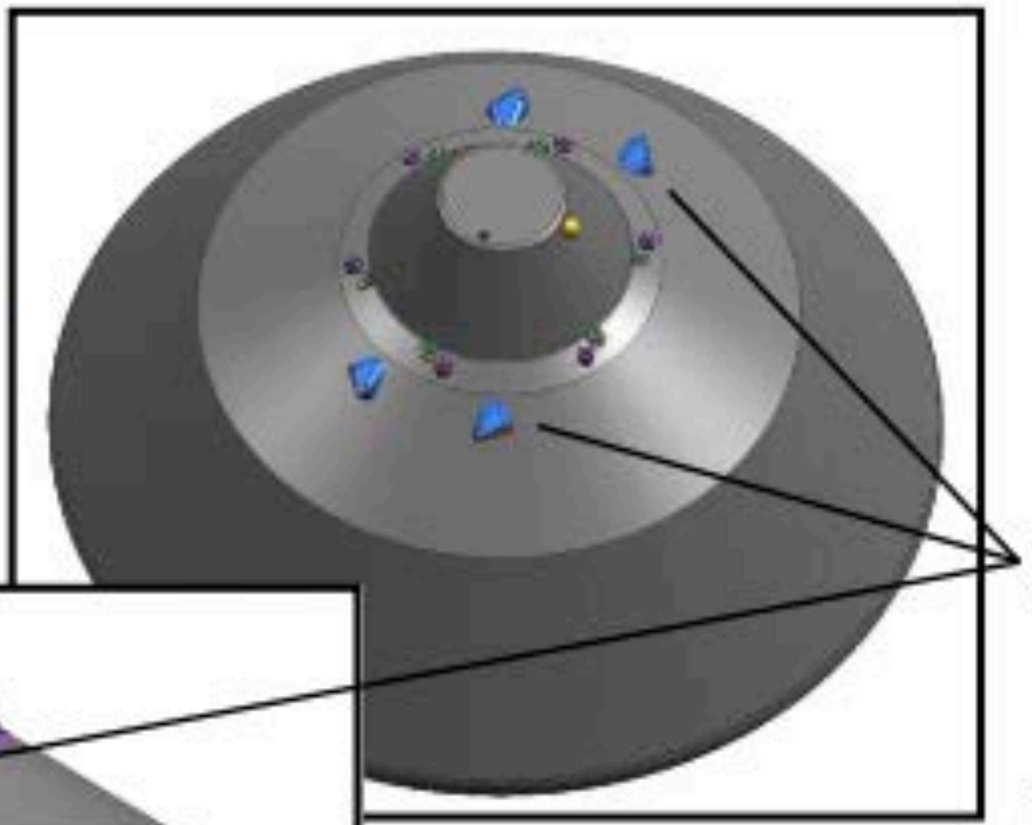

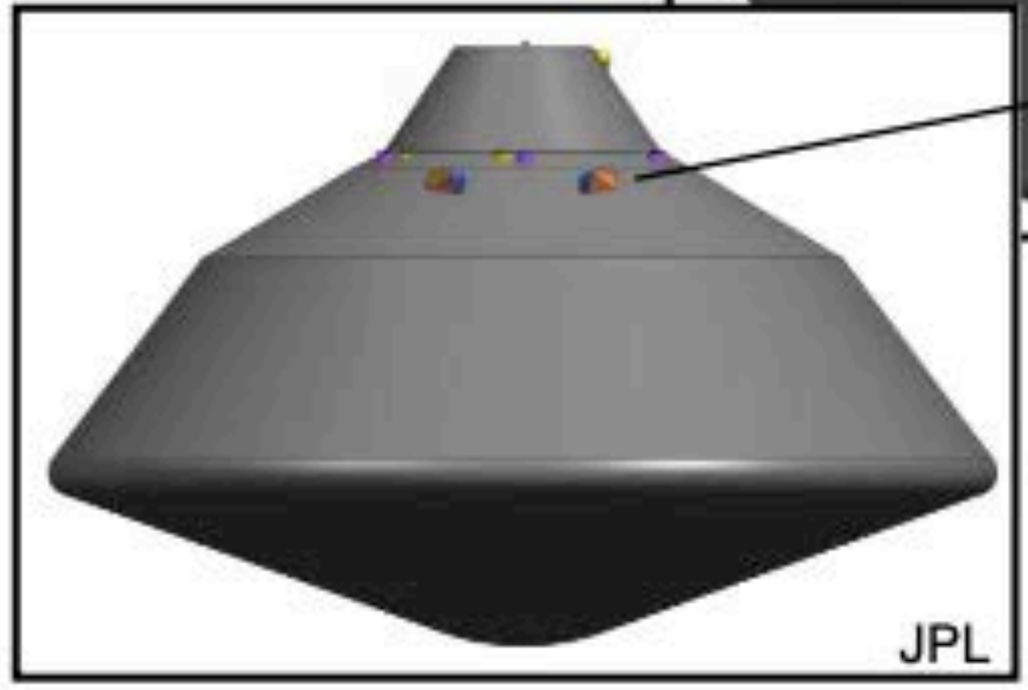

- **MSL backshell design requires canted thrusters for control authority**
- **Thrusters sticking into the flow; must be designed to withstand aerothermal environment**
  - no validation of our methods for this application

Shock Layer Radiation

- **Shock layer radiation is highly non-equilibrium, non-blackbody**
  - Titan analysis showed order of magnitude differences between equilibrium&accurate model
- **Not important for Mars missions to date, but critical for HMMES**
  - importance increases with velocity & vehicle size
  - primary radiator, CO(4+) emits in UV

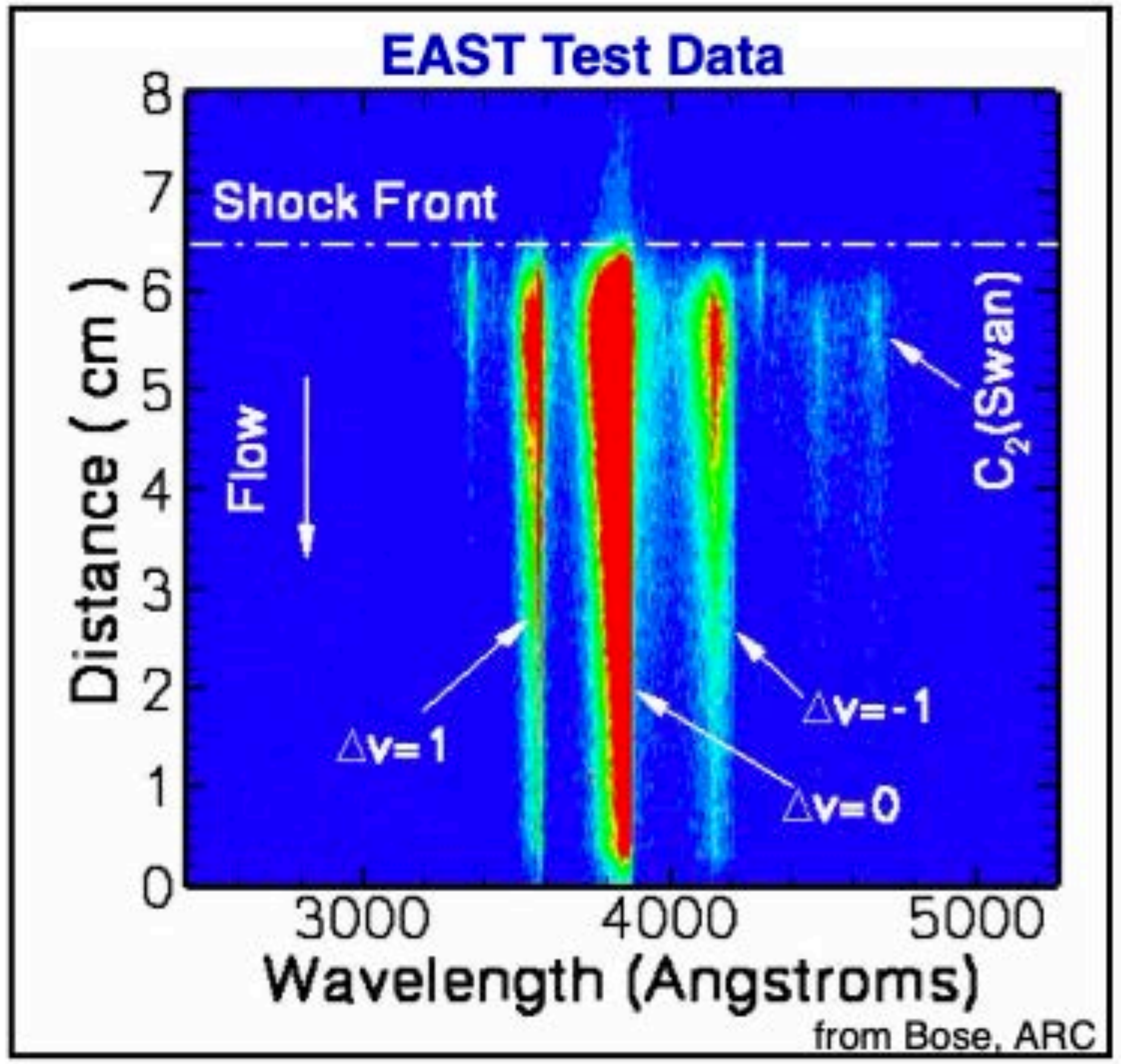

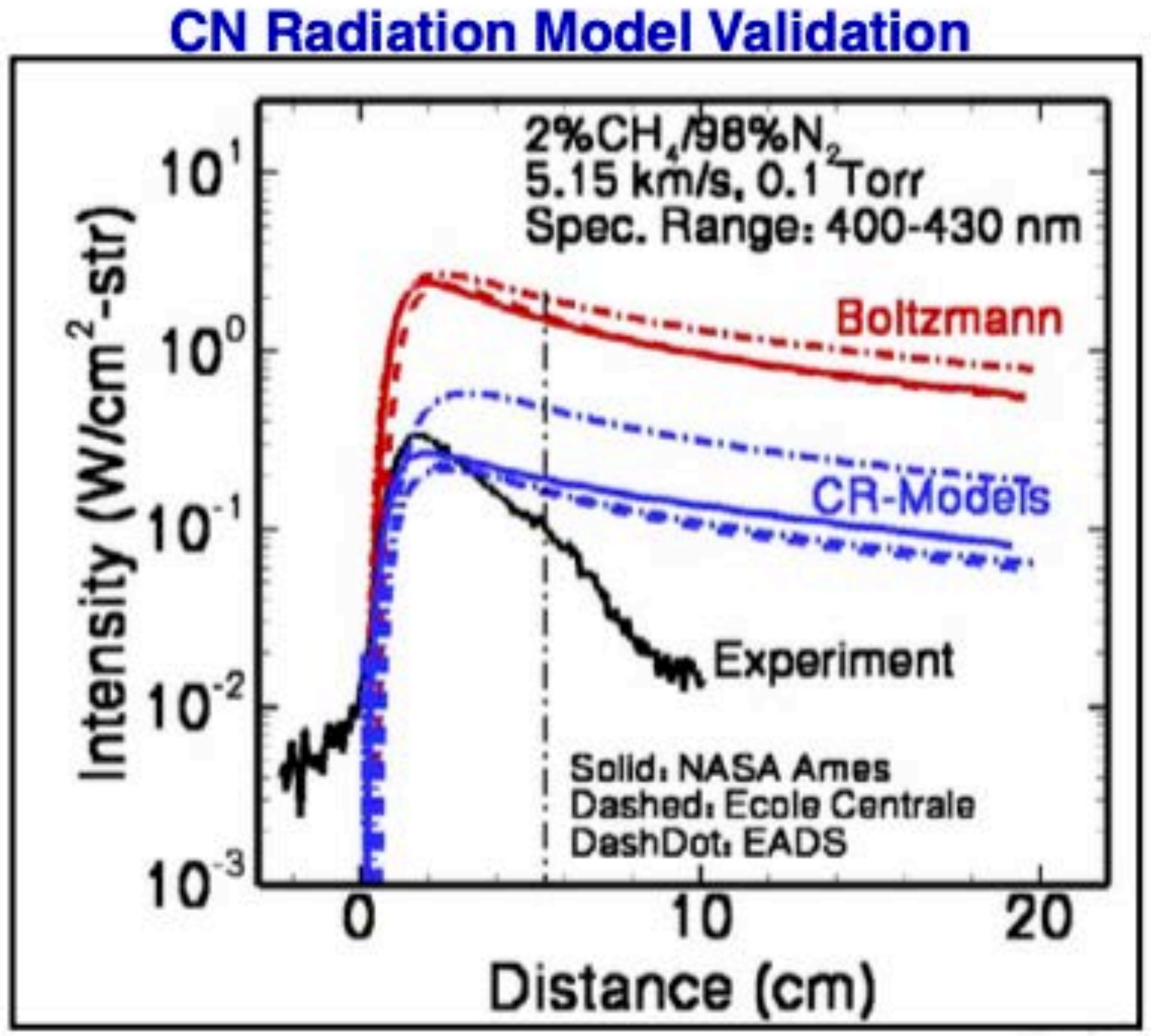

- **What are the key gaps?**
  - obtain additional shock tube data for Mars entries
  - build collisional-radiative models for all atomic and molecular radiators
  - compute excitation rates from QM
  - develop medium-fidelity methods for design
  - develop models for coupling to fluid dynamics

Flowfield-Radiation-Ablation Coupling

Titan Radiation Coupling

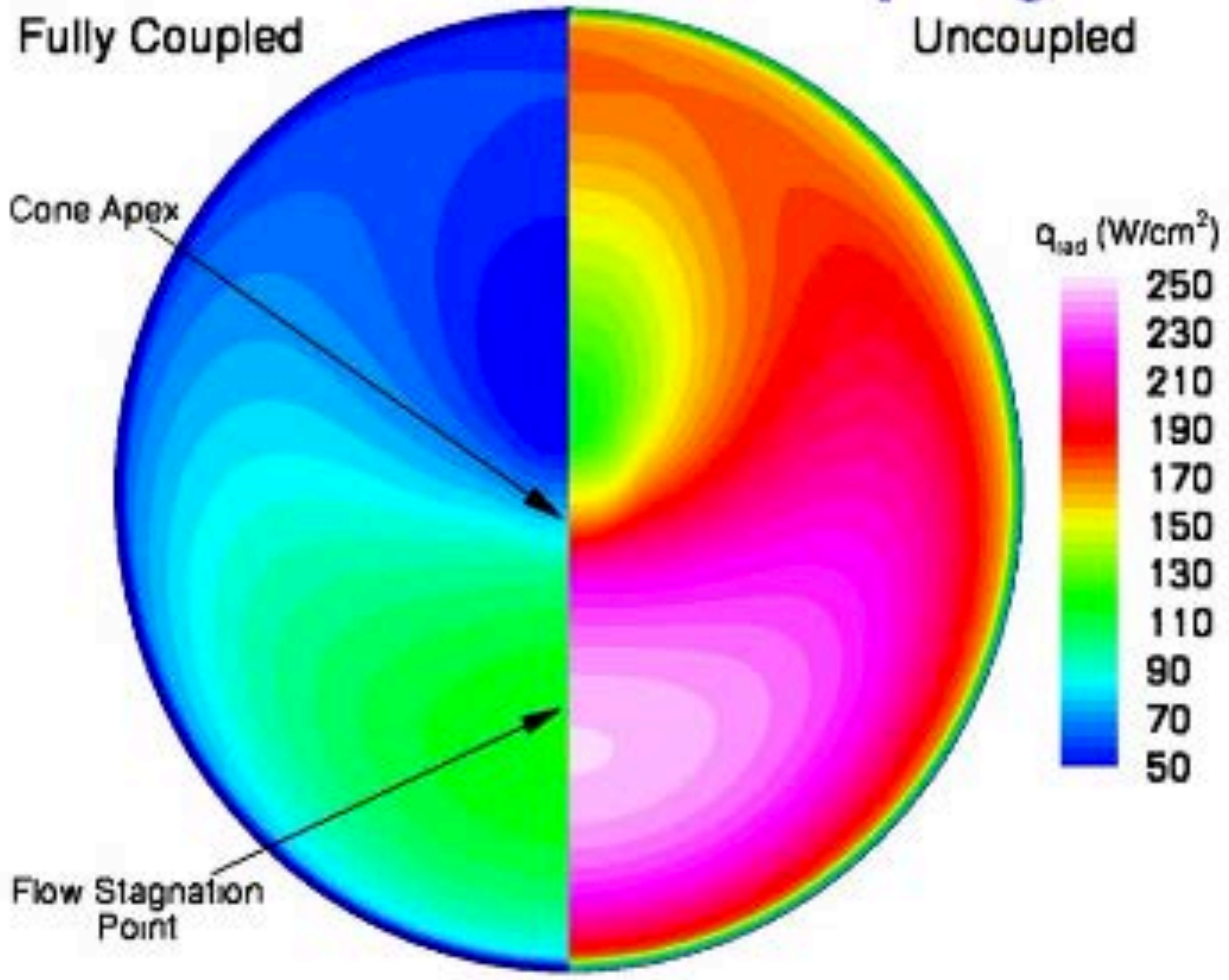

Stardust Ablation Coupling

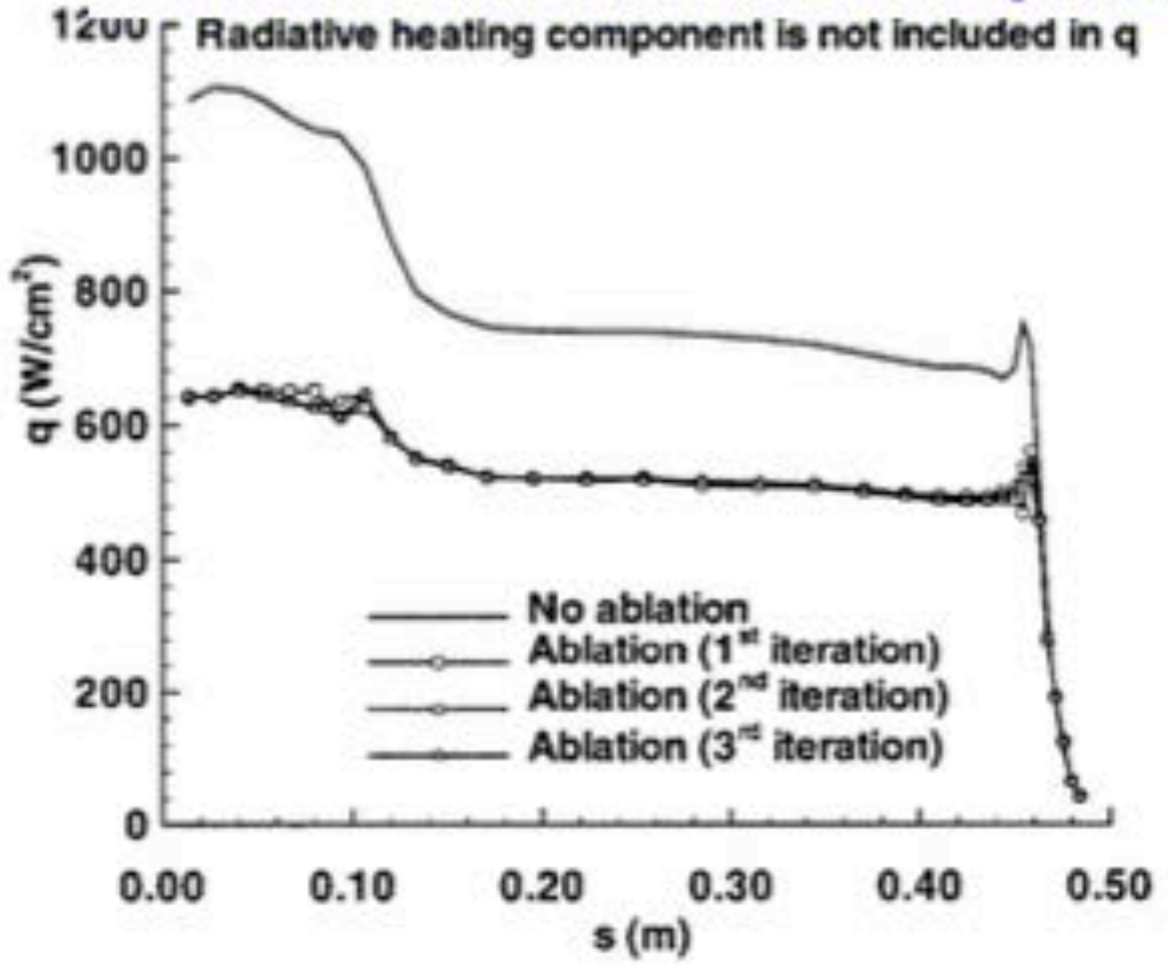

➢ Flowfield-Radiation (adiabatic cooling)

- Engineering approximation

$$\Gamma = 2q_{rad}/(\tfrac{1}{2}\rho_\infty V_\infty^3) \qquad q_{coup}/q_{unc} = 1/(1+\upsilon\Gamma^{0.7})$$

- Loose coupling is also possible
- More accurate answer requires simultaneous solution of the Navier-Stokes and radiative transfer equations; not possible except for limiting cases

➢ Flowfield-Ablation

- Blowing reduces heat transfer
- Ablation products mix with boundary layer gases
- Typically solved via loose-coupling approximation

➢ Radiation-Ablation

- Injected ablation products can absorb/emit radiation

➢ Ablation-Trajectory

- Significant ablation can lead to changes in aerodynamics/trajectory/GN&C
- Primarily a concern for RV's

TPS-Boundary Layer Interaction

- **We have already discussed gas-surface and ablation coupling, but other interactions are important**
- **Ablation induced distributed roughness**
  - Surface roughness generated on TPS surface as a consequence of ablation.
  - Strong interaction with boundary layer - increased heating and shear stress result
  - Heating augmentation from zero to factor of three possible over turbulent smooth wall
- **Discrete roughness**
  - Due to gaps, repairs, geometrics singularities, etc.
  - Generate local heating and shear augmentation factors which must be accommodated
- **For MSL:**
  - Distributed roughness adds about 20% to heating (pattern roughness not expected)
  - Discrete roughness adds another 40% locally in areas of gaps or repairs)

Pattern Roughness on RV Nosetip

Protruding Gap Filler in Arc Jet Test

TPS-Boundary Layer Interaction (2)

➢Melt layer interactions

- One class of ablators uses a glassy substrate material
- Energetically favorable; glass vaporization is highly endothermic
- Can cause strongly coupled instabilities in environments where glass melts but does not vaporize
- Interactions or instabilities can range from minor to catastrophic

Melt Flow induced by stream wise vortices

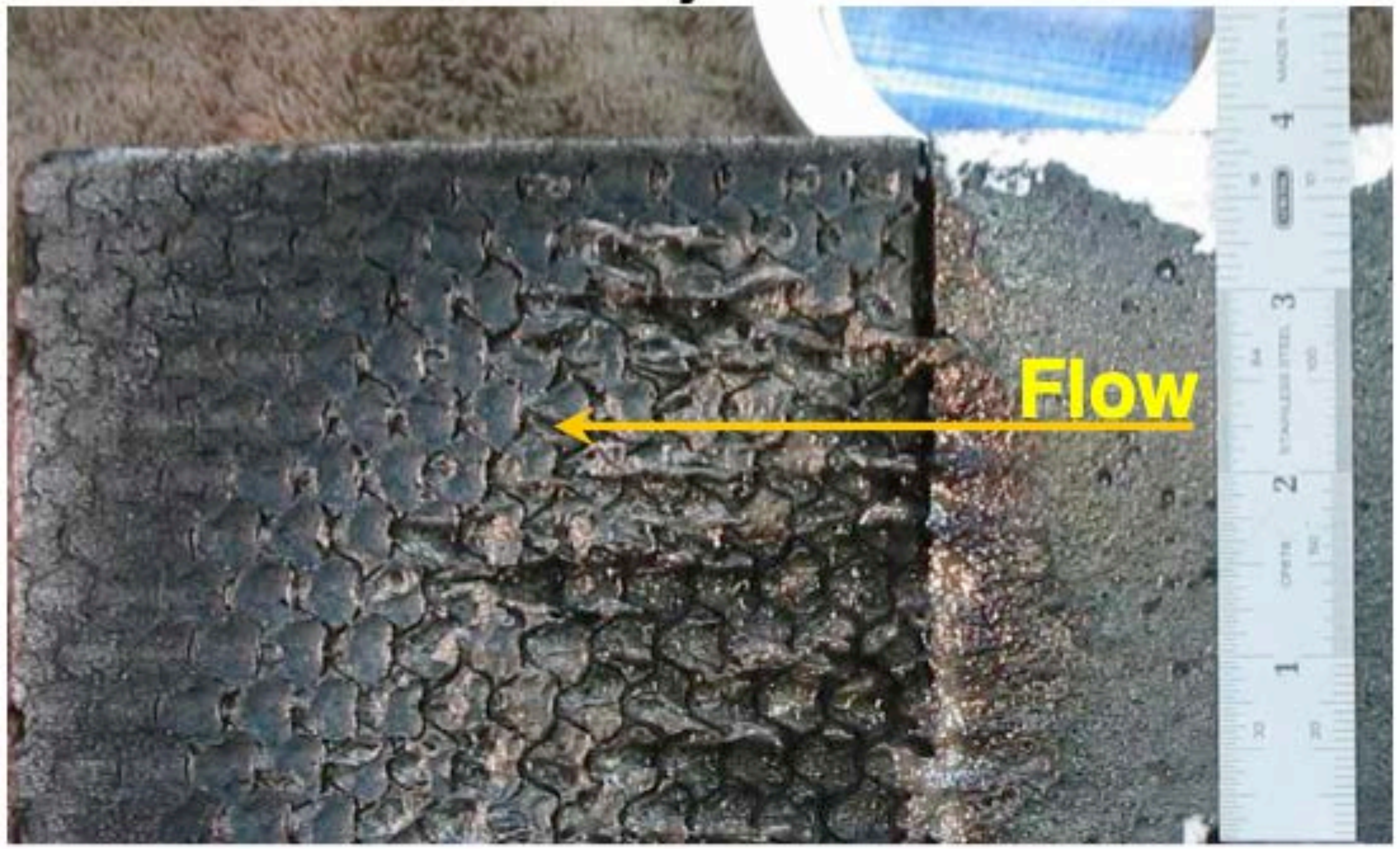

➢What to do?

- Simple solution: don't fly glassy ablators in such environments
- Better long term solution: develop models of the boundary layer surface interaction

Research topic: Better models for all aspects of material / fluid interactions

Shape Optimization

- **The primary reason we continue to use 70° sphere cones for Mars entry is "heritage"**
  - argument is weak: clear finding of MSL aerothermal peer review last summer
- **Non-optimal from aerothermal perspective**
  - expansion around nose leads to boundary layer instabilities, early transition, high heating levels
- **Modified ellipsoid aeroshell has significant advantages with same aerodynamics**
  - for Mars aerocapture this shape led to 50% lower heat flux, potential 67% TPS mass savings

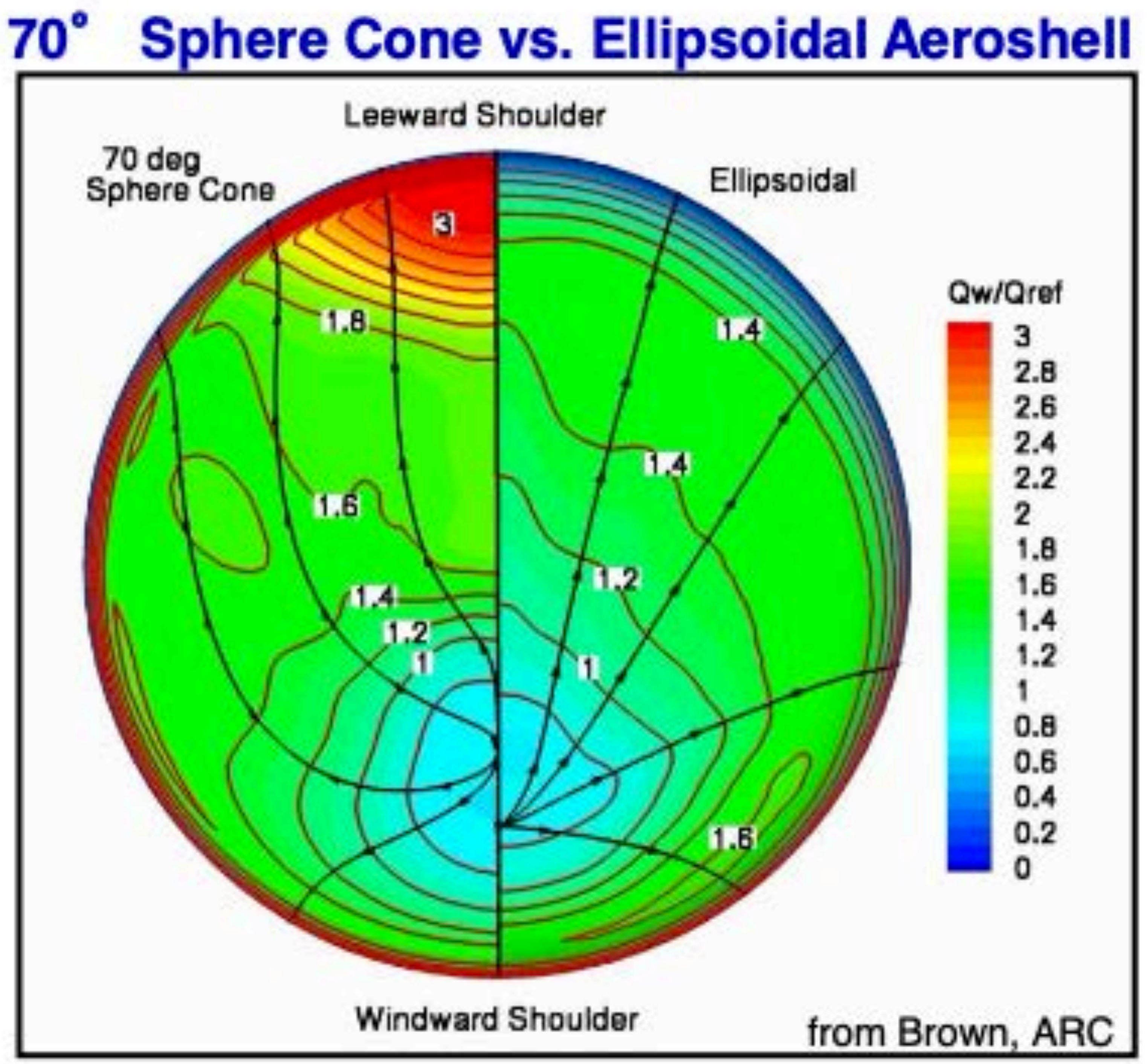

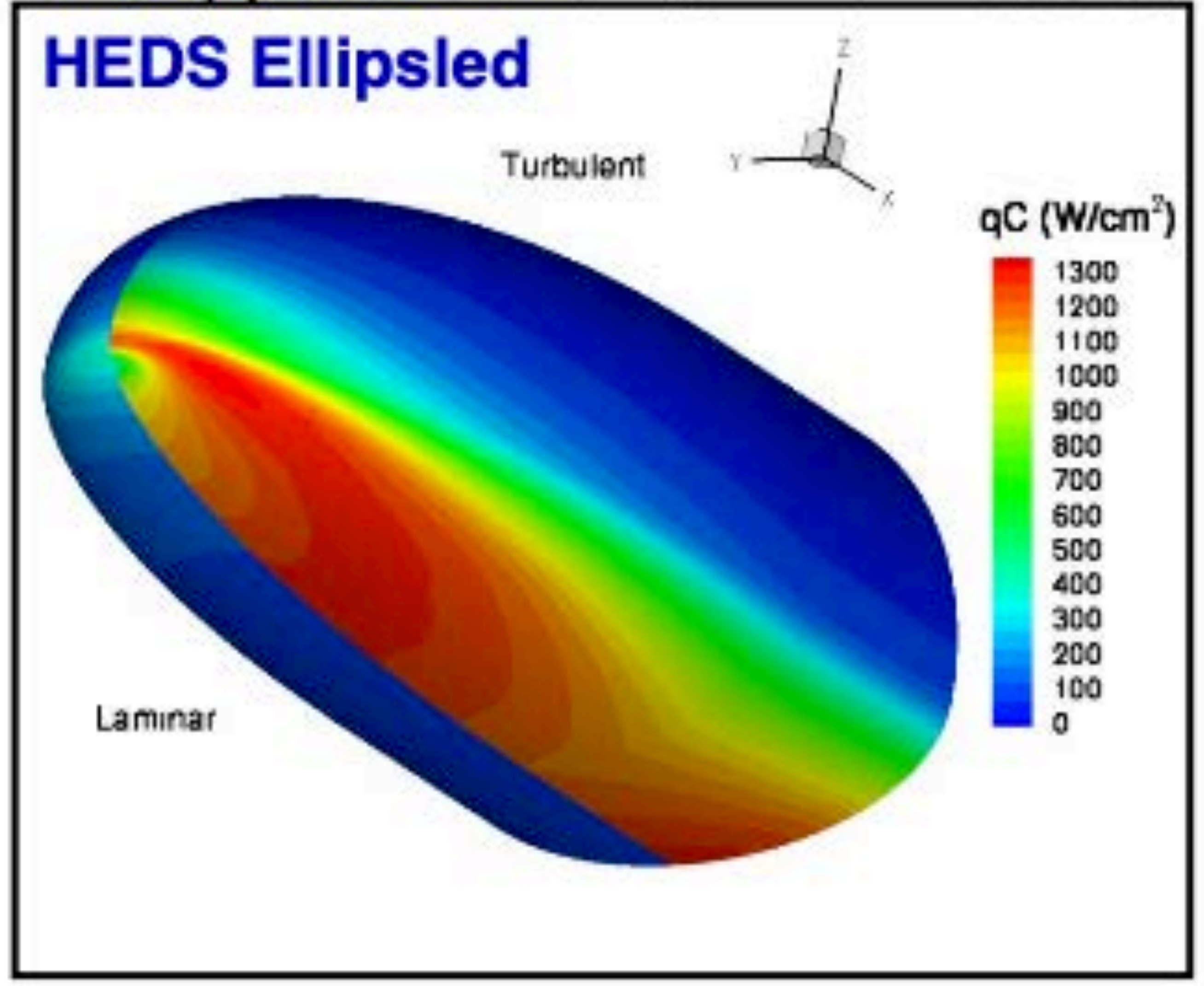

- **For large entry masses other shapes (e.g. ellipsled, biconic, bent biconic) should be explored as well**

→ **A full shape optimization study should be part of any future Mars systems analysis**

Validation: AS-202 Flight Data

Afterbody Calorimeter Placement

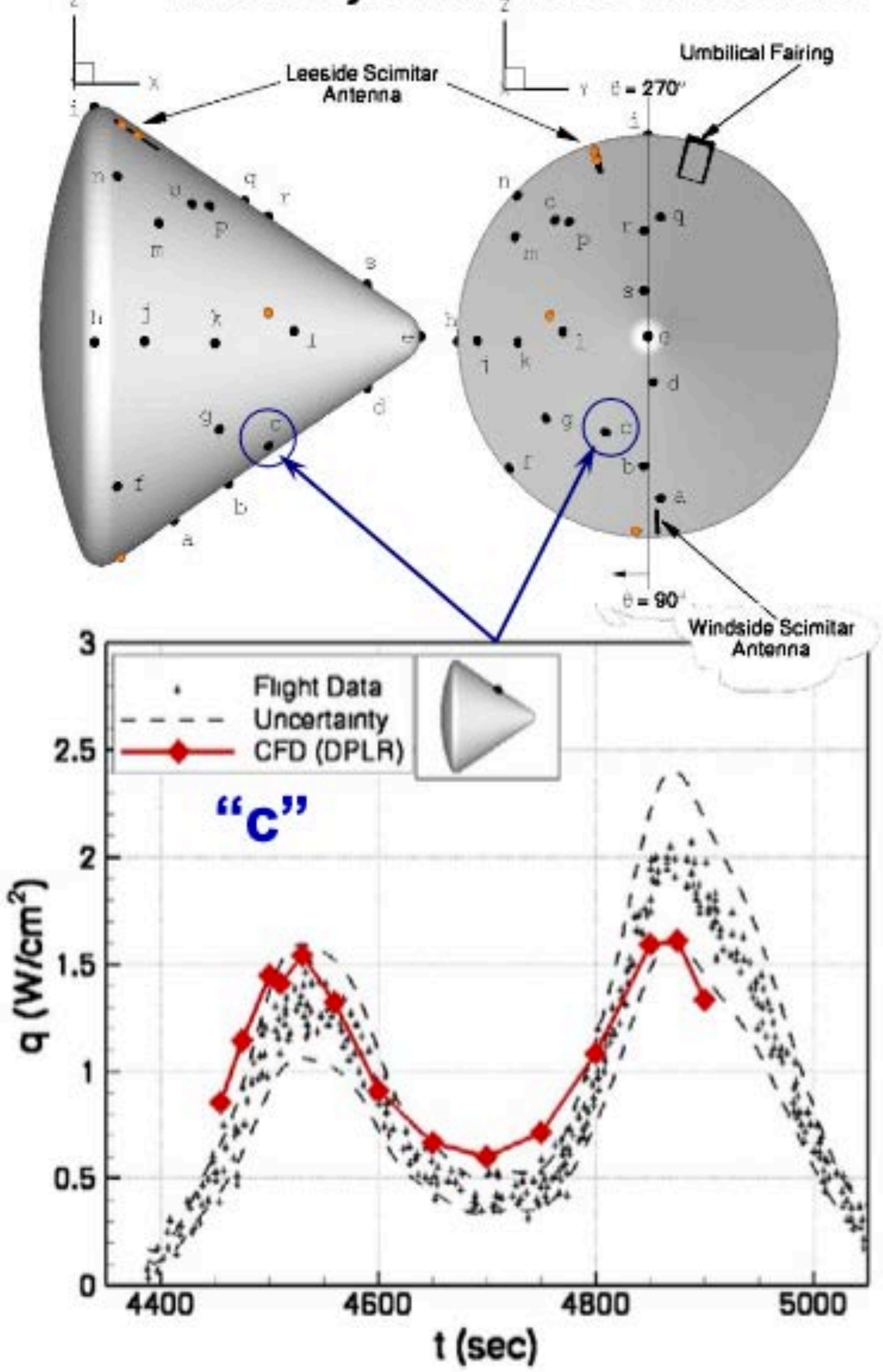

- **Problem**: Current uncertainty on afterbody heating predictions is very high
- **Goal**: reduce uncertainty levels by validation with flight data

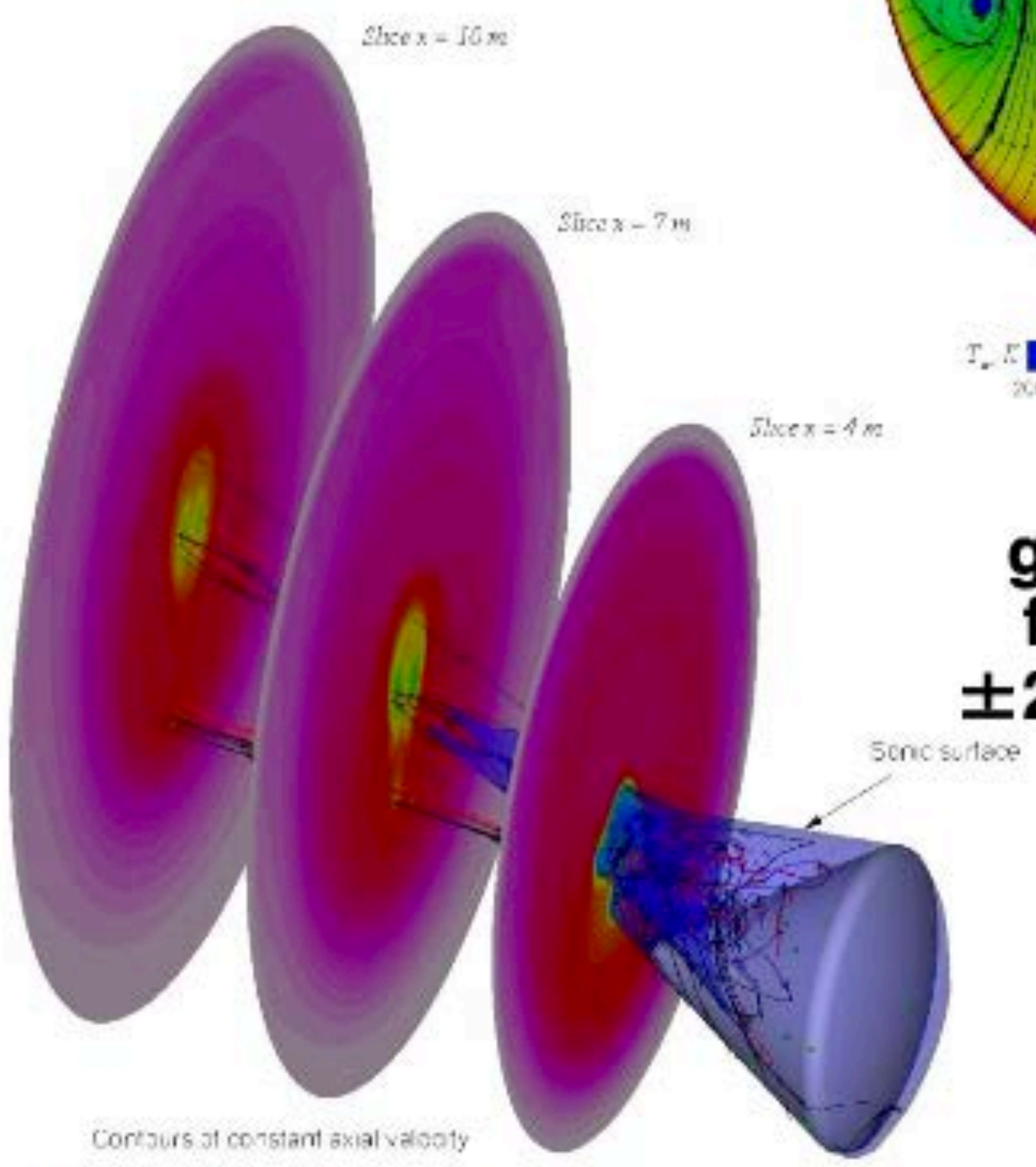

Ref: AIAA 2004-2456

Surface Oilflow
t= 4900 s, $Re_D = 7.6\times10^5$

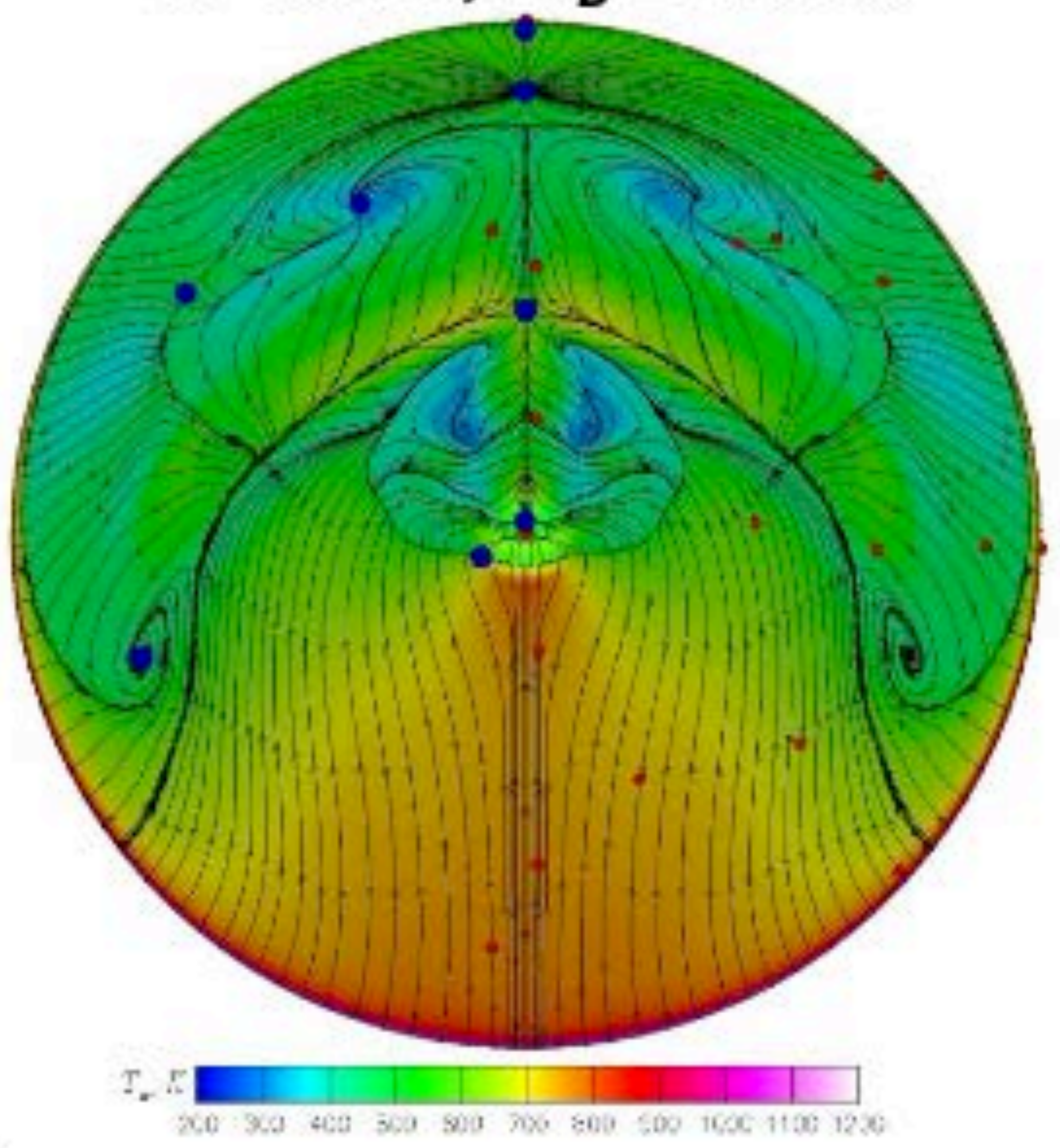

⇒Computations generally agree with flight data to within ±20% uncertainty at 15 of 19 calorimeter locations.

Flight Data: MER-B Heatshield

- Unique opportunity to observe in-situ flight hardware during Opportunity extended mission
- Multiple images of (inverted) heatshield made with cameras and micro-imager
- Work ongoing to compare visualized material response to predictions

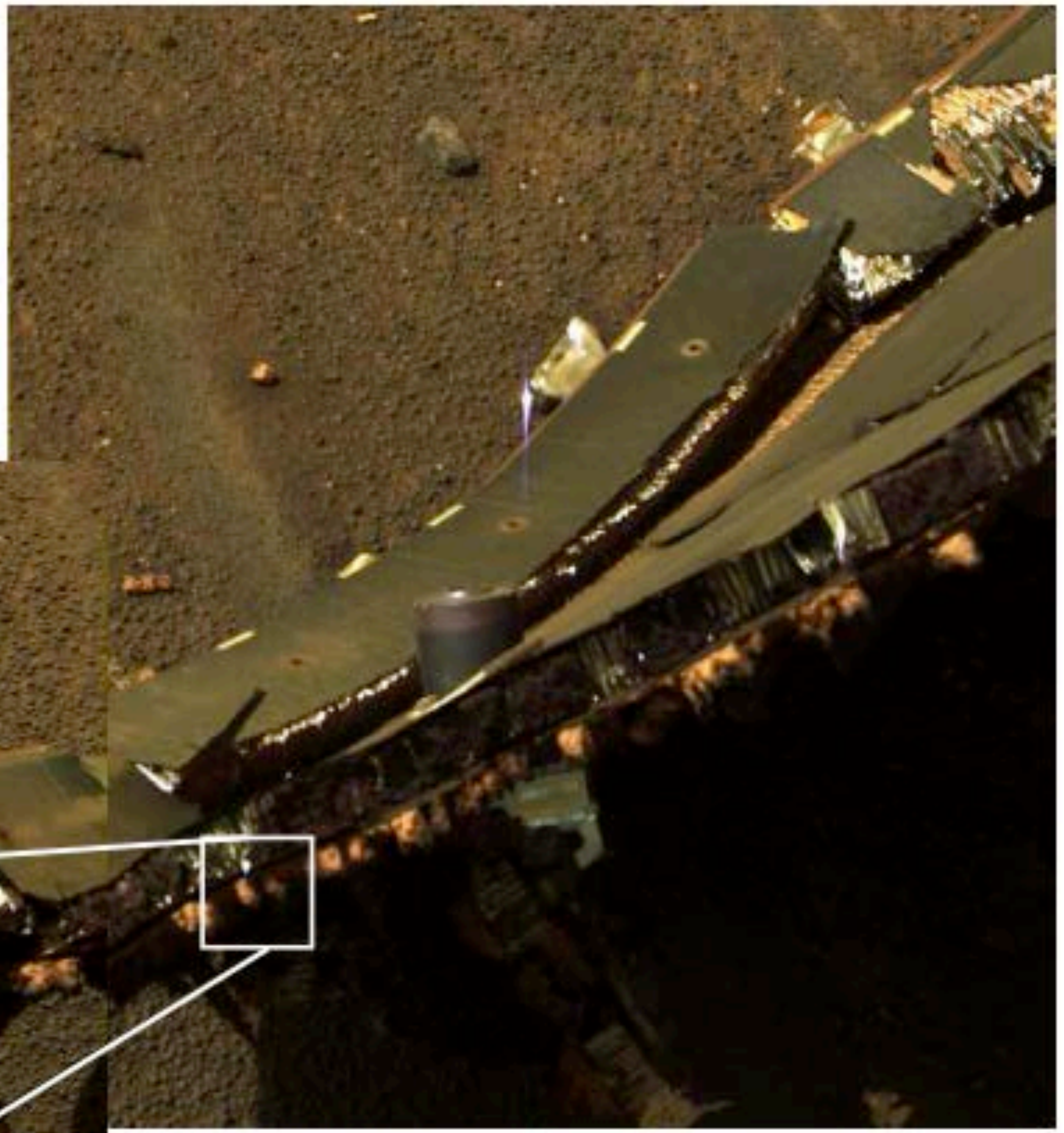

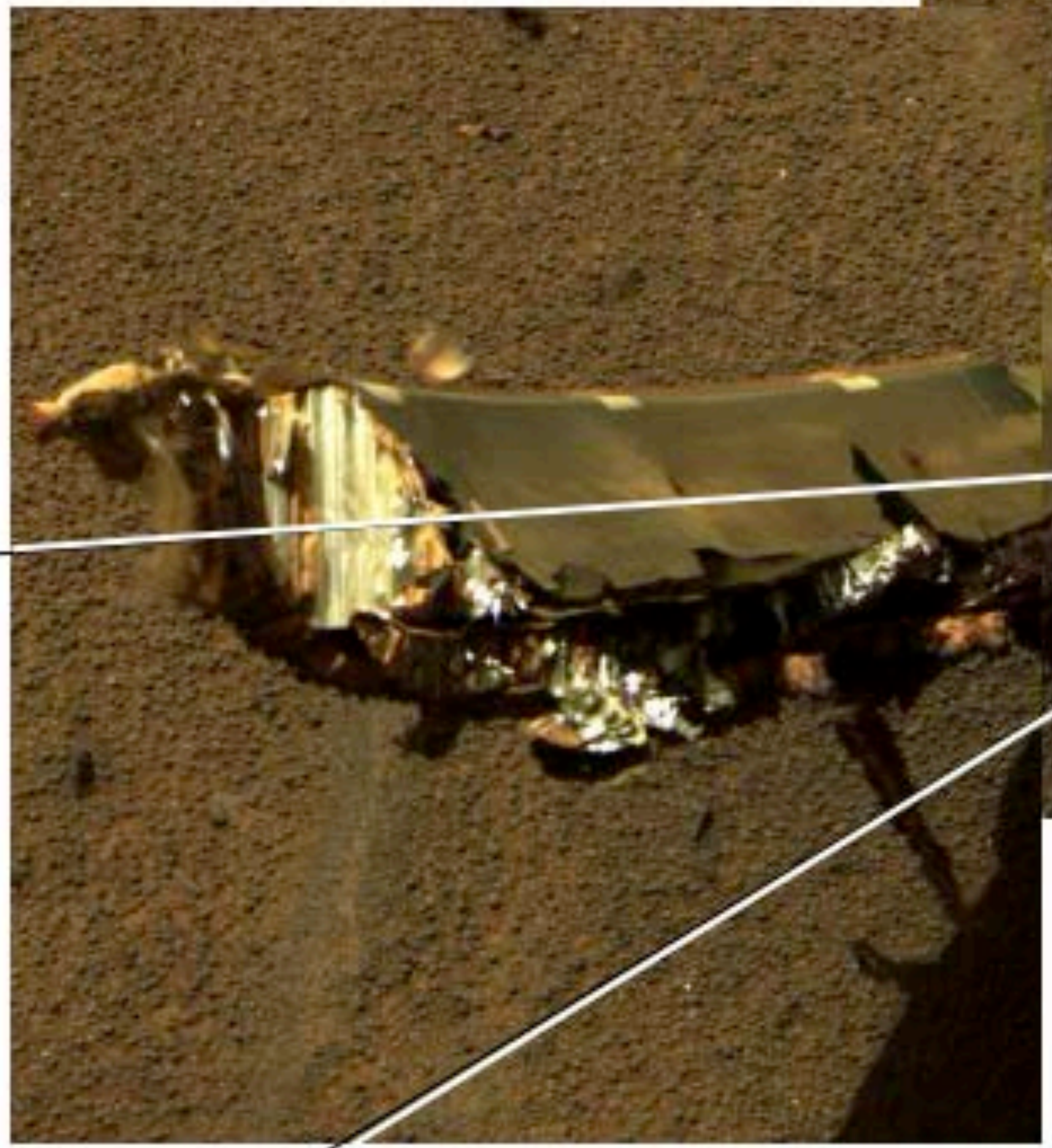

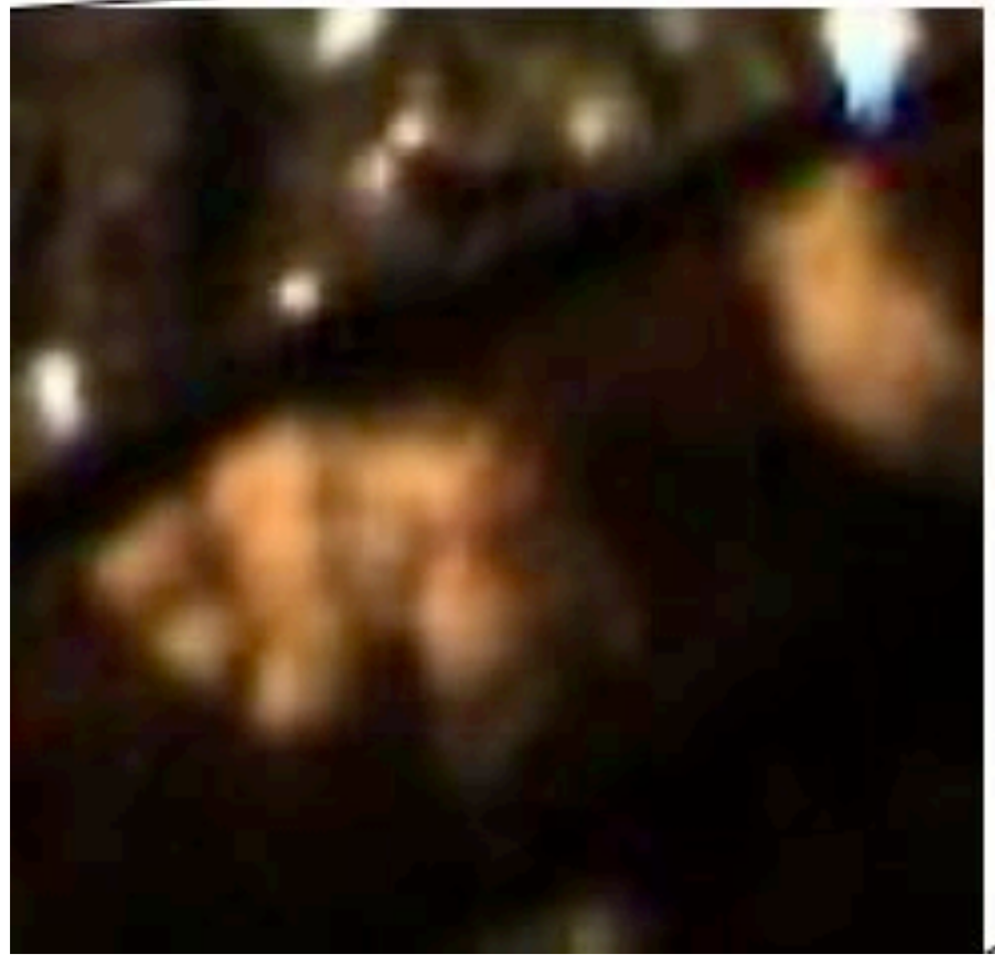

Image courtesy Christine Szalai, JPL

→ Flight data are the gold standard for final model validation

Flight Data: MEDLI

MSL Heatshield Layout

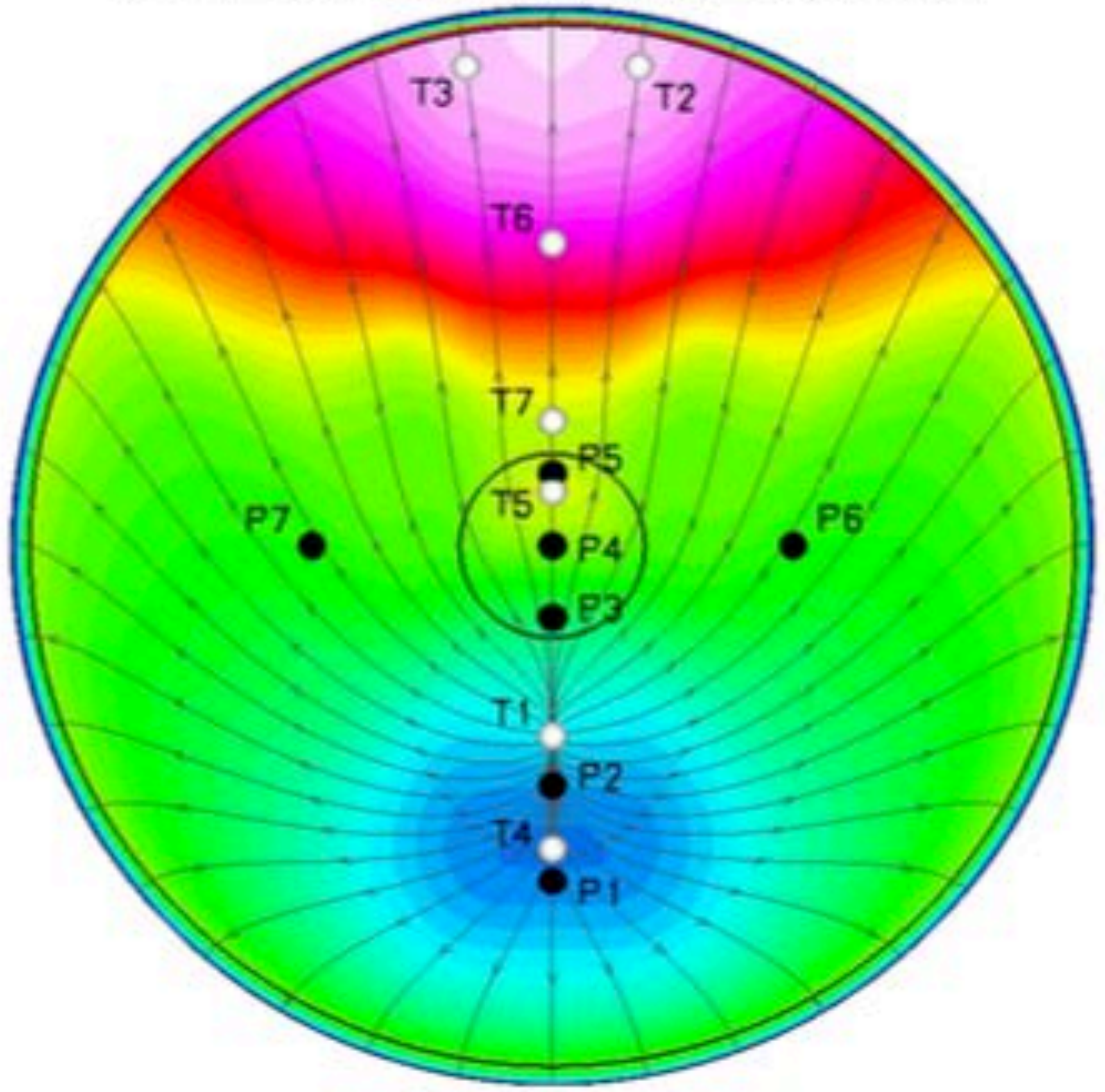

- HQ approval for MSL instrumentation suite!
- High TRL sensors to be installed in seven locations on heatshield
- Flight data obtained will go a long way toward validating ARMD-developed tools to drive down uncertainties discussed herein
- No backshell instrumentation (backshell is on critical path)

Recession Sensor

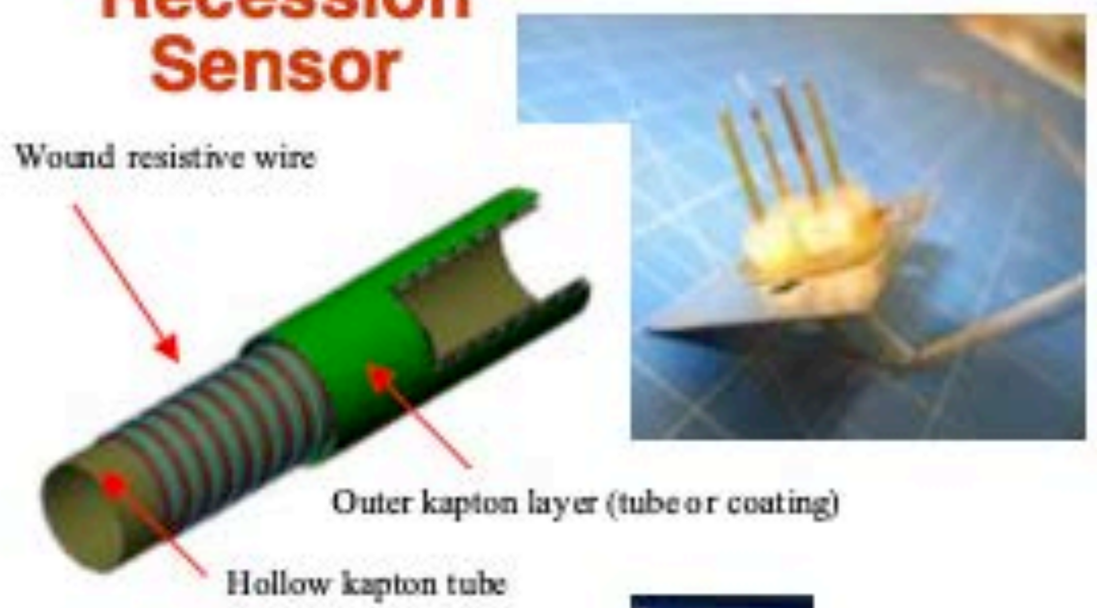

Thermocouple Plug

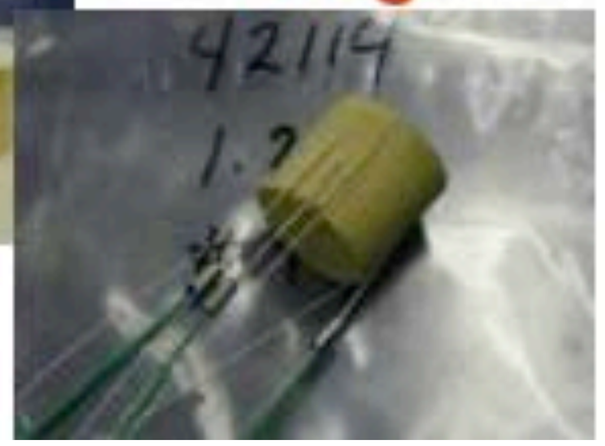

Pressure Sensor